FIRE BEHAVIOR PREDICTION AND FUEL MODELING OF FLAMMABLE SHRUB UNDERSTORIES IN NORTHEASTERN PINE - OAK FORESTS

by

Michael E. Dell'Orfano

A Thesis

Submitted to the Faculty

of the

WORCESTER POLYTECHNIC INSTITUTE

in partial fulfillment of the requirements for the

Degree of Master of Science

in

Fire Protection Engineering

by

Michael E. Dell'Orfano

August 1996

APPROVED:

Prof. Nicholas A. Dembsey, Advisor

Richard D. Pehrson, Reader

Prof. Richard L.P. Custer, Co-advisor

Prof. David A. Lucht, Director
Center for Firesafety Studies

Acknowledgments

This thesis would not have been possible without the financial and logistical support provided by the National Park Service for the prescribed burns at Cape Cod National Seashore. This support was given through a grant to Professor William A. Patterson, III at the University of Massachusetts, Amherst, and I would like to thank Professor Patterson for the generous amount of time and interest he gave my thesis. Thanks also to Dave Crary at Cape Cod National Seashore and Dr. Wendy R. Catchpole of the University of South Wales for the valuable data and up-to-date information.

I would also like to thank Professor Nicholas Dembsey and Professor Richard Custer for their enthusiasm, guidance and interest in expanding the scope of fire protection engineering at Worcester Polytechnic Institute. Your time and sharing of your knowledge is greatly appreciated. Thank you also to Richard Pehrson for his technical reading and help with the finishing touches.

The completion of this thesis has been a long road and I couldn't have done it without the love and support of my mom and dad through all of the ups and downs. Thanks to all of my family and great friends and to Brandi and Pokey who have always stood, and barked, by my side. Thanks especially to the firefighters at West Station in Auburn, MA for the good times and good calls. But none of this would have happened without the Orange County Fire Authority introducing me to my true love, fighting wildfires. Time to head back West!

Thank you Boston! Goodnight!

Abstract

This thesis evaluates the effectiveness of BEHAVE: Fire Behavior Prediction and Fuel Modeling System in predicting fire behavior in the Northeastern pine - oak forest. This fuel complex is composed primarily of a litter and huckleberry shrub understory with a pitch pine and oak overstory. Measurements of fuel bed physical characteristics, weather and fire behavior are taken from a series of prescribed burn studies in Cape Cod National Seashore in Massachusetts. Site-specific fuel models are constructed which provide the necessary inputs for fire predictions. Observed spread rates and flame lengths are over-predicted by BEHAVE for burns conducted during the winter (dormant season) and under-predicted for burns conducted during the summer (growing season). Attempts to improve winter predictions are successful when the litter moisture is adjusted in order to account for the live wintergreen which increases the overall moisture content of the surface fuels. A sensitivity study is performed where each input parameter is varied over a reasonable interval in order to view its impact on predictions. The model's high sensitivity to fuel bed depth and 1-hr surface-area-to-volume ratio appear to be the cause for fire prediction deviations during the winter, while the high live fuel moisture contents appear to overwhelm and suppress fire behavior predictions during the summer. It is concluded that BEHAVE's representation of fuel complexes as a homogeneous fuel bed with constant properties does not take into account the unique features of the litter and shrub components. An alternative, simple model of fire spread is developed which treats each component as a separate fuel bed. The model is based on a measurement of the heat release rate which can be determined directly through the principle of oxygen consumption calorimetry. Future work using small- and large-scale testing apparatus will help determine the ignition process of the live shrubs and the effect of parameters such as moisture content on the burning characteristics of the fuels.

Table of Contents

List of Tables

List of Figures

Nomenclature

A	weighted surface area [dimensionless]
A_d	cross-sectional area of combustion interface [m^2]
a	fuel absroptivity
c_s	specific heat of fuel bed [kJ/kg-K]
c_p	specific heat of air [kJ/kg-K]
d	fuel bed depth, m
$\frac{dw}{dt}$	mass loss rate per unit area of fire front [lb/ft^2-min]
F	view factor
F_L	flame length, ft
f	weighting factor [dimensionless]
g	acceleration of gravity [m/s^2]
H_A	heat per unit area [Btu/ft^2]
H_F	flame height [m]
h	heat content [Btu/lb]
h_w	half-width of confidence interval
$\vec{I}$	vector sum of all heat fluxes
I_B	fireline intensity [Btu/ft-s]
I_p	propagating flux [Btu/ft^2-min]
$(I_p)_o$	no-wind, no-slope propagating flux [Btu/ft^2-min]
I_R	reaction intensity [Btu/ft^2-min]

$I_{x,ig}$ horizontal heat flux absorbed by a unit volume of fuel at time of ignition [Btu/ft^2-min]

k_g gas-phase conductivity [kW/m-K]

L flame length [m]

L_c preheating distance in gas-phase conduction [m]

M_f fuel moisture content (percent of oven-dry weight)

$M_{x,\,dead}$ dead fuel moisture of extinction [fraction]

$M_{x,living}$ live fuel moisture of extinction [fraction]

m mass of fuel [kg]

$\dot{m}$ mass loss rate [kg/s]

$\dot{m}_e$ experimentally determined mass loss rate [lb/min]

n random sample size

P_w width of weighting platform [ft]

Q_{ig} heat of preignition [Btu/lb]

Q_{ef} effective heat [cal/g]

$\dot{Q}$ heat release rate [kW]

$\dot{Q}^*$ dimensionless heat release rate

$\dot{Q}_r$ radiant heat release rate [kW]

$\dot{q}_{cond}$ gas-phase conduction forward heat flux [kW]

$\dot{q}_f$ forward heat flux due to flames above fuel bed [kW]

$\dot{q}_o$ forward heat flux through combustion interface [kW]

$\dot{q}_r$ radiative forward heat flux through combustion interface [kW]

R rate of spread [ft/min]

S_T fuel particle total mineral content

T_f flame temperature [K]

T_o initial temperature [K]

T_p pyrolysis temperature [K]

T_∞ ambient air temperature [K]

t_r flame residence time [min]

t_b burnout time [s]

U midflame windspeed [ft/min]

U_w windspeed [m/s]

V quasi-steady rate of spread [m/s]

w_o oven-dry fuel loading [lb/ft^2]

w_n net fuel loading [lb/ft^2]

z percentile of the standard normal distribution

Greek Symbols

α fraction of living fuel

$1-\alpha$ confidence coefficient

β packing ratio

β_{op} optimum packing ratio

χ_b fraction of heat release rate released through combustion interface

χ_{cond} fraction of heat release rate transferred by gas-phase conduction

χ_r fraction of heat release rate transferred by radiation

Δ flaming zone depth [m]

ΔH_c effective heat of combustion [kJ/kg]

Δh enthalpy change [kJ/kg]

ΔV unit volume

δ fuel bed depth [ft]

$\left(\frac{\partial I_z}{\partial z}\right)_{z_c}$ gradient of vertical heat flux at a constant depth, z_c [Btu/ft^3-min]

ε effective heating number

ϕ angle of slope inclination

ϕ_s slope coefficient

ϕ_w wind coefficient

Γ reaction velocity [min^{-1}]

Γ' potential reaction velocity [min^{-1}]

Γ'_{max} maximum reaction velocity [min^{-1}]

γ parameter based on definition of flame height

η_δ reaction zone efficiency

η_M moisture damping coefficient

η_s mineral damping coefficient

Σ summation

θ angle between flame and the perpendicular to the fuel bed

ρ_b oven-dry bulk density/fuel bed bulk density [lb/ft^3, kg/m^3]

ρ_{be} effective bulk density [lb/ft^3]

ρ_p oven-dry particle density [lb/ft^3]

ρ_∞ ambient air density [kg/m^3]

σ surface-area-to-volume ratio [ft^{-1}]

τ_R reaction time [min]

ω population standard deviation

ξ propagating flux ratio

Symbols/Superscripts

~ weighted value of parameter

∂ partial derivative

' per unit length

" per unit area

1. Introduction

An extensive study has been conducted in the Cape Cod region of Massachusetts for the purposes of analyzing the physical characteristics and fire behavior of a fuel complex found in the northeastern United States (W. A. Patterson III, personal communication, 1995). The fuel complex is the pine-oak forest which is composed of a litter and shrub understory, and a pitch pine and oak overstory. Data have been collected from a series of measurements of fuel bed physical characteristics and subsequent prescribed burns. The purpose of this thesis is to use these data to construct standardized fuel models which represent the characteristics of the fuel complex necessary for fire behavior predictions. The effectiveness of current wildfire simulation models in predicting fire behavior in the pine - oak forests will be evaluated.

The pine - oak forest is located primarily near the coastline of the northeastern United States from the mid - Atlantic north through central New England. A unique characteristic of this fuel complex is the predominantly huckleberry (Gaylussacia baccata) shrub understory which is very flammable due to its ease of ignition and ability to sustain combustion even under high moisture conditions. The potential fire behavior of these fuels was seen in Long Island, New York in late August, 1995 when two individual fires burned 9,500 acres and a number of houses and businesses (McFadden, 1995a,b). This pine barren fuel complex had a large fuel loading of primarily a scrub oak and huckleberry shrub understory. Under extreme drought and high wind conditions, fires whipped through this understory and upward into the pine overstory producing flame lengths over

40 feet. Similar fire behavior was observed in southern Miles Standish State Forest near Plymouth, Massachusetts in 1957 (W. A. Patterson III, personal communication, 1996). The scrub oak/huckleberry understory together with a pitch pine overstory burned over 15,000 acres in under two days. The running crown fire jumped a four - lane highway and produced flame lengths over 100 feet.

This thesis will focus on the fuel complex found in the Cape Cod National Seashore which is composed of a pitch pine and oak overstory with a predominantly huckleberry shrub understory. These fuels create a great deal of concern due to their fire behavior potential and the threat of fire to neighboring communities. There is a significant wildland/urban interface with over 600 houses, businesses and other structures in and around the Cape Cod National Seashore (Crary, 1987; D. W. Crary, Jr., personal communication, 1996). The entire Cape Cod area is also a major attraction for tourism, especially in the summer months, resulting in heavy traffic flow, emergency egress difficulties and increased potential of careless fires. Due to aggressive firefighting procedures in this area over the past 50 years, there is also an increased accumulation of these hazardous fuels creating a potential for catastrophic fire. Therefore, it is of great interest to study the various means of reducing these fuel loads, the behavior of these fuels in fire, and the potential to model and predict the behavior of a fire spreading through this fuel complex.

The field of wildland fire modeling is currently in a transitional period, marked by a re-evaluation of well established methods of predicting fire behavior, as new concepts and techniques are introduced to better understand the behavior of a spreading wildfire. The

past 30 years have seen large steps toward the use of predictive tools to simulate the growth, spread and effects of all types of wildland fires. In the early 1970's, a mathematical model was developed as a first attempt to produce a complete predictive package that could represent the physical and chemical characteristics of various fuel complexes and mathematically predict the behavior of a fire moving through these types of fuels (Frandsen, 1971; Rothermel, 1972). Several of these concepts and ideas were used concurrently in the development of the National Fire Danger Rating System (NFDRS) (Bradshaw, Deeming, Burgan, & Cohen, 1984; Burgan, 1988), which uses daily observations of temperature, humidity, precipitation amounts and duration, and wind speeds to establish the fire hazard in the region where the measurements were taken. The NFDRS is still being used to obtain important weather data and establish various levels of fire danger and their corresponding suppression requirements.

In the late 1970's and early 1980's, attempts were made to incorporate the theoretical and empirical relationships developed by Frandsen (1971) and Rothermel (1972) into a set of tools that could easily be used by land managers, firefighters and other field personnel to model the behavior of fires before or during their occurrence. Several improvements and additions were made to the original mathematical concepts and incorporated into a set of nomograms, or charts, that would allow one to graphically predict the rates of spread, flame lengths and various other measures of behavior of a fire burning in a particular fuel complex (Albini, 1976a, 1976b). With the introduction of advanced calculators (Rothermel, 1983), this process could be performed easily.

A set of computer programs was developed in the mid-1980's called BEHAVE: Fire Behavior Prediction and Fuel Modeling System (Andrews, 1986; Andrews & Chase, 1989; Burgan & Rothermel, 1984). The BEHAVE system consists of fuel models that are used in conjunction with fire prediction models in order to estimate various measurements of fire behavior and fire growth patterns. The fuel models of BEHAVE numerically describe a fuel complex through such parameters as fuel loading, size, arrangement and chemical properties. The fire prediction models incorporate these fuel models along with several environmental parameters into a set of equations which predict the speed, size and various measures of intensity of a fire moving through the fuel complex. This is different from the NFDRS which was designed to establish the fire risk in an area through such parameters as a spread component and burn index.

These models are still in wide use today and have been utilized in several aspects of land management and wildfire suppression. BEHAVE was used to help resolve fuel modification and urban planning issues in the wildland/urban interface of the Oakland/Berkeley Hills area of California (Rice & Martin, 1985). By predicting the potential fire behavior in the area's northern coastal scrub fuels, debates were resolved on the fire hazard of this fuel complex and the placement of fuel breaks.

Another use of BEHAVE's predictive capabilities is in the planning for the prescribed burning of an area. This technique of fuel management is the application of fire to a forest or other wildland area, under a specific range of weather conditions, in order to achieve specific management objectives (Mobley, Jackson, Balmer, Ruziska, & Hough, 1973). Prescribed fires can be used to reduce hazardous fuel accumulations, improve

wildlife habitat, prepare a site for planting or seeding, control disease, enhance the appearance of an area, etc. Such land management procedures have not been utilized extensively in regions of the northeastern United States.

This thesis will use the data obtained from prescribed burns conducted at Cape Cod National Seashore in Massachusetts to evaluate the effectiveness of BEHAVE in predicting fire behavior in the pine - oak forest fuel complex. The structure of the thesis will include an overview of the theoretical and experimental basis of BEHAVE, including a discussion of the mechanisms by which a fire spreads and how these are mathematically represented within the fire prediction model. A description of BEHAVE itself follows, including the necessary input parameters required to obtain fire predictions. This leads to a description of the fuel complex under analysis and how it fits into the theoretical assumptions of BEHAVE.

The fuel and fire prediction models within BEHAVE will be analyzed next. Site-specific fuel models for several experimental plots will be constructed. The fire behavior predictions for the fuel models will be compared with observations of fire behavior during the prescribed burns. After developing initial conclusions about BEHAVE's predictions based on these comparisons, a more in-depth analysis will be performed on the fire prediction model. This analysis will include an evaluation of how each parameter affects the outcome of fire behavior predictions, and the effectiveness of the data collection techniques used to obtain these parameters. An understanding of the strengths and weaknesses of BEHAVE will be obtained from this analysis along with suggestions for improving the outcome of fire behavior predictions. The thesis will conclude with a

discussion of an alternative, simple model of fire spread based on quantitative measures of the unique burning characteristics of the fuel components. Suggestions for future work will also be made.

2. Background

2.1 Fire Spread Mechanisms

Figure 2.1 provides an illustration of the different potential components of a fuel complex. The lowest component above the soil is a layer of dead and decomposing fuel particles called the duff layer. This layer can support a smoldering fire for long periods of time, although it will not usually contribute to the active flaming front. Typically, surface fires will spread through the next layer of fuels, composed of grass or litter (freshly fallen leaves, needles, and other debris). Above the litter is an intermediate layer of fuel, varying in compactness and height and composed of slash fuels (produced by logging, etc.) and shrubs, or "ladder" fuels. This layer is marked by dead branches, live fuels or other accumulations which can provide continuous fuels from the lower layers to the overstory. The fire behavior within these intermediate layers will vary depending on the characteristics of the species, climate of the region and other variables. The overstory, or top layer, is usually marked by trees which can vary in compactness from an open stand (sparsely populated trees) to a closed stand (densely populated trees). Surface fires will not usually involve the overstory, although the trees can become scorched, damaged or killed under conditions of large flame lengths or extended exposure to high fire temperatures. When the overstory is ignited, it can support a crown fire where the fire moves through the tree canopy, sometimes independent of the surface fire below.

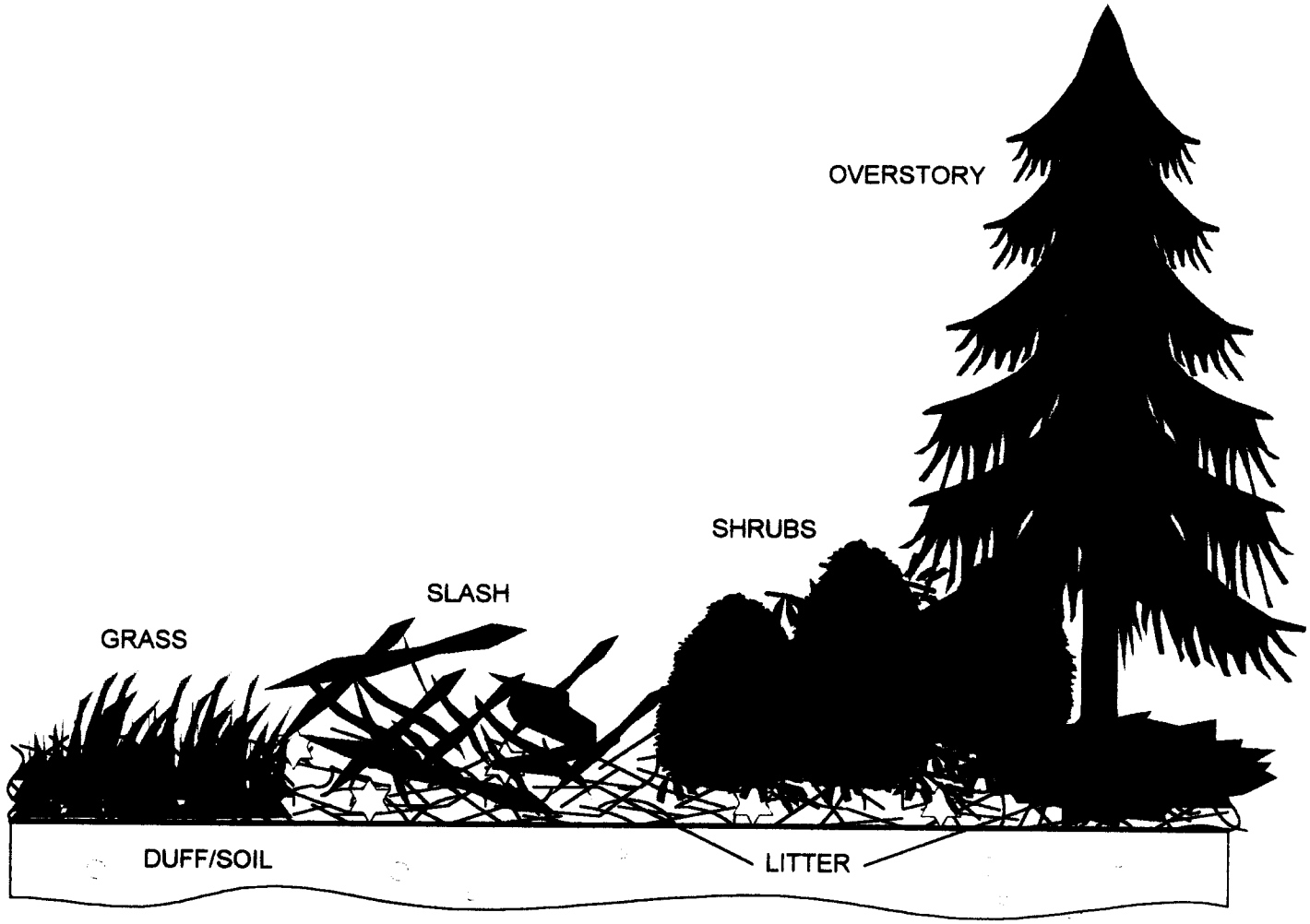

Figure 2.1: Components of a fuel complex.

Fires spreading through wildland fuels are typically modeled as following an elliptical pattern of spread that is altered by topography, wind and varying fuel types (Anderson, 1983). Figure 2.2 gives an illustration of the basic components of a spreading fire. The portion of a fire spreading in the direction of the wind is considered a head fire, and is usually the portion at the highest level of fire behavior (flame lengths and spread rates). With varying topography and wind conditions, the fire may spread aggressively in varying directions causing several independent head fires, or converging fire fronts. A fire spreading perpendicular to the wind direction, or along the sides of a fire, is called a flank fire and is usually of intermediate fire behavior. Fires spreading against the wind are backing fires and typically have the lowest level of fire behavior.

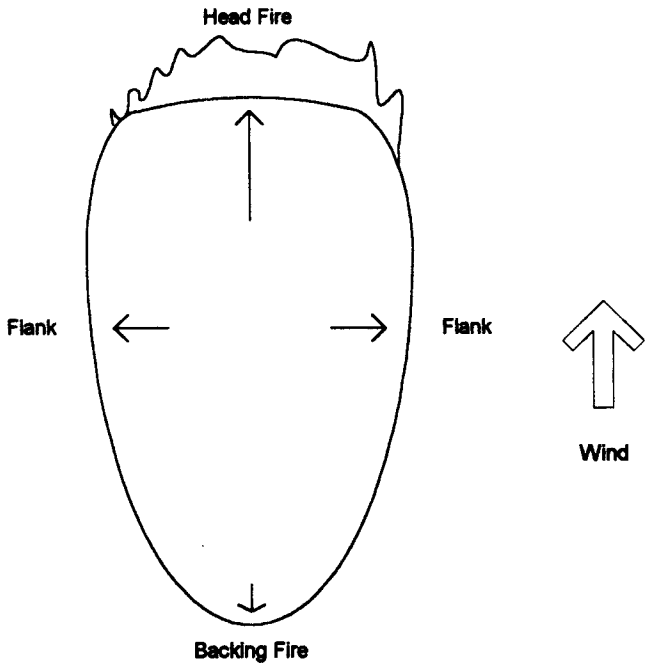

Figure 2.2: Components of a spreading fire.

The spread of fire through wildland fuels can be viewed as a series of ignitions (Fons, 1946) where the fire front, or flaming zone, moves through a fuel bed heating the potential fuel ahead. As this fuel is heated, its moisture content at the surface decreases as the water is evaporated. The surface of the potential fuel eventually becomes sufficiently hot to undergo the process of pyrolysis, or thermal degradation of solids to produce char and combustible gases (Kanury, 1995). This gas-air mixture is then ignited by the advancing flames and the fuel becomes part of the flaming zone.

Figure 2.3 represents a fire spreading through a porous fuel bed, of constant depth, toward a unit volume of potential fuel. This unit volume is the smallest volume that retains the characteristics of the fuel bed (Frandsen, 1971). As the potential fuel approaches the flaming zone, it is heated by the mechanisms of radiation and convection from both the flames above the fuel and from the flames within the fuel bed itself. Because the majority of the heat rises, the contribution of convective heating from the flames above the fuel is small under no-wind, no-slope conditions. However, when the addition of wind or slope (Figures 2.4 and 2.5, respectively) causes the flames to be bent over the potential fuel, heat transfer from this flaming region becomes more significant, as the fuel is exposed to more convection, radiation and direct flame contact (Rothermel, 1972).

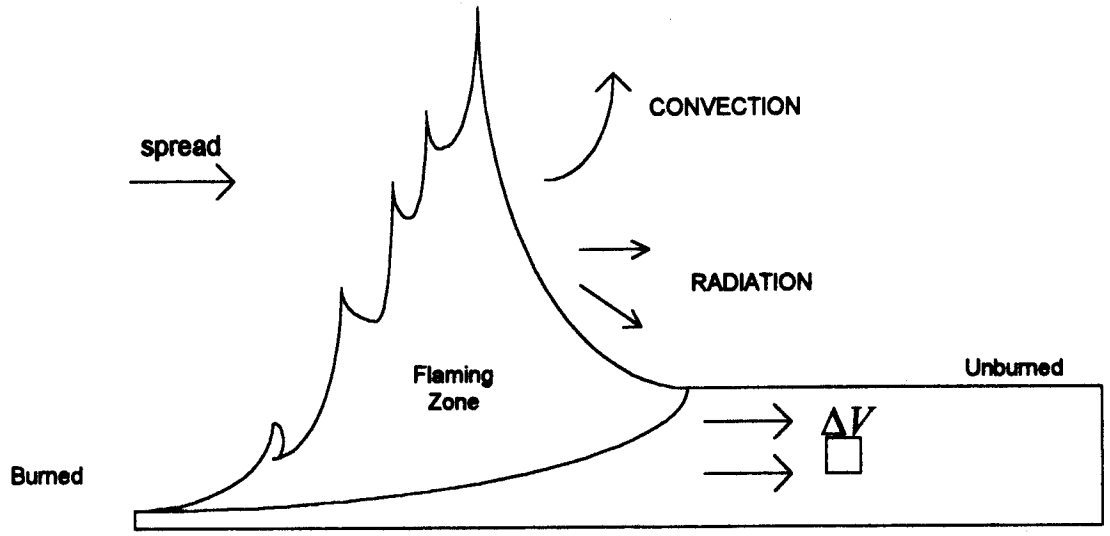

Figure 2.3: Characterization of a flame front moving through a fuel bed under no wind, no slope conditions.

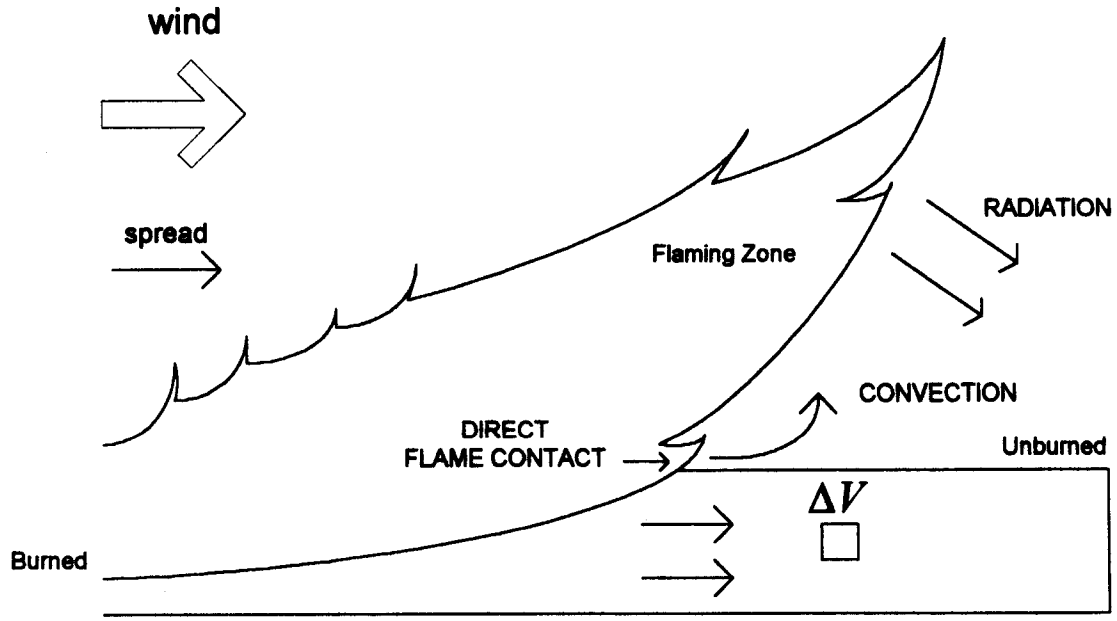

Figure 2.4: Characterization of a flame front moving through a fuel bed under wind conditions.

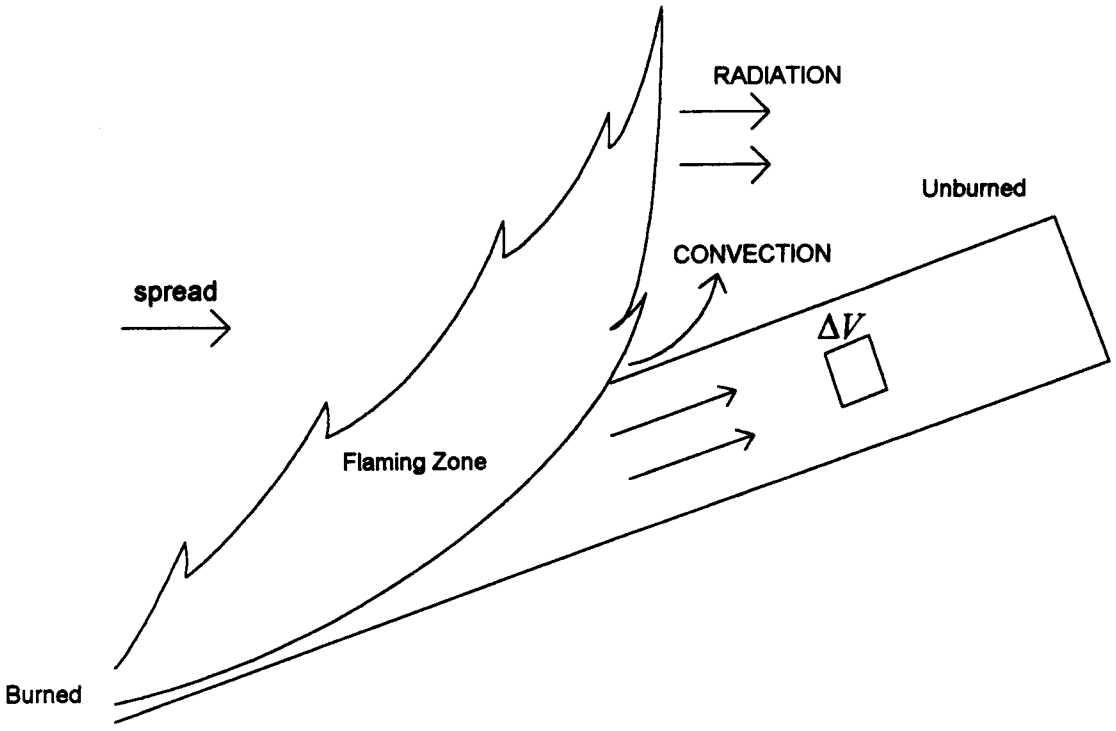

Figure 2.5: Characterization of a flame front moving through a fuel bed under upslope conditions.

2.2 A Mathematical Model for Fire Spread

Frandsen (1971) developed a theoretical rate of spread equation for a fire burning through a porous, homogeneous fuel bed of constant depth. This was accomplished by applying the conservation of energy principle to a unit volume of fuel lying within the fuel bed and ahead of the advancing flaming zone. Figure 2.6 shows the vector sum of all heat fluxes, $\bar{I}$, and the net heat absorbed per unit volume, $\rho_{be}Q_{ig}$, as the unit volume, ΔV, approaches the fixed combustion zone interface (Frandsen, 1971). The coordinate system is defined with the x-axis horizontal, the z-axis vertical and the y-axis parallel to the fire front (out of the page in Figure 2.6).

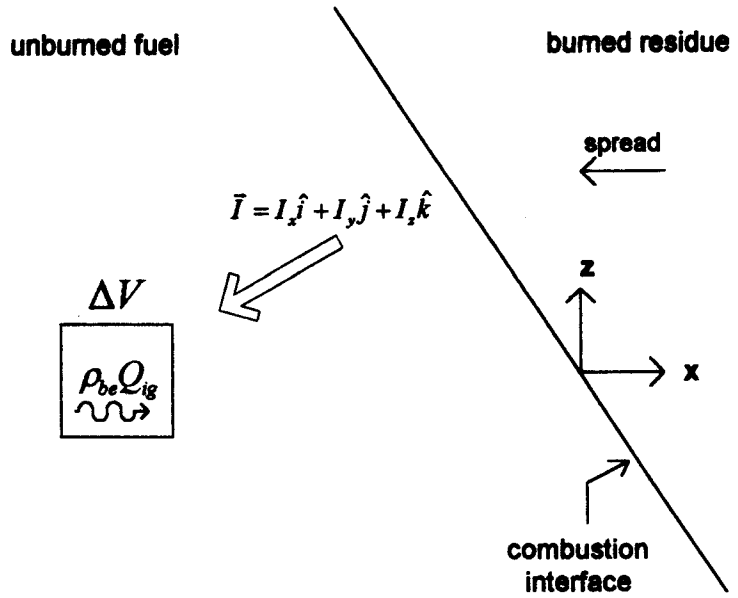

Figure 2.6: Energy balance applied to a unit volume of fuel ahead of the advancing flame front.

Both the horizontal and vertical components of the heat flux incident on the unit volume were considered, although only for heating within the fuel bed itself. Heat transfer from the flames above the fuel was not included explicitly. The flame front is assumed to be sufficiently wide to discount the heat transfer in the y-direction due to symmetry. The theoretical rate of spread equation was written as:

$$R = \frac{I_{xig} + \int_{-\infty}^{0} \left(\frac{a_z}{\hat{a}}\right)_{z_c} dx}{\rho_{be} Q_{ig}} \text{ [ft/min]}, \qquad (2.1)$$

where:

R = quasi-steady rate of spread [ft/min],

I_{xig} = horizontal heat flux absorbed by the unit volume of fuel at the time of ignition [btu/ft^2-min],

ρ_{be} = effective bulk density (amount of fuel per unit volume of the fuel bed raised to ignition ahead of the advancing fire) [lb/ft^3],

Q_{ig} = heat of preignition (heat required to bring a unit weight of fuel to ignition) [Btu/lb],

$\left(\frac{\partial I_z}{\partial z}\right)_{z_c}$ = gradient of the vertical heat flux at a constant depth z_c [btu/ft^3-min].

(∂ denotes the partial derivative)

Equation 2.1 is viewed as the ratio of the heat flux received from the flaming zone to the heat required to ignite the potential volume of fuel, or $I_p/\rho_{be}Q_{ig}$, where I_p is the propagating flux (Frandsen, 1971; Rothermel, 1972). The assumption of a quasi-steady rate of spread is valid when all fuel and environmental conditions are held constant.

Rothermel (1972) developed experimental and analytical methods of evaluation to provide an approximate solution to equation 2.1 in terms of measurable fuel and environmental properties. This was brought about by the introduction of several new terms and correlations based primarily on experimental data. The final form of the spread equation is:

$$R = \frac{I_R \xi (1 + \phi_w + \phi_s)}{\rho_b \varepsilon Q_{ig}} \text{ [ft / min]}, \tag{2.2}$$

where:

I_R = Reaction Intensity [Btu/ft^2-min],

ξ = Propagating Flux Ratio, 0 to 1,

ϕ_w = Wind Coefficient, 0 to 1,

ϕ_s = Slope Coefficient, 0 to 1,

ρ_b = Oven-dry Bulk Density [lb/ft^3],

ε = Effective Heating Number, 0 to 1.

Equation 2.2 is used to predict the spread of fires and different measures of intensity within the flaming zone. The residual burning of fuels after the flame front has passed, however, is not accounted for.

As in equation 2.1, the numerator of equation 2.2 is the driving force of the fire and is defined as the propagating flux, I_p, or the proportion of the total heat release rate per unit area that is received by the potential fuel ahead of the flame front. In order to evaluate this quantity, it is assumed that the propagating flux under no-wind, no-slope conditions, $(I_p)_o$, is proportional to the reaction intensity, I_R, or the heat release rate per unit area of the fire front (Rothermel, 1972). The proportionality constant is ξ, or the fraction of the total heat release rate that is actually received by the potential fuel. The no-

wind, no-slope propagating flux is written as $(I_p)_o = \xi I_R$. Additional heat transfer, from the flames above the fuel, by convection, radiation, and direct flame contact, due to increases in wind and slope, is accounted for through the wind and slope coefficients, respectively.

The source of the no-wind, no-slope propagating flux is the reaction intensity, I_R, and can be written as:

$$I_R = -\frac{dw}{dt} h \ [\text{Btu} / \text{ft}^2 \text{ - min}], \tag{2.3}$$

where:

h = heat content of fuel [Btu/lb],

$\frac{dw}{dt}$ = mass loss rate per unit area of the fire front [lb/ft^2-min].

The heat content, or heat of combustion, is a chemical property of the fuel, defined as the total amount of heat released when a unit mass of fuel is oxidized completely (Drysdale, 1985).

In order to estimate the mass loss rate term of equation 2.3, several new terms are introduced to produce the final relation:

$$I_R = w_n h \Gamma' \eta_M \eta_s = w_n h \Gamma, \tag{2.4}$$

where:

w_n = net fuel loading [lb/ft^2],

Γ' = potential reaction velocity [min^{-1}],

η_M = moisture damping coefficient, 1 to 0,

η_s = mineral damping coefficient, 1 to 0,

Γ = reaction velocity [min^{-1}].

The product of $\Gamma'\eta_M\eta_s$ is the reaction velocity, Γ, and represents the completeness and rate of fuel consumption. It is defined as,

$$\Gamma = \frac{\eta_\delta}{\tau_R} \ [\text{min}^{-1}], \tag{2.5}$$

or the ratio of the reaction zone efficiency, η_δ, to the time for the fire front to travel the depth of one flaming zone (reaction time),τ_R. The reaction velocity is dependent on the properties, size and arrangement of fuel particles in the fuel bed.

In the denominator of equation 2.2, the effective bulk density term of equation 2.1 is written in terms of a measurable oven-dry bulk density, ρ_b, and an effective heating number, ε. The oven-dry bulk density is,

$$\rho_b = w_o/\delta \ [\text{lb/ft}^3], \tag{2.6}$$

where w_o is the oven-dry, or no-moisture, fuel loading, and δ is the fuel bed depth. The oven-dry fuel loading is related to the net fuel loading by the relation (Albini, 1976a),

$$w_n = w_o(1-S_T) \approx w_o \ [lb/ft^2], \tag{2.7}$$

where S_T (approximated as 0.0555) is the fuel particle total mineral content (Burgan & Rothermel, 1984). The effective heating number is the fraction of a fuel particle that must be heated for ignition and increases as the fuel diameter becomes smaller. Thus, the product of the oven-dry bulk density and the effective heating number indicates the weight of fuel, per cubic foot, which must be heated to the ignition temperature. The heat of preignition, Q_{ig}, is the amount of heat required to ignite this fuel, per unit weight (Burgan & Rothermel, 1984). The effective heating number and the heat of preignition are written as (Rothermel, 1972):

$$\varepsilon = \exp(-138/\sigma). \tag{2.8}$$

$$Q_{ig} = 250 + 1{,}116M_f. \tag{2.9}$$

where σ is the surface-area-to-volume (S/V) ratio, or fuel particle size, and M_f is the fuel moisture content expressed as a percentage of the oven-dry weight.

Substituting equations 2.4 and 2.6 - 2.9 into equation 2.2, we have,

$$R \approx \frac{h\Gamma' \eta_M \eta_s \delta \xi (1 + \phi_w + \phi_s)}{[\exp(-138/\sigma)][250 + 1{,}116 M_f]} \quad [\text{ft/min}]. \tag{2.10}$$

Equation 2.10 represents an approximate rate of spread equation. Several empirical correlations were derived from small-scale laboratory experiments in order to express the variables in terms of measurable parameters.

2.2.1 Experimental Methods

A series of tests were conducted involving the construction of small-scale fuel beds composed of either wood excelsior (fine fuels), ¼" sticks, or ½" sticks (Rothermel, 1972; Rothermel & Anderson, 1966). These fuel beds represent a homogeneous fuel array of constant depth and were constructed in either a wood crib fashion, as a series of tripods, or in a uniformly packed bed of excelsior (Fons, Bruce, & Pong, 1959; Rothermel 1972). Fuel beds in the reaction velocity experiments were approximately 3 ft wide, 5-to-8 ft long, and 4-to-6 inches deep. The parameters varied in the experiments were the surface-area-to-volume ratio, σ, and the fuel bed packing ratio, β. The packing ratio of a fuel bed is defined as the ratio of the oven-dry bulk density to the oven-dry particle density, $\beta = \rho_b/\rho_p$, and was varied by altering the depth and loading of the excelsior, or the space between sticks in the wood crib and tripod arrays. A load cell, or weighting platform, was also utilized in order to measure the mass loss rate and reaction time, as the quasi-steady fires burned through the fuel beds.

The reaction velocity, Γ, was experimentally determined by evaluating the reaction zone efficiency in equation 2.5 as $\eta_\delta = \dot{m}_e/(w_n R P_w)$, where $\dot{m}_e$ is the experimentally determined mass loss rate, and P_w is the width of the weighting platform used in the experiments. The potential reaction velocity, Γ', was determined by dividing the experimentally determined Γ by η_M and η_s in order to separate Γ from the effects of the moisture and minerals of the fuels that were used in the experiments (Rothermel, 1972). This allowed Γ' to be correlated only to the physical features of the fuel array.

From these experiments, it was found that there exists an optimum packing ratio, β_{op}, where an ideal balance between fuel and air is achieved, providing maximum burning conditions. The important parameters were determined to be σ, β, β_{op}, and the ratio β/β_{op}, which is a measure of how close the fuel bed is to its optimum packing ratio. The variables ε, β_{op}, Γ', ξ, ϕ_w, and ϕ_s are all directly correlated to combinations of these parameters, as shown in equations 2.11 to 2.15.

$$\beta_{op} = 3.348\sigma^{-.8189}, \tag{2.11}$$

$$\Gamma' = \Gamma'_{max}(\beta/\beta_{op})^A \exp[A(1-\beta/\beta_{op})] \ [\text{min}^{-1}], \tag{2.12a}$$

$$\Gamma'_{max} = \sigma^{1.5}(495+.0594\sigma^{1.5})^{-1} \ [\text{min}^{-1}], \tag{2.12b}$$

$$A = 133\sigma^{-0.7913} \ \text{(Albini, 1976a)}, \tag{2.12c}$$

$$\xi = (192+0.2595\sigma)^{-1}\exp[(0.792+0.6811\sigma^{.5})(\beta+0.1)], \tag{2.13}$$

$$\phi_w = CU^B\left(\frac{\beta}{\beta_{op}}\right)^{-E}, \tag{2.14a}$$

$$C = 7.47\exp(-0.133\sigma^{.55}), \tag{2.14b}$$

$$B = 0.02526\sigma^{.54}, \quad (2.14c)$$

$$E = 0.715\exp(-3.59x10^{-4}\sigma), \quad (2.14d)$$

U = midflame windspeed [ft / min],

$$\phi_s = 5.275\beta^{-.3}(\tan\phi)^2, \quad (2.15)$$

$\tan\phi$ = slope.

2.2.2 Modeling Fire Spread through Actual Fuel Beds

The above equations were derived under the assumption that a fire is spreading through a homogeneous fuel bed with constant properties and under constant environmental conditions. Actual forests, grasslands and shrub fields, however, are often composed of several different fuel components, particle sizes and arrangements. It was assumed that these variations within a fuel complex could be accounted for by grouping the fuel into categories according to similar properties, such as size class, living fuels and dead fuels (Rothermel, 1972). This concept was then incorporated into the development of fuel models, which numerically represent each component of a fuel complex - litter, grass, shrubs and slash - by size class, fuel load, and fuel properties. These fuel models provide the necessary input parameters to the fire spread equations and will be discussed later in this chapter.

A weighting procedure was developed in order to account for the variations in fuel parameters and condense them into values which represent the entire fuel complex (Burgan & Rothermel, 1984; Rothermel, 1972). This procedure is based on the assumption that heat transfer, moisture evaporation and other combustion processes all occur through the surface of fuels (Rothermel, 1972). Fine fuels (0-.25 inch diameter)

have the highest surface-area-to-volume ratios, react the fastest to these processes and are the primary carrier of the fire. The majority of the weighting procedure, then, is based on a measure of the amount of surface area that is contributed by each fuel size class and category.

There are two categories of fuels, dead and live, within a fuel complex. The dead fuels are divided into three size classes based on a corresponding timelag class, or the theoretical time required for a fuel particle to lose approximately 2/3 of the initial moisture content above equilibrium (Fosberg & Schroeder, 1971). Equilibrium moisture content is the moisture content a fuel particle would obtain if left in a steady-state environment long enough to obtain equilibrium (Bradshaw et al., 1984). The timelag and corresponding size classes are as follows:

- 1-hour: 0 - .25 inch,
- 10-hour: .25 - 1 inch,
- 100-hour: 1 - 3 inch.

Live fuels include the live herbaceous, hb (grasses, ferns) and live woody, wd (leaves, 0 - .25 inch diameter twigs) classes.

Dimensionless weighting factors, f_k, represent the contribution of each size class and category. The weighting factors are defined as (Burgan & Rothermel, 1984):

$$f_{1\text{-hr}} = A_{1\text{-hr}}/A_{dead}, \tag{2.16a}$$

$$f_{10\text{-hr}} = A_{10\text{-hr}}/A_{dead}, \tag{2.16b}$$

$$f_{100\text{-hr}} = A_{100\text{-hr}}/A_{dead}, \tag{2.16c}$$

$$f_{hb} = A_{hb}/A_{live}, \tag{2.16d}$$

$$f_{wd} = A_{wd}/A_{live}, \tag{2.16e}$$

$$f_{dead} = A_{dead}/(A_{dead} + A_{live}), \tag{2.16f}$$

$$f_{live} = A_{live}/(A_{dead} + A_{live}), \tag{2.16g}$$

where the dimensionless $A_{1\text{-}hr}, \ldots, A_{wd}$ in equations 2.16a-e are based on the mean values of oven-dry fuel loading, surface-area-to-volume ratio and oven-dry particle density of that size class:

$$A_j = [(\sigma)_j\ (w_j)]/(\rho_p)_j. \tag{2.17}$$

Then, $A_{dead} = A_{1\text{-}hr} + A_{10\text{-}hr} + A_{100\text{-}hr}$ and $A_{live} = A_{hb} + A_{wd}$.

From the above weighting factors, characteristic values of each input parameter used to evaluate the fire spread equations are determined. For instance, the weighted heat content of a fuel complex is,

$$h_{complex} = f_{dead}h_{dead} + f_{hb}h_{hb} + f_{wd}h_{wd}\ \ [\text{Btu/lb}]. \tag{2.18}$$

A slightly different method is used to calculate the mean fuel bed depth for the fuel complex. Here, the depth of each of the i = 1 to 4 fuel components (grass, litter, shrubs, slash) is weighted by the ratio of the oven-dry load of each component, $(w_o)_i$, to the total oven-dry load, $(w_o)_T$. That is,

$$\delta_{complex} = \sum_{i=1}^{4} \delta_i (w_o)_i / (w_o)_T \quad [\text{ft}]. \tag{2.19}$$

The reaction intensity, equation 2.4, becomes (Albini, 1976a):

$$I_R = \Gamma' \sum_{i=1}^{4} (\tilde{w}_n)_i (\tilde{h}_i)(\tilde{\eta}_s)_i (\tilde{\eta}_M)_i \quad [\text{Btu} / \text{ft}^2 / \text{min}]. \tag{2.20}$$

where the ~ denotes the weighted, characteristic parameters for each of the fuel components. The potential reaction velocity, Γ', is similarly calculated by substituting characteristic values of S/V ratio and a mean value of packing ratio into equations 2.11 and 2.12a - 2.12c. Each of the characteristic parameters is then substituted into equation 2.2 in order to calculate the rate of fire spread through a fuel complex.

2.3 BEHAVE: Fire Behavior Prediction and Fuel Modeling System

2.3.1 Overview

BEHAVE incorporates the mathematical model of fire spread developed by Rothermel (1972) and given by the equations in section 2.2, along with previously indicated revisions by Albini (1976a, 1976b), into a set of computer programs for use in wildfire suppression, prescribed burn planning, fire reconstruction, or other land management needs (Andrews & Chase, 1989; Andrews, 1986; Burgan & Rothermel, 1984). The programs run in an MS-DOS environment, and are relatively easy to use.

Figure 2.7 shows the structure of the BEHAVE system, along with a brief description of each of the programs and modules (Andrews, 1986).

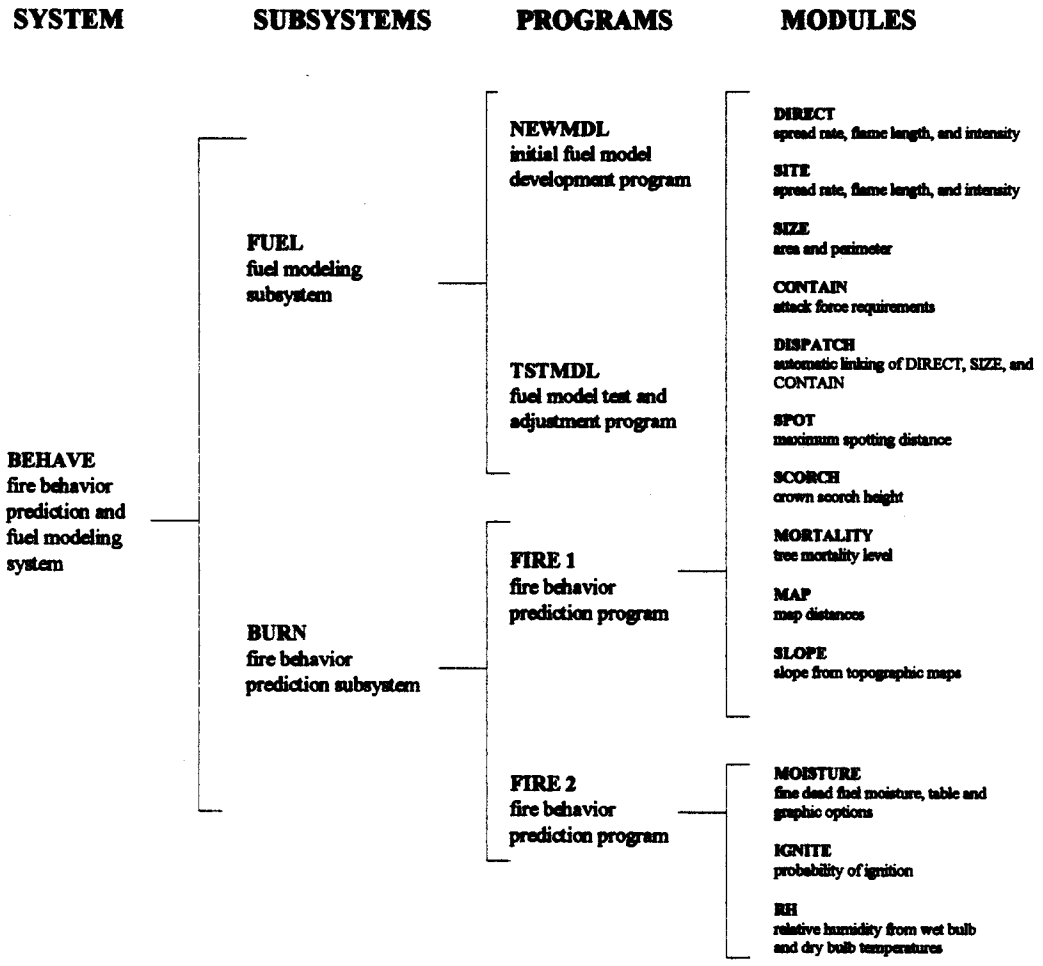

Figure 2.7: BEHAVE system structure.

The programs predict the spread and different measures of intensity of fires burning in a quasi-steady state, independent of the source of ignition, and spreading in an elliptical pattern (Andrews, 1986). Only fires burning in surface fuels, within about 6 feet

of and contiguous to the ground, are modeled. The system is not applicable to ground (duff) fires, crown fires, or other severe fire conditions such as a 'blow-up' or firestorm situation. All fuel properties, wind, and slope conditions are assumed to be constant throughout the prediction time.

The major fire behavior parameters predicted by BEHAVE are the rate of spread, reaction intensity, heat per unit area, fireline intensity and flame length, each of which is measured within the flaming zone. The rate of spread and reaction intensity (equations 2.2 and 2.4, respectively) come directly from Rothermel's mathematical model of fire spread, as discussed in section 2.2. The heat per unit area (equation 2.21) is defined as the heat released from a square foot of fuel while the flaming zone is in that area. Fireline intensity (equation 2.22) is the heat released per second from a foot-wide section of fuel extending from the front to the rear of the flaming zone. Flame length (equation 2.23) is written in terms of fireline intensity. The following are the equations used by BEHAVE to predict these parameters (Andrews, 1986):

Rate of Spread

$$R = \frac{I_R \xi (1 + \phi_w + \phi_s)}{\rho_b \varepsilon Q_{ig}} \quad \text{[Chains/hr, 1 Chain = 66 Feet]} \tag{2.2}$$

Reaction Intensity

$$I_R = w_n h \Gamma' \eta_M \eta_s \quad \text{[Btu/ft}^2\text{/min]}, \tag{2.4}$$

Heat Per Unit Area

$$H_A = I_R \bullet t_r \ [Btu/ft^2], \tag{2.21}$$

t_r = flame residence time [min],

Fireline Intensity

$$I_B = (I_R \bullet R \bullet t_r)/60 \ [Btu/ft/s], \tag{2.22}$$

Flame Length

$$F_L = 0.45 I_B^{0.46} \ [ft]. \tag{2.23}$$

2.3.2 Fuel Models

BEHAVE incorporates the use of fuel models to represent a particular fuel complex and provide the necessary input parameters to the fire behavior equations. These models were developed as a substitute to on-the-spot sampling of fuel input parameters, during or before a prescribed burn or wildfire, which can be time-consuming and costly (Rothermel, 1972). Land managers can choose a fuel model that closely fits the vegetation of interest, by either using one of the 13 standard fuel models, or by creating a custom fuel model through the FUELS subsystem of BEHAVE.

Currently, there are 13 Northern Forest Fire Laboratory (NFFL) fuel models developed for input to the BEHAVE system, see Table 2.1 (Andrews, 1986). Each represents typical fuel complexes found in North America. These are also being referred to as the Fire Behavior Prediction System (FBPS) fuel models (W. A. Patterson III, personal communication, 1996).

Table 2.1: The 13 NFFL fuel models.

Fuel Model	*Typical Fuel Complex*
	Grass and Grass Dominated
1	Short grass
2	Timber (grass and understory)
3	Tall Grass
	Chaparral and Shrub Fields
4	Chaparral (6ft)
5	Brush (2ft)
6	Dormant brush, hardwood slash
7	Southern rough
	Timber Litter
8	Closed timber litter
9	Hardwood litter
10	Timber (litter and understory)
	Slash
11	Light logging slash
12	Medium logging slash
13	Heavy logging slash

Fuel models represent a particular fuel complex through such parameters as fuel loading, surface-area-to-volume ratio, fuel bed depth, heat content and moisture of extinction. The moisture of extinction is defined as the upper limit of dead fuel moisture content beyond which the fire will no longer spread with a uniform front (Rothermel, 1983). If fuel moistures exceed this value, they will no longer contribute to the spreading fire, and predicted fire behavior may reach zero. This parameter is calculated by the

program and is based on experimental data obtained by measuring the moisture of extinction at various packing ratios for the 13 NFFL fuel models (Burgan & Rothermel, 1984). From these data, it was determined that the moistures of extinction for dead litter, grass, and slash components behave according to the relationship $M_{x,cp} = 100(0.12 + 4.8\beta_{cp})$, where $M_{x,cp}$ is the component moisture of extinction, and β_{cp} is the component packing ratio. For the dead shrub components, $M_{x,cp} = 0.35$ for shrubs with leaves that contain oils and waxes and $M_{x,cp} = 0.20$ for those that do not. Then, a similar weighting procedure is used to find the dead fuel moisture of extinction for the fuel model, M_x, as for the characteristic fuel bed depth,

$$M_{x,dead} = \sum_{i=1}^{4} M_{x,i}(w_o)_i / (w_o)_o. \tag{2.24}$$

Heat content values are chosen as 8,000 Btu/lb for each of the 13 NFFL fuel models. Some fuel factors required as input to the fire spread equations are held constant, as they have little effect on the outcome of fire behavior predictions, are reasonably similar amongst various fuel types, and/or are difficult to measure. These include the particle density, 32 lb/ft^3; total mineral content, 0.0555; effective mineral content, 0.010; 10-hr S/V ratio, 109 ft^{-1}; and 100-hr S/V ratio, 30 ft^{-1} (Burgan & Rothermel, 1984). Figure 2.8 shows the final form of a fuel model, specifically the NFFL fuel model #1, composed of short grasses up to one foot in height.

NFFL FUEL MODEL #1

LOADS, T/AC		S/V RATIOS, 1/FT		OTHER	
1 HR	0.74	1 HR	3500.	DEPTH, FT	1.00
10 HR	0.00	LIVE HERB	190.	HEAT CONTENT, BTU/LB	8000.
100 HR	0.00	LIVE WOODY	190.	EXT MOISTURE, %	12.
LIVE HERB	0.00	SIGMA	3500.	PACKING RATIO	0.00106
LIVE WOODY	0.00			PR/OPR	0.25

Figure 2.8: Final numerical values of NFFL fuel model #1

2.3.2.1 Custom Fuel Models

The FUEL subsystem of BEHAVE allows users to construct site-specific fuel models or modify the standard NFFL models by using the NEWMDL program. The fire behavior characteristics can then be tested under simulated environmental conditions with the TSTMDL program (Burgan & Rothermel, 1984). Constructing a new fuel model may be necessary when fuel conditions are not well represented by the standard NFFL models. This has been done in fuel complexes such as Southern palmetto-gallberry (Hough & Albini, 1978), California chaparral (Rothermel & Philpot, 1973), and Alaska's black spruce forests (Norum, 1982).

To develop a custom fuel model, the fuel complex is divided into four components (litter, grass, shrubs and slash), each of which is further divided into the dead fuel size classes and/or live fuel classes. The litter, shrub and slash components can contain 1-, 10- and 100-hr fuels. Shrubs can also include additional live herbaceous and woody fuels. The grass component can contain 1-hr and/or live herbaceous fuels. The fuel loading, depth and percent coverage are entered into the program NEWMDL for each of the

relevant fuel components in the area of interest. Both the fuel load and depth estimates are adjusted depending on the percent coverage of each component. For the live grass fuels, the model also allows users to construct a dynamic model, which accounts for the drying of the grasses through the season (Andrews, 1986). This is done by transferring a fraction of the live herbaceous fuel load to the 1-hour dead fuel load, for live fuel moistures between 30 and 120%.

The 1-hour dead, live herbaceous and live woody surface-area-to-volume ratios must also be estimated for each of the appropriate components. Values can range from 192 ft^{-1} for course fuels to 3,500 ft^{-1} for fine fuels. Heat content values are also required for the dead and live fuel categories and can range from 7,000 to 12,000 Btu/lb. Lower heat contents are suggested by the program for fuels of low volatility, such as solid wood, grasses and hardwood leaves, and higher values are suggested for fuels which are highly volatile, such as those that contain oils and waxes (Burgan & Rothermel, 1984). As discussed earlier, moisture of extinction values are provided by the program, although they can be manipulated between 10 and 60% by the user.

2.3.3 Inputs/Outputs of the Fire Prediction Model

The DIRECT module of the FIRE 1 program is the main source for fire behavior predictions within BEHAVE. The following are its input and output parameters (Andrews & Chase, 1989):

Table 2.2: Input/output parameters of the DIRECT module of BEHAVE.

Input	Output
Fuel model	Rate of Spread, ch/h
1-hr fuel moisture, %	Heat per unit area, Btu/ft^2
10-hr fuel moisture, %	Fireline intensity, Btu/ft/s
100-hr fuel moisture, %	Flame length, ft
Live herbaceous moisture, %	Reaction intensity, Btu/ft^2/min
Live woody moisture, %	Effective windspeed, mi/h
Midflame windspeed, mi/h	Direction of maximum spread
Slope, %	
Direction of wind vector	
Direction for spread calculations	

The input parameters include the fuel model which supplies the physical and chemical characteristics of the fuel bed and several environmental parameters which represent the weather conditions and topography during the proposed time of burning. The temperature and relative humidity are represented by the dead fuel moisture contents, while the live fuel moisture contents depend on the stage of plant development, time of year, extent of drought, and other complex, species-dependent processes. The midflame windspeed corresponds to the windspeed at a height above the surface fuel equivalent to the mid-level height of flames (Rothermel, 1983). The DIRECT module allows users to indicate the slope of the terrain, the direction of the wind with respect to the slope and the direction for spread predictions.

The DIRECT module predicts each of the fire behavior parameters of equations 2.2, 2.4 and 2.21 to 2.23. Predictions can be obtained for head, flanking or backing fires depending on the slope and wind conditions indicated. Equation 2.2 recognizes the contribution of both the slope and wind effects on the rate of spread, although interactions between them are not recognized (Burgan & Rothermel, 1984). The effective windspeed

in Table 2.2 depends on the midflame windspeed, slope and fuel model, and gives an indication of the relative effects of different combinations of wind and slope on predictions (Andrews, 1986).

3. Pine - Oak Forests

The fuel complex under study is the northeastern pine - oak forest with a flammable shrub understory, see Appendix A, located from the mid-Atlantic coast north through central New England. This fuel complex is of particular interest as it and similar fuel complexes in the Northeast are incorporated into extensive prescribed burn plans for the purposes of fuel reduction, species regeneration and education. Several plots containing the pine - oak forests with a huckleberry shrub understory have been studied as part of a joint effort between members of the Cape Cod National Seashore and the Department of Forestry and Wildlife Management at the University of Massachusetts at Amherst (Crary, 1987). The purpose of this 10-year study is to examine the effects of fire on the various species within the complex, and obtain data for fuel modeling and fire behavior prediction purposes (W. A. Patterson III, personal communication, 1995). This thesis will focus on the fuel complex located in the Lombard/Paradise Hollow area at the tip of Cape Cod in Truro, Massachusetts. Variations of this fuel complex are located in other areas throughout the Northeast, including scrub oak barrens with a scattered pitch pine overstory in central Massachusetts, and grass/huckleberry fields found on islands off of Cape Cod, including Martha's Vineyard and Nantucket.

3.1 Description

The pine - oak forest is characterized by three of the dominant fuel components shown in Figure 2.1. The bottom litter component, usually ranging from one to six inches

in depth, is composed primarily of oak and shrub leaves along with some pine needles, with close to 100% ground coverage. The intermediate, shrub component is dominated by huckleberry (Gaylussacia baccata), along with additional shrubs including blueberry (Vaccinium vacillans and V. angustifolum), and wintergreen (Gaultheria procumbans). The huckleberry can reach heights of 4 to 6 feet, and the total shrub component usually has about 65-70% ground coverage. The overstory is composed of white and black oak (Quercus alba and Q. velutina), and pitch pine (Pinus rigida). Overstory heights average between 30 to 50 feet, with approximately 80% canopy closure. The plots in the Cape Cod area also contain a small amount of scrub oak (Quercus ilicifolia), with cover of about 5% and heights up to 6 feet.

It is appropriate to utilize this fuel complex as a means of validating the mathematical model developed by Rothermel (1972) and incorporated into BEHAVE. The litter and shrub fuel components fit within the porous fuel bed assumptions of the model and are generally continuous. Shrub heights are under six feet tall and contiguous to the ground, and observed fire behavior tends to exhibit the "series of ignitions" assumption that is the basis of the spread equations (Frandsen, 1971).

The pitch pine and oak overstory can also contribute to the overall fire behavior under extreme conditions, however the model will not adequately predict the behavior of fires spreading from the surface fuels vertically to the overstory. The information can, however, be used to predict the possibility of overstory scorching from a surface fire, which may lead to a crown fire or the torching of individual trees.

3.2 Fire Behavior

Appendix B establishes general guidelines which help quantify and classify various hazard levels of fire behavior. This provides a practical method of indicating significant changes in fire behavior and portraying the relative fire danger of a particular fuel complex. Throughout this analysis, the primary fire behavior characteristics of interest will be the spread rate and flame length. These are the most visible characteristics of a fire, and often dictate the necessary actions for suppression and control efforts. Tables 3.1 (Andrews, 1986; National Wildfire Coordinating Group, 1989; Rothermel, 1983) and 3.2 (developed in Appendix B) give general interpretations of the various hazard levels of flame lengths and spread rates, respectively.

Table 3.1: Fire suppression interpretations of flame lengths.

Flame Length (ft)	Interpretations
<4	Fire can generally be attacked at the head or flanks by persons using handtools. Hand line should hold the fire.
4-8	Fires are too intense for direct attack on the head by persons using handtools. Handline cannot be relied on to hold the fire. Effective equipment: dozers, pumpers, retardant aircraft.
8-11	Fires may present serious control problems - torching, crowning, and spotting. Control efforts at the fire head will probably by ineffective.
>11	Crowning, spotting, and major fire runs are probable. Control efforts at the head of the fire are ineffective.

Table 3.2: Fire suppression interpretations of spread rates.

Spread Rate, ft/min	Interpretations
< 5	Very slow rate of spread. Corresponds to average 20-person crew line production rate in short brush over an extended period.
5-30	Range of spread rates that can be handled by average 20-person crew doing fast line construction on an initial attack. Lower values correspond to line production rates in short brush (fuel model 5). Higher values for litter/timber fuels (fuel model 9).
30-100	Dozer and tractor-plow fireline production rates. Production rates are generally faster in shrub fuels than timber.
100-260	Walking speeds of firefighters moving away from the fire.
260-530	Jogging speeds of firefighters moving away from the fire.
530+	Estimated speeds in extreme wildfire conditions. Firefighters would have to run from the head of the fire.

The primary focus of the fuel modeling and fire behavior prediction analysis is the litter and shrub components of the pine - oak forests. A description of fire spread through this understory depends a great deal on the season in which it is burned. A distinction is made between the dormant season (fall, winter, and early spring) and the growing season (spring, summer). The major distinguishing factors between these two seasons are the variations in live fuel moisture contents and the presence of leaves on the live fuels during the growing season.

3.2.1 Dormant Season Fire Behavior

The primary means of fire spread in this fuel complex is through fuel in the litter and shrub components. The litter layer is readily ignitable and will sustain a spreading fire under most conditions. This layer of fuels is largely consumed during a fire, and has been observed to produce flame lengths in the range of 1 to 2 feet. This often produces a sufficient exposure to the intermediate layer of shrubs, and in particular the huckleberry, to cause ignition.

During the dormant season, the low fuel moistures of the live huckleberry stems and the dead litter fuels will significantly increase the overall fire behavior. Average live moisture contents for the months of March and April range from about 65 to 70%. These shrubs also tend to retain their dead stems, providing fuels for vertical fire spread. Even under the more controlled levels of environmental conditions (lower winds, higher relative humidity) during prescribed fires, flame lengths produced by the litter and huckleberry components have exceeded 10 feet (W. A. Patterson III, personal communication, 1996). Fires during the dormant season are typically the most intense, with greater levels of fire behavior and fuel consumption than in the summer, growing season. This can be attributed to a combination of the lower live fuel moistures and a lack of an overstory canopy, causing a higher sun exposure and increased drying of the fuels below.

3.2.2 Growing Season Fire Behavior

During the growing season, the mechanisms of fire spread are similar to the dormant season. However, live moisture contents of the shrubs are higher, ranging

between 65 and 70% for the stems and between 125 and 180% for the leaves. The leaves contain a high ether extractive content, which includes the various waxes, oils, terpenes, and fats present in many plant fuels (Philpot, 1969b). These ether extractives have been found to increase the flammability of live fuels by facilitating the initiation of combustion at higher moisture conditions and increasing the burning rate (Philpot, 1969a; Shafizadeh, Chin, & DeGroot, 1977). This behavior is unique to the region as most broadleafed, deciduous plants in the Northeast will only burn under extereme drought or fire conditions (Crary, 1987).

Overall, prescribed fires during the growing season tend to produce a level of fire behavior that is about ½ to ¾ that of the dormant season, usually just charring the stems and killing the leaves of the huckleberry (W. A. Patterson III, personal communication, 1996). However, ignition of the huckleberry can produce flame lengths similar to those during the dormant season, displaying somewhat of a mini "crown fire" effect as the fire burns through the shrubs. Previous summer prescribed burns in patches of huckleberry have been reported to produce flame lengths in excess of 15 ft (Crary, 1987).

4. Testing BEHAVE

4.1 Prescribed Burn Studies

The series of prescribed burns and fuel modification experiments were conducted from 1986 to 1996 in the Lombard/Paradise Hollow area of Truro, Massachusetts. Fuel bed physical characteristics and fire behavior data have been collected from several experimental plots containing the pine - oak forests with a predominantly huckleberry shrub understory (Crary, 1987; Patterson, 1986; Patterson, Saunders, & Horton, 1984). Information from these studies was used in this thesis for the development of site-specific fuel models and for comparison of observed fire behavior with predictions obtained from BEHAVE.

The research site is located on 17 acres between the Lombard and Paradise Hollows within the Cape Cod National Seashore (Crary, 1987). Several 20 m x 20 m study plots were designated as either a burn, mowed, or control plot, where the corresponding treatment was prescribed burning, mechanical fuel height reduction, or no treatment, respectively, see Figure 4.1. The treatments were conducted at 1-, 2-, 3-, 4-, or 5-year intervals, during the 'Winter' (primarily March and April) or 'Summer' (July). For example, plot K12 is designated as a BW3A plot, or a plot that was **B**urned in the **W**inter every **3** years. The designation of A, B, C, etc. indicates replicate treatments. Several larger control plots were designated as TP, or Test Plot. Plot TP01 was approximately 70 m x 70 m and plot TP06 was approximately 80 m x 40 m.

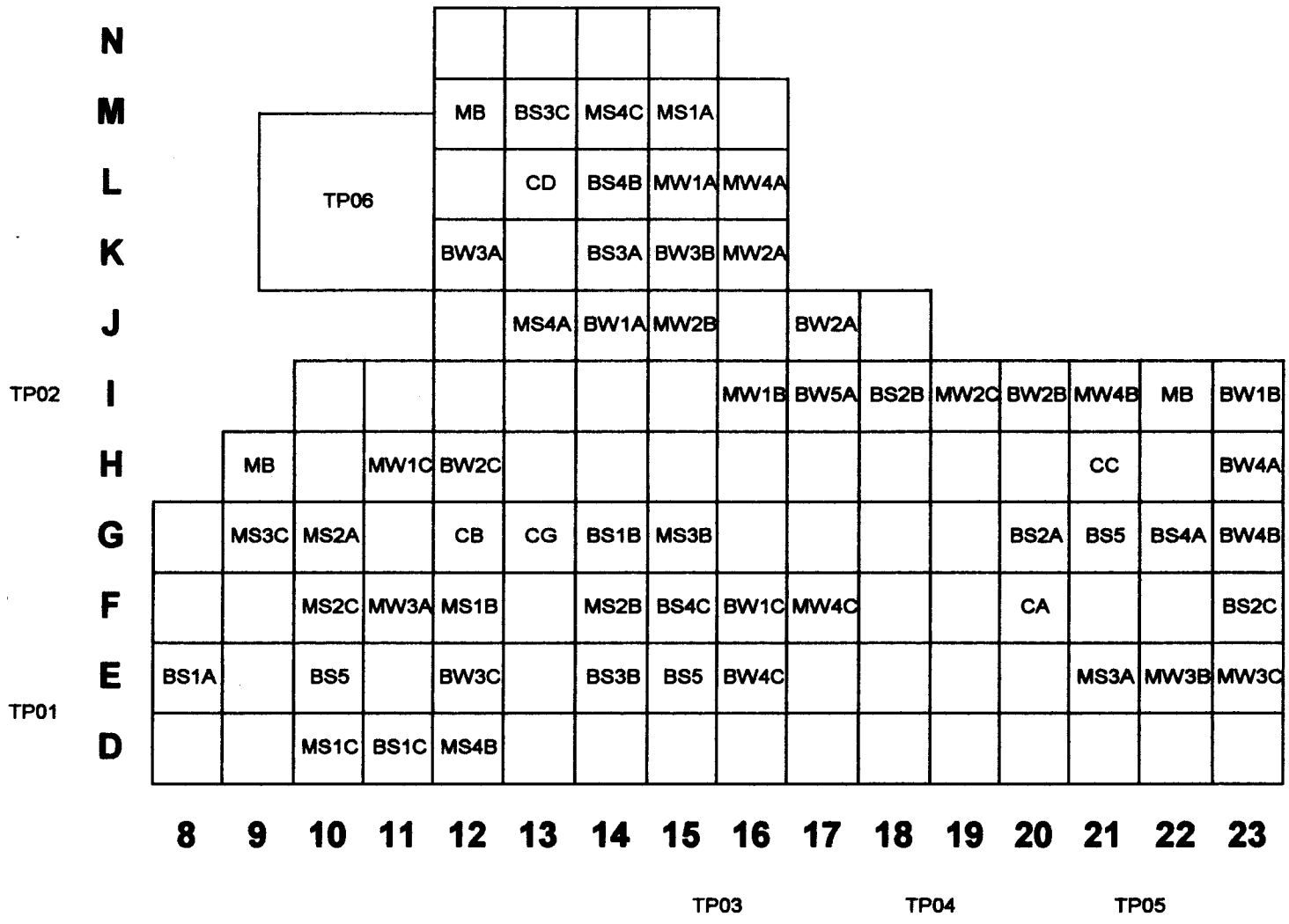

Figure 4.1: Lombard/Paradise Hollow prescribed burn research plots.

The data from 9 experimental plots (4 summer and 5 winter) and 2 of the larger control plots (which have recently undergone summer burn treatments) were used in the analysis of BEHAVE. These will be referred to as 'experimental' and 'control' plots, respectively. Table 4.1 gives the plot, treatment, date, and an abbreviation that is used throughout the remainder of the text to denote each individual plot.

Table 4.1: Prescribed burn plot information.

Plot	Treatment	Date of Burn	Abbreviation
I18	BS2B	7/30/92	I1892S
K12	BW3A	4/24/89	K1289W
K14	BS3A	7/28/89	K1489S
E12	BW3C	3/18/92	E1292W
K15	BW3B	4/06/92	K1592W
K14	BS3A	7/30/92	K1492S
M13	BS3C	7/31/92	M1392S
G23	BW4B	3/28/90	G2390W
I17	BW5A	4/07/92	I1792W
TP01	Control	8/04/95	TP01S
TP06	Control	7/22/96	TP06S

Each of the experimental plots contained 36 metal stake-flags, see Figure 4.2. These flag points aided in the measurement of fire behavior characteristics including spread rates, flame lengths, flame heights and flame depths, by enabling an observer to note the arrival of the fire front at a specific flag. All of the measurements were made visually by one person for the purpose of uniformity. Spread rates were calculated either by dividing the distance of fire travel by the elapsed time and recorded directly as a rate, or by merely noting the arrival of the fire at a particular flag alongside constantly recorded time intervals. In the latter method it was often difficult to calculate the spread rates, as the procedure of noting the arrival of the fire at various flags was inconsistent and often

focused on several sides of the fire at the same time making the path of the fire difficult to follow. Flame heights were also recorded visually using 4-ft reference stakes with 1-ft interval markings. A visual estimation of flame angle was made in order to measure the flame lengths. Wind speeds were recorded at each time interval, along with an indication of whether the fire observation was of a head, backing or flanking fire. There were no significant slope changes from zero for any of the 20 m x 20 m burn plots.

Fire behavior measurements were obtained using different methods for the control plots. Head fire spread rates were recorded using a system of 10 timers spaced in three rows on a 10 m x 15 m grid for plot TP06S and a 10 m x 10 m grid for plot TP01S. The timers were activated at a temperature of 200°C using 1.5 mm type k mineral insulated stainless steel sheathed (310) insulated junction thermocouples. The spread rates were calculated from the difference between timer activation times and the distance of fire travel. Head fire flame lengths were approximated from observers' estimates and pictures taken during the burns. The slope of plot TP01S and TP06S ranged from 0-3% and 0-7%, respectively.

The fires were started either as a point source at the middle of the plot, or as a series of strip head or line fires. The ignition source was a single match for the point source ignitions, and a driptorch for the strip head fire ignitions, see Figure 4.2. The fires reached a steady state of spread fairly quickly and were allowed to burn either uninhibited until burnout or completed with a ring fire ignition pattern. Any adjustments to fire behavior, through the use of a ring fire or the converging of multiple fire fronts, were not included in the data analysis.

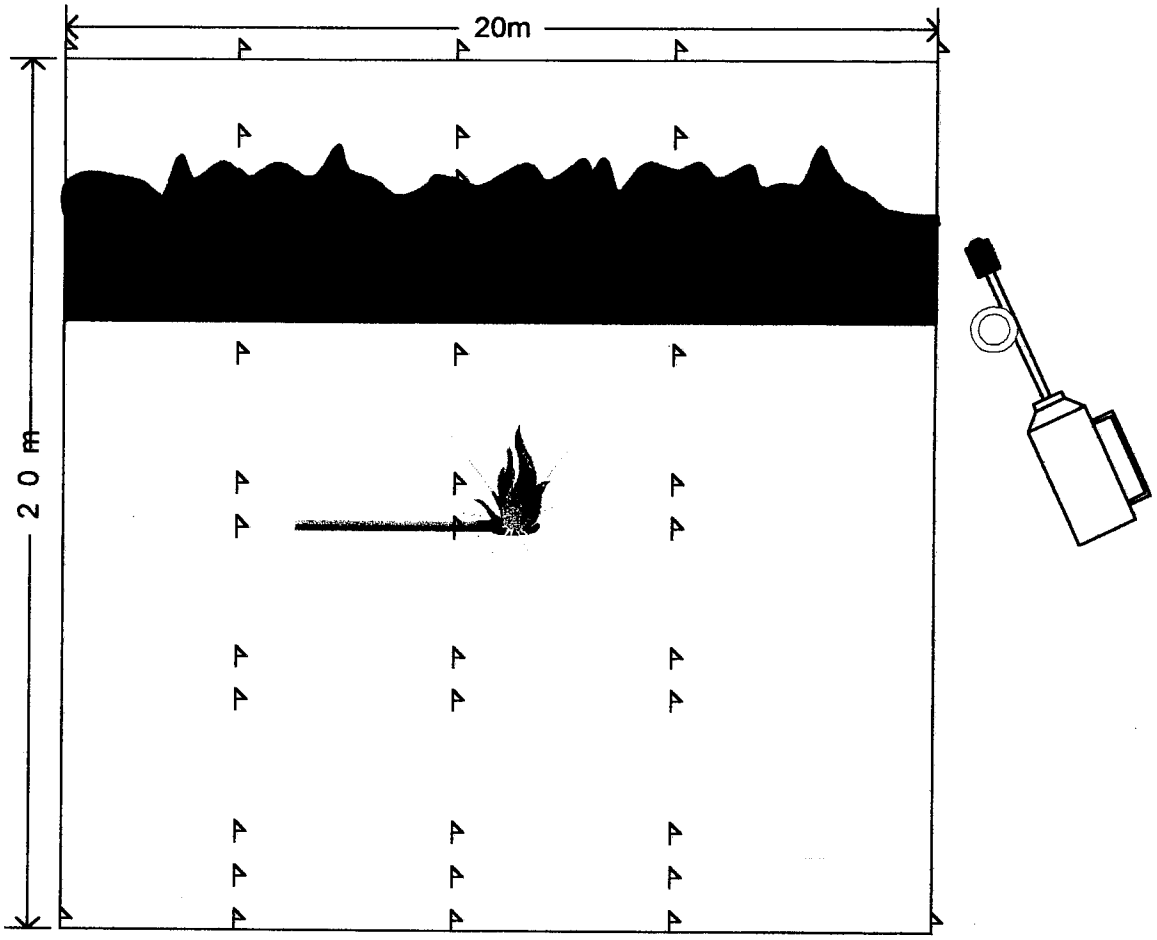

Figure 4.2: Layout of experimental burn plots.

4.2 Custom Fuel Models

Site-specific fuel models were developed for each of the 9 experimental and 2 control burn plots, based on fuel data collected prior to each burn. This was done in order to match the specific fuel conditions of each plot as closely as possible when testing the effectiveness of BEHAVE in predicting fire behavior. Each input parameter will be discussed, along with the corresponding measuring techniques utilized. Figures C.1 through C.11 in Appendix C show the data, by fuel component, used to construct each custom fuel model, along with the final set of numerical data used as input to the fire prediction model.

4.2.1 Fuel Load

4.2.1.1 Experimental Plots

All of the dead, downed fuel load, with the exception of the leaves and pine needles in the litter layer, was determined using the downed woody fuel inventory method described by Brown (1974). This inventory procedure is based on the planar intersect technique, where lines are laid out from random sample points to establish a sample plane. Pieces of dead, woody fuel which cross this plane are counted, along with measurements of fuel and duff depth, in order to estimate the total fuel load, by size class, present on a particular plot of land. Results of the downed woody fuel inventories for each of the burn plots are shown in Table 4.2 (Patterson, 1996).

Table 4.2: Results of the 1992 downed woody fuel inventory.

	Fuel Loads (tons/acre)						Fuel Depths (inches)						
Plot	Ave. 1-hr	Ave. 10-hr	Ave. 100-hr	Ave. 1000-hr Sound	Ave. 1000-hr Rotten	Ave. Downed Woody Fuel	Duff Depths		Fuel Depths			Ave. Duff Depth	Ave. Fuel Depth
I1892S	1.2	0.19	3.05	3.2	0	7.63	1.7	0.5	1.5	0.5	0	1.1	0.67
K1289W	1.2	0	2.67	1.02	0	4.88	1.5	1.1	0	0.5	1	1.3	0.5
K1489S	1.54	0.06	3.81	0	0	5.42	1.1	1.5	1	2	0	1.3	1
E1292W	1.23	0.03	1.14	0	0	2.41	1.5	2.4	1	0.5	0	1.95	0.5
K1592W	0.73	0.13	2.29	3.59	0.76	7.49	1.5	0.9	0	0.5	4	1.2	1.5
K1492S	1.54	0.06	3.81	0	0	5.42	1.1	1.5	1	2	0	1.3	1
M1392S	1.27	0.22	0.38	2.14	0	4.02	1.2	1.2	1.5	1	1.5	1.2	1.33
G2390W	1.39	0.32	3.05	1.86	0	6.62	2.1	2.9	1	5	6	2.5	4
I1792W	0.63	0.12	0.87	0	0.1	1.72						2.8	5.57

While this downed woody fuel inventory was conducted for each of the experimental plots in early summer of 1992, the results were used as fuel load estimates for each of the plots under study regardless of when the burn actually took place. This is a reasonable estimate for plots that were burned in late summer 1992 as they were burned after the inventory (I1892S, K1492S, and M1392S). Also, plot I1792W had not been burned before 1992 and so the average values of five untreated, experimental plots were used for reasonable fuel loading estimates. Some error in using the 1992 fuel inventory may occur for plots E1292W, K1592W and G2390W, where the inventory took place after the burn. This may result in an under-estimation of the fuel load, particularly the 1-hr fuel sticks that are usually consumed the most during the burns.

The numbers of times that each plot had been burned prior to the burn under study is also an important factor (W. A. Patterson III, personal communication, 1996), particularly for plots K1489S and K1289W. Plot K1489S had been burned twice before the 1992 inventory and plot K1289W had been burned three times. However, both had only been burned once prior to the 1989 burn. It has been found that the first burns in this fuel complex tend to be of sufficient intensity to consume most of the litter layer and kill, but not fully consume the shrubs. Over the next three years prior to the 1989 burn, the litter accumulates again and the dead shrubs remain standing. Under dry 1- and 10-hr fuel conditions, the second burn will produce fire behavior similar to the initial burn. After this second burn, there is a substantial drop in shrub height, standing dead load and corresponding fire behavior. This would result in a lower dead fuel accumulation in 1992 than was actually present in 1989.

Errors in approximating the downed fuel loads from the 1992 inventory would be small, particularly for the overall 1-hr fuel load, as the majority of this parameter was represented by the leaf and needle content of the litter layer. This quantity was determined by a separate means, called "biomass plots" (Patterson, 1996). In this procedure, small subplots were inventoried in the fall before each burn. All dead and live material from four 100 cm x 40 cm subplots per plot was collected, separated and weighed on an oven-dry basis to determine the litter, standing dead, live leaf and live twig fuel loads. The values from the four biomass plots were averaged in order to produce the appropriate loads for each burn plot, see Table 4.3.

Table 4.3: Biomass plot data obtained prior to each prescribed burn.

	Fuel Load (tons/acre)		
Plot	Standing Dead	Litter Load	Live Woody Load
I1892S	0.16	3.9	0.35
K1289W	0.3	4.2	1.95
K1489S	0.72	3.5	1.18
E1292W	0.1	3.6	1.87
K1592W	0.51	4.4	4.35
K1492S	0.62	4.3	1.04
M1392S	0.08	4.6	0.57
G2390W	0.02	5.5	2.03
I1792W	0.42	9.4	3.20

These biomass plots were conducted before the burns and had to be corrected to account for any subsequent litter accumulation during the winter. This was done by measuring the total litter fall in control plots over a 3-year period. It was found that on average 350 g/m^2 (1.6 tons/acre) of leaves and needles accumulate annually.

When constructing the custom fuel models for the experimental plots, the litter component was composed of the leaf and needle loading obtained from the biomass plots. The shrub component was composed of the 1-, 10-, and 100-hour fuel loads determined from the downed woody fuel inventory, and the standing dead and live woody fuel loads determined from the biomass plots. Parameter values for the shrub component, shown in Figures C.1 through C.9, have been reduced according to the percent coverage for each plot, as discussed later.

4.2.1.2 Control Plots

The fuel loading for control plots TP01S and TP06S was estimated using inventory data collected in 1985 before treatments began in the research area (Crary, 1987). Biomass plots were averaged from a total of 48 samples to yield all necessary data, see Table 4.4. Litter loads also included downed woody fuel of all sizes and so a separate fuel inventory was not necessary.

Table 4.4: Biomass plot data for control plots.

Fuel Load (tons/acre)				
Litter/1-hr Load	10-hr Load	100-hr Load	Standing Dead	Live Woody Load
5.86	0.12	0.30	0.23	1.43

When constructing the custom fuel models for the control plots, the litter component was composed of the leaf and needle loading and all of the downed woody fuel obtained from the 1985 biomass plots. The shrub component was composed of the standing dead and live woody fuel loads determined from the same source. Parameter

values for the shrub component, shown in Figures C.10 and C.11, have been reduced according to the percent coverage.

4.2.2 Surface-Area-to-Volume Ratio

Measurements of 1-hr and live woody S/V ratios had not been made for this fuel complex. Thus, values of 2000, 1500 and 1350 ft^{-1} for the litter, 1-hr shrub and live woody S/V ratios, respectively, were used in the custom fuel models (W. A. Patterson III, personal communication, 1996). The sensitivity of fire behavior predictions to this parameter will be discussed later.

4.2.3 Fuel Bed Depth

The program NEWMDL requires a depth estimate for each of the components appropriate to a fuel complex. For the experimental plots, a series of live fuel height measurements were conducted before each burn (Patterson, 1996). Fifteen 100 cm x 20 cm subplots were sampled in order to estimate the average height of each shrub and tree species. Since the huckleberry was the tallest and most dominant of the shrubs, its average height was taken as the shrub depth. Shrub heights for the control plots were estimated from pictures taken prior to the burns and were found to be roughly 3 feet for the huckleberry in each plot. Average shrub heights for each of the major species present on the burn plots are given in Table 4.5.

Table 4.5: Live shrub heights for the major species within each burn plot.

Average Live Fuel Heights (cm)				
Plot	Gaylussacia baccata	Vaccinium vacillans	Gaultheria procumbans	Vaccinium angustifolum
I1892S	22.7	17.2	5.3	10.7
K1289W	57.4	37.0	11.5	
K1489S	56.1	23.5	10.4	15.9
E1292W	55.7	23.3	9.3	17.9
K1592W	52.7	30.7	10.7	18.8
K1492S	32.9	16.9	7.3	12.8
M1392S	31.7	23.5	9.3	9.4
G2390W	72.1	31.2	15.2	13.3
I1792W	119.5	44.5	11.1	
TP01S	99.0			
TP06S	99.0			

No direct measurements of litter depth were taken. Estimates of litter depth were based on average fuel depth measurements obtained from the 1992 downed woody fuel inventory, see Table 4.2. This measurement is meant to represent the height above the duff layer of all dead fuel, at each sample point. The fuel depth measurements, however, usually corresponded to the litter depth due to the low amounts of downed fuel on the experimental plots. For the untreated plots, the litter depth averaged 5 to 6 inches. For the burn plots, litter depth was close to 1 inch due to consumption during previous prescribed burns. A value of 5.75 inches, obtained from the average of all untreated, experimental plots in 1992, was used for the control plot litter depths.

4.2.4 Percent Coverage

An estimate of the percent ground coverage is required for each of the fuel components in the custom fuel model. For coverage of less than 100%, the values of fuel load, S/V ratio and fuel bed depth for that component are reduced by multiplying those

values by the percent coverage. While the litter layer could reasonably be assumed to cover 100% of the plot, this was not the case for the shrubs. The average coverage for shrubs in this type of fuel complex is usually between 65 and 70%, for untreated plots. The coverage is usually less for plots that are burned more frequently, as the shrubs are given less time to re-grow. Based on the interval at which the plot was burned, along with shrub height data taken before the burn, an overall percent coverage was assigned for each burn plot, see Table 4.6:

Table 4.6: Shrub component percent ground coverage.

Plot	% Coverage
I1892S	40
K1289W	60
K1489S	60
E1292W	80
K1592W	70
K1492S	50
M1392S	50
G2390W	75
I1792W	85
TP01S	75
TP06S	65

4.2.5 Heat Content

Values for heat content have not been found in the literature for fuels in this complex (Fahnestock, 1970; Golley, 1961; Kelsey, Shafizadeh, & Lowery, 1979; Richards, 1940; Susott, 1982; Susott, DeGroot, & Shafizadeh, 1975; Susott, Shafizadeh, & Aanerud, 1979). Therefore, a value of 8000 Btu/lb was used for each of the live and dead fuel components, as was done with the 13 NFFL fuel models. The NEWMDL

program suggests higher values, closer to 9500 Btu/lb, for shrubs which contain oils and waxes. The heat content would appear to depend greatly on the season in which the fuel is burned and whether or not leaves are present. This will be discussed later.

4.3 Environmental Parameters

The prescribed burns were conducted on days of moderate fire and weather conditions (low winds and high relative humidity) due to concerns with possible extreme fire behavior. This resulted in lower levels of fire behavior not indicative of the true potential discussed in Chapter 3. Table D.1 of Appendix D gives a sense of the various levels of relative humidity and 1-hr fuel moistures, and their fire hazard interpretation (National Wildfire Coordinating Group, 1989). Exceptions to this table have been found in Cape Cod National Seashore where fuel moistures of 12-15% have been recorded on days of 70-90% relative humidity (W. A. Patterson III, personal communication, 1996). The relationship between fuel moistures and fire hazard, however, appear to be reasonable. Live fuel moistures are not controlled by the same environmental factors as dead fuel moisture, although there are general guidelines to assist in estimating this parameter. Table D.2 gives guidelines for estimating live fuel moisture contents based on the stage of plant development (Rothermel, 1983). Again, the pine - oak forest fuel complex deviates from this table, with live shrub moistures usually not exceeding 200% in all stages of development. Table D.3 gives a scale of windspeeds for comparison to those encountered during the prescribed burns (National Wildfire Coordinating Group, 1989).

Fuel moisture data were collected on the day of the burn. The litter, live leaf and live stem moistures were all determined by collecting and drying samples prior to the time of ignition. The 1-, 10- and 100-hour fuel moistures were determined using a 'Protimeter' wood moisture meter which gives a direct, electronic reading of fuel moisture when inserted into the fuel stick. The ranges and average values are given in Table 4.7.

Table 4.7: Fuel moistures present on the day of each burn.

	Litter Moisture, %			1-hr Moisture, %			10-hr Moisture, %		
Plot	Min.	Ave.	Max.	Min.	Ave.	Max.	Min.	Ave.	Max.
I1892S	12.2	15.7	18.2	10.8	16.3	22.9	12.2	15.4	18.5
K1289W			8			8	8	15.8	37.7
K1489S				13.4	15.5	16.5	12.7	16.5	21
E1292W	12.4	13	13.6	9.3	20.4	33.8	9.7	33.4	46.2
K1592W	9.9	11.1	12.7	8	11.4	26.3	8	24.9	46
K1492S	8.6	9.3	10.6	12.7	14.4	19.7	11.6	15.1	22.8
M1392S	10.4	13.6	17.1	8	11.9	28.8	8.9	16.3	27.5
G2390W				8.6	9.7	12.1	8.7	27.6	53
I1792W		19.2		8.7	17.9	35.3	11.6	38.7	59.5
TP01S		18.4			14.4			20	
TP06S		12.4			13.2			13.9	

	100-hr Moisture, %			Live Leaf Moisture, %			Live Stem Moisture, %		
Plot	Min.	Ave.	Max.	Min.	Ave.	Max.	Min.	Ave.	Max.
I1892S	12.4	28.8	54.2	122.8	144.6	161	100	105.5	118.3
K1289W	8	27.3	43.2				24.8	33.6	45.1
K1489S		43			160			99	
E1292W	18.4	34.7	49				67.7	69	70.3
K1592W	17.4	36.4	48				64.6	65.3	66
K1492S	11	22.3	53.1	147.4	161.3	180.9	96.2	99.7	108.3
M1392S	9.2	22.9	52	129.8	147.1	165.5	86.1	91.6	97.6
G2390W	26.3	34.8	40.8				24.3	26.3	31.6
I1792W	12.8	35.9	45.1				56.8	58.2	59.6
TP01S		20.9			158.4			70	
TP06S		14.6			181.1			71.1	

Table 4.8 gives the range of midflame windspeeds recorded during the course of each prescribed burn, along with average slope, temperature and relative humidity. Temperature and relative humidity measurements were obtained through the use of a psychrometer, found in the standard belt weather kit (Mobley et al., 1973). Wind measurements were also made on-site, using a hand-held electronic anemometer.

Table 4.8: Weather information recorded during each burn.

		Midflame Windspeed, mi/h			Slope, %	Temperature, °F		Relative Humidity, %
Plot	Time of Burn	Min.	Ave.	Max.	Ave.	Dry Bulb	Wet Bulb	Ave.
I1892S	1400	0	0.6	1.2	0	70	63	69
K1289W	1015	0	2.0	5.0	0			
K1489S	1430	0	1.0	5.0	0	82	73	61
E1292W	1415	0	1.3	3.5	0	38	31	40
K1592W	1245	0.7	2.9	6.2	0	50	41	44
K1492S	1430	0	0.5	1.8	0	73	64	61
M1392S	1200	0	0.2	1.8	0	76	64	53
G2390W	1000	0	2.0	6.0	0	40	32	36
I1792W	1000	0	0.9	3.5	0	48	38	36
TP01S	1300	0	2	4	0-3	83		78
TP06S	1430	2	2.5	4	7	77		45

For fire behavior predictions, average values of midflame windspeed were used as input to BEHAVE, along with average values of each of the appropriate fuel moistures. The average litter moisture was used for the 1-hr fuels whenever available, due to the larger fuel load contribution of litter in this size class. Similarly, average live leaf moistures were used for live woody fuel moisture estimates during the summer burns, as they are the major carrier of fire through the shrubs during this season.

4.4 Observed vs. Predicted Fire Behavior

4.4.1 Results

The purpose of the comparison between observed and predicted fire behavior was to analyze the effectiveness of BEHAVE in predicting fire behavior in this fuel complex, based on site-specific fuel models and average environmental conditions. These predictions were compared to the average observed fire behavior recorded during each burn. Tables 4.9 and 4.10 give the range of fire behavior observed on each of the burn plots, along with the corresponding predictions. One predicted value was obtained for each of the plots from the DIRECT module of BEHAVE.

Table 4.9: Observed and predicted spread rates.

Head Fire Spread Rates (ft/min)						
	Observed			Predicted	Error, %	
Plot	Min.	Ave.	Max.		Under	Over
K1289W	2.0	3.8	6.5	6.6		74
K1592W	1.5	5.5	12.0	7.7		40
G2390W	1.7	4.0	6.5	10.1		153
I1892S	0.5	1.0	1.0	0.25	75	
K1489S	6.0	9.1	12.5	2.2	76	
K1492S	1.0	1.1	1.3	1.1	-	-
M1392S	1.1	2.6	5.0	0.5	81	
TP01S	11.8	14.0	15.0	4.4	69	
TP06S	20.0	26.0	26.0	6.6	75	
AVE.					**75**	**89**

Table 4.10: Observed and predicted flame lengths.

Head Fire Flame Lengths (ft)						
	Observed			Predicted	Error, %	
Plot	Min.	Ave.	Max.		Under	Over
K1289W	1.0	2.4	4.0	5.0		108
E1292W	1.0	1.3	2.2	4.2		223
K1592W	1.3	2.1	3.5	5.6		167
G2390W	1.0	3.7	8.0	6.8		84
I1792W	3.0	4.0	5.0	5.9		48
I1892S	0.8	0.8	1.0	0.4	50	
K1489S	3.5	5.4	11.0	2.5	54	
K1492S	0.8	1.9	3.3	1.2	37	
M1392S	1.2	2.0	2.8	0.8	60	
TP01S	3.0	5.0	8.0	3.7	26	
TP06S	3.0	5.0	7.0	4.8	4	
AVE.					**39**	**126**

Figures 4.3 and 4.4 graphically show the results of the comparison for spread rates and flame lengths, respectively. The x-axis represents the observed values of fire behavior, where the data points correspond to the average recorded spread rate or flame length during the burn. The purpose of the error bars was to evaluate the accuracy of predictions when the entire range of the observed fire behavior was considered. The y-axis represents the predicted value of spread rate and flame length for each of the burn plots. For plots I1892S and M1392S, a value of zero was predicted for spread rates, as a result of the program rounding predictions less than 0.5 ft/min down to zero. For ease of comparison with observed values, the non-rounded value was obtained from the graphs available in the TSTMDL program of BEHAVE.

The 45-degree line on each of the figures represents the line of exact agreement between the observed and predicted fire behavior. Fire behavior (spread rates and flame

lengths) is over-predicted (above the 45-degree line) for the winter burns, and under-predicted (below the 45-degree line) during the summer. Tables 4.9 and 4.10 give the percent under- or over-prediction for spread rates and flame lengths, respectively, expressed as a percent of the observed values.

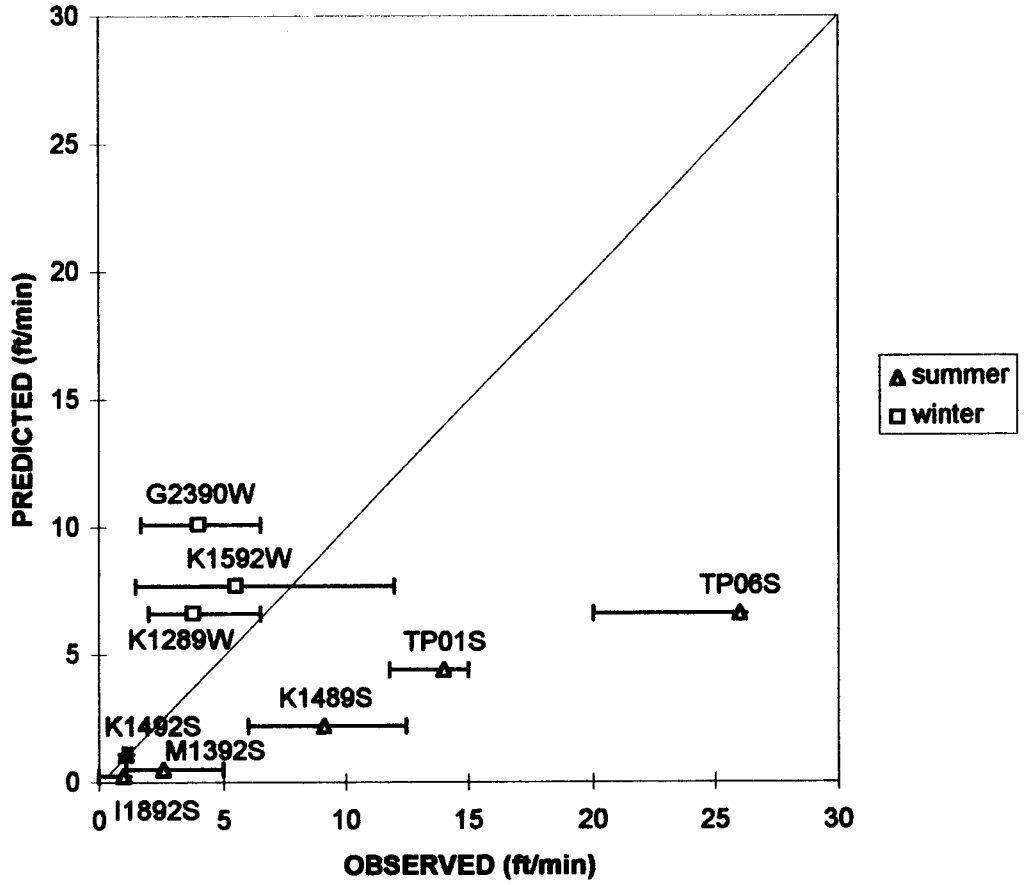

Figure 4.3: Predicted vs. observed head fire spread rates.

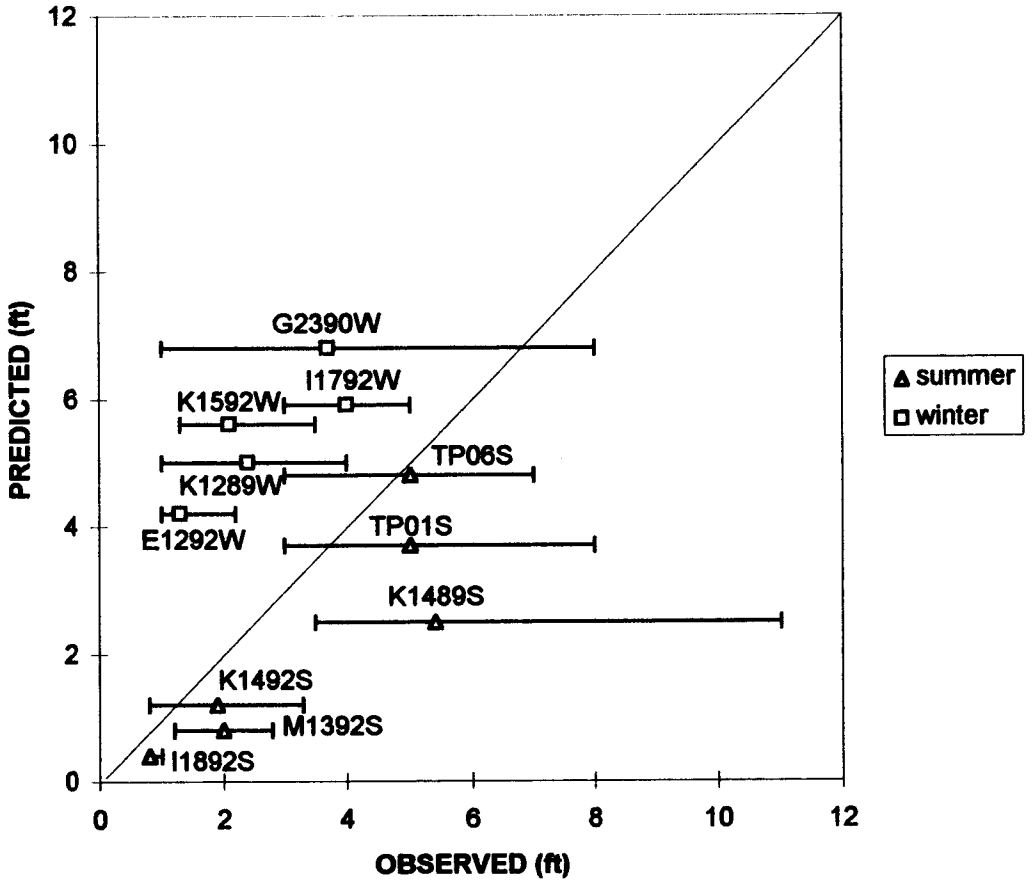

Figure 4.4: Predicted vs. observed head fire flame lengths.

4.4.2 Discussion

One main objective of the prescribed burns was to collect the necessary data to effectively evaluate the potential fire behavior of this fuel complex in the future. From an initial overview, the errors in predictions obtained from BEHAVE were high, generally greater than 50% when comparing predictions to the average observed spread rates and flame lengths. However, because the prescribed burns were not conducted under carefully controlled experimental conditions, with discontinuities in fuel bed and environmental characteristics, it is also beneficial to compare fire behavior predictions with the complete range of observed behavior. In this case, deviations of predictions from observations are narrowed for many of the plots, as the error bars in Figures 4.3 and 4.4 indicate that some of the fire behavior observations were similar to predictions. More significant deviations, however, are realized for plot K1489S where observed flame lengths reached values well over the predictions. Also, for plots G2390W, K1489S, TP01S and TP06S, Figure 4.3 shows that their whole range of observed spread rates fell outside predictions. This discussion will analyze the possible causes of the deviations of predictions from observations along with their significance.

From a practical point of view, as outlined in the various hazard levels of flame lengths and spread rates in Tables 3.1 and 3.2, the levels of fire behavior observed during each prescribed burn were generally low, as was the predicted fire behavior. The majority of observed and predicted spread rates fell in the first level or lower end of the second hazard level (0-30 ft/min) as indicated in Table 3.2 and, in fact, never exceeded a value of

approximately 10 ft/min. These spread rates are quite slow, and do not create a great deal of concern when planning for a prescribed burn or suppression efforts during a wildfire. Similarly, when considering the various hazard levels established for flame lengths in Table 3.1, observed and predicted values tended to stay within the first two levels (0-8 ft). These flame lengths are acceptable for most prescribed burn operations, as the necessary precautions are usually taken to help ensure containment, including handtools, water supply and pre-established firebreaks. One interesting plot, however, was K1489S, which exhibited a wide range of recorded flame lengths, some of which reached 11 feet. The deviation of predictions from observed flame lengths, in this case, are significant from a fire suppression interpretation. Similarly, the under-prediction of spread rates for plots TP01S and TP06S were significant and will be analyzed further.

The size of the experimental plots may be a contributing factor to the deviations of predictions from observed fire behavior. Winter plot predictions over-estimated the potential of the fuel complex which may indicate that the fires on the 20 m x 20 m plots were not able to reach a full steady-state of spread. However, the fire behavior during the summer was consistently under-estimated, indicating that other, more complex factors are causing inaccuracies in predictions. This is supported when considering the larger control plots which were also under-predicted.

The clear difference in the results of the comparison between observed and predicted fire behavior based on the season in which the plots were burned raises questions as to the seasonal variations in the flammability of the fuels and how fuels are represented within the fire prediction model. The main differences between the winter and

summer months are the characteristics of the live shrub component, including the presence of leaves with high moisture contents during the summer. In previous prescribed burns of this fuel complex, whether or not the live fuels have contributed to observed fire behavior has depended greatly on the litter layer's ability to support a hot enough fire that would heat the shrubs sufficiently to sustain fire spread (W. A. Patterson III, personal communication, 1996). This, in turn, seems to be dependent on the environmental factors present on the day of the burn, namely the moisture contents of the dead fuels and the wind speeds.

On burns of low intensity, the primary carrier of the fire is usually the litter layer, which would make this fuel complex similar to NFFL fuel model 9, characterized by closed long-needle conifer and hardwood stands with a litter layer that will support a strong surface fire (Rothermel, 1983). Figure 4.5 shows the values of the fuel model parameters used in this standard fuel model.

```
STATIC 9. NFFL FUEL MODEL 9

   LOADS, T/AC            S/V RATIOS, 1/FT            OTHER
   -----------            ----------------   --------------------------
   1 HR          2.92     1 HR        2500.  DEPTH, FT              0.20
   10 HR         0.41     LIVE HERB    190.  HEAT CONTENT, BTU/LB   8000.
   100 HR        0.15     LIVE WOODY   190.  EXT MOISTURE, %          25.
   LIVE HERB     0.00
   LIVE WOODY    0.00
```

Figure 4.5: NFFL fuel model 9 parameters.

For comparison purposes, fuel model 9 was used to predict fire behavior for each of the burn plots. The results (Tables 4.11 and 4.12) indicate that the plots that exhibited lower levels of spread rates and flame lengths were predicted well by fuel model 9, but it

under-predicted in nearly ever other case, suggesting the importance of the additional shrub component within the fuel complex. Other NFFL fuel models, such as the shrub group (fuel models 4-7 shown in Figure 2.1), may also be used in limited cases, although several aspects of these models differ from the characteristics of the pine-oak forests, producing large deviations in predictions, see Tables 4.11 and 4.12. It is important that a custom fuel model be used to evaluate fire behavior in this fuel complex, in order to account for the unique interactions between fuel components.

Table 4.11: Spread rate (ft/min) predictions using NFFL fuel models.

Plot	Observed	Custom	NFFL 9	NFFL 4	NFFL 5	NFFL 6	NFFL 7
K1289W	3.8	6.6	2.2	42.42	15.15	9.9	12.12
K1592W	5.5	7.7	3.3	41.41	5.5	13.13	13.13
G2390W	4	10.1	2.2	40.4	15.15	9.9	11.11
I1892S	1.0	0.25	1.1	2.2	0	2.2	2.2
K1489S	9.1	2.2	1.1	7.7	2.2	5.5	5.5
K1492S	1.1	1.1	1.1	4.4	1.1	3.3	2.2
M1392S	2.6	0.5	1.1	2.2	0	1.1	1.1
TP01S	14.0	4.4	1.1	3.3	1.1	6.6	5.5
TP06S	26.0	6.6	2.2	9.9	2.2	10.1	7.7

Table 4.12: Flame length (ft) predictions using NFFL fuel models.

Plot	Observed	Custom	NFFL 9	NFFL 4	NFFL 5	NFFL 6	NFFL 7
K1289W	2.4	5.0	1.5	15.6	5.2	3.3	3.9
E1292W	1.3	4.2	1.1	4.4	1.1	2.3	2.5
K1592W	2.1	5.6	1.7	14.2	1.8	3.6	3.9
G2390W	3.7	6.8	1.4	14.6	5.1	3.1	3.7
I1792W	4.0	5.9	0.7	0	0.1	1.2	2
I1892S	0.8	0.4	0.8	2.3	0.5	1.6	1.5
K1489S	5.4	2.5	0.9	2.6	0.6	1.9	1.8
K1492S	1.9	1.2	0.9	4.6	0.6	1.8	2.5
M1392S	2.0	0.8	0.8	2.2	0.5	1.3	1.2
TP01S	5.0	3.7	1.0	1.8	0.4	2.3	2.4
TP06S	5.0	4.8	1.5	5.0	1.2	3.4	2.9

There are several parameters within the fuel and prediction models that could account for the various fire behavior encountered during the burning of each plot, and the deviations of predictions from these observations. The most obvious of these, which usually produce direct effects on fire behavior, are the environmental parameters, including the wind speed and fuel moisture contents.

4.4.2.1 Environmental Parameters

Midflame windspeeds were generally low during the prescribed burns, although the burns with the highest recorded winds (plots K1289W, K1592W, G2390W, K1489S, TP01S, and TP06S) as shown in Table 4.8, tended to have the highest observed spread rates and flame lengths. Their corresponding predictions followed this trend, with the exception of plot K1489S, see Tables 4.9 and 4.10.

Burns that were conducted under conditions of low moisture content did not always result in higher observed or predicted fire behavior. Recall that 1-hr moisture contents were determined from the litter moisture estimates whenever available. This is generally reasonable, as the litter fuels composed most of the 1-hr component. However, both the litter and 1-hr moisture contents together varied widely, see Table 4.7, suggesting some non-uniformity within the burn plots. Similarly, the 10- and 100-hr moisture contents also had a wide range of recorded values. Whether or not these variations would have a strong impact on fire behavior predictions needs to be analyzed further.

With respect to seasonal differences, the litter layer is usually drier during the winter and early spring than in the summer, which would help account for the expected

increase in fire behavior described in Chapter 3. For the burn plots under study, however, there was no consistent trend in dead fuel moisture contents between the winter and summer. The measured live fuel moistures shown in Table 4.7 did vary widely, especially when considering both the leaves and stems during the summer. For example, the range of possible live fuel moistures for plot M1392S ranged from about 85% to 165%. The moisture contents of the live fuels used for fire behavior predictions had the greatest seasonal difference among plots, averaging about 50% for stems in the winter and 160% for leaves during the summer. This division between summer and winter values is consistent with results where the lower winter live fuel moistures corresponded to over-predictions and higher summer values to under-predictions.

Another aspect to consider is the interaction between the live and dead fuels. Woitkiewicz (1996) found that a possible explanation for lower levels of fire behavior in the winter burns may be due to the abundance of Gaultheria procumbens (wintergreen) on the forest floor. These live fuels average a moisture content of about 130% during this season and are very short, ranging from 1-2 inches on frequently burned plots to 5-7 inches on untreated plots (W. A. Patterson III, personal communication, 1996). Therefore, the wintergreen is an integral part of the litter layer and can actually decrease fire behavior when there are sufficient quantities.

One way to represent the multiple sources of fuel moisture within the same layer of fuels is to calculate an adjusted fuel moisture which takes into account the ratio of the amount of the dry litter fuels to the wet wintergreen. This adjusted moisture content is defined as (Woitkiewicz, 1996):

adj. moisture = [total mass H_2O/total dry mass] x 100. [%] (4.1)

The mass of water is defined as the product of the oven-dry mass of the fuel and its moisture content. For instance, from the biomass plots of K1289W, there was 113.5 g of wintergreen at 130% moisture content and 948.5 g of litter at 8% moisture content. Therefore, there are 147.8 g of water in the wintergreen and 75.9 g of water in the litter for a total mass H_2O = 223.7 g and total dry mass = 1062 g. The adjusted moisture content is then 21.1%. This is a large difference compared to the value for litter of 8% and may help account for the lower levels of fire behavior during the prescribed burns. A similar calculation was performed for each of the winter plots and their adjusted moisture contents are shown in Table 4.13.

Table 4.13: Adjusted fuel moisture for winter surface fuels.

Plot	Litter Moisture Content, %	Adjusted Moisture Content, %
K1289W	8	21.1
E1292W	13	27.8
K1592W	11.1	27.5
G2390W	9.7	22.2
I1792W	19.2	22.3

The result of using these adjusted fuel moistures as 1-hr fuel moistures in the fire predictions model was a decrease in predicted spread rates and flame lengths, see Tables 4.14 and 4.15, respectively. Predictions were improved as there was less of an over-

prediction for each plot, see Figures 4.6 and 4.7. This same exercise was not performed for the summer plots as their fire behavior was already under-predicted.

Table 4.14: Observed vs. predicted spread rates using adjusted litter moisture content.

	Observed			Predicted	
Plot	Min.	Ave.	Max.	Original	Adjusted
K1289W	2.0	3.8	6.5	6.6	4.4
K1592W	1.5	5.5	12.0	7.7	4.4
G2390W	1.7	4.0	6.5	10.0	6.6

Table 4.15: Observed vs. predicted flame lengths using adjusted litter moisture content.

	Observed			Predicted	
Plot	Min.	Ave.	Max.	Original	Adjusted
K1289W	1.0	2.4	4.0	5.0	3.6
E1292W	1.0	1.3	2.2	4.2	3.4
K1592W	1.3	2.1	3.5	5.6	3.8
G2390W	1.0	3.7	8.0	6.8	4.9
I1792W	3.0	4.0	5.0	5.9	5.0

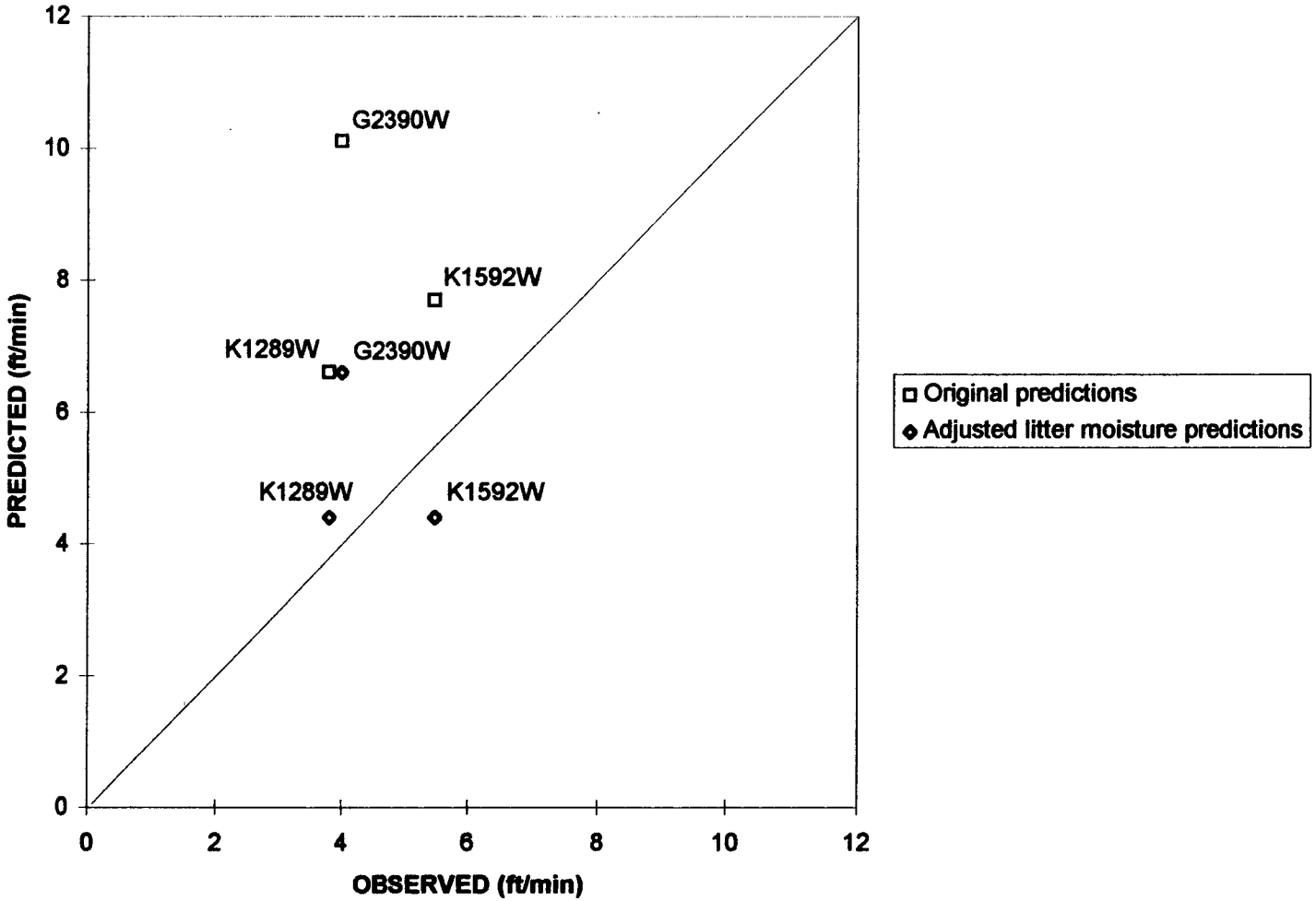

Figure 4.6: Comparison of original spread rate predictions with those based on adjusted litter moisture.

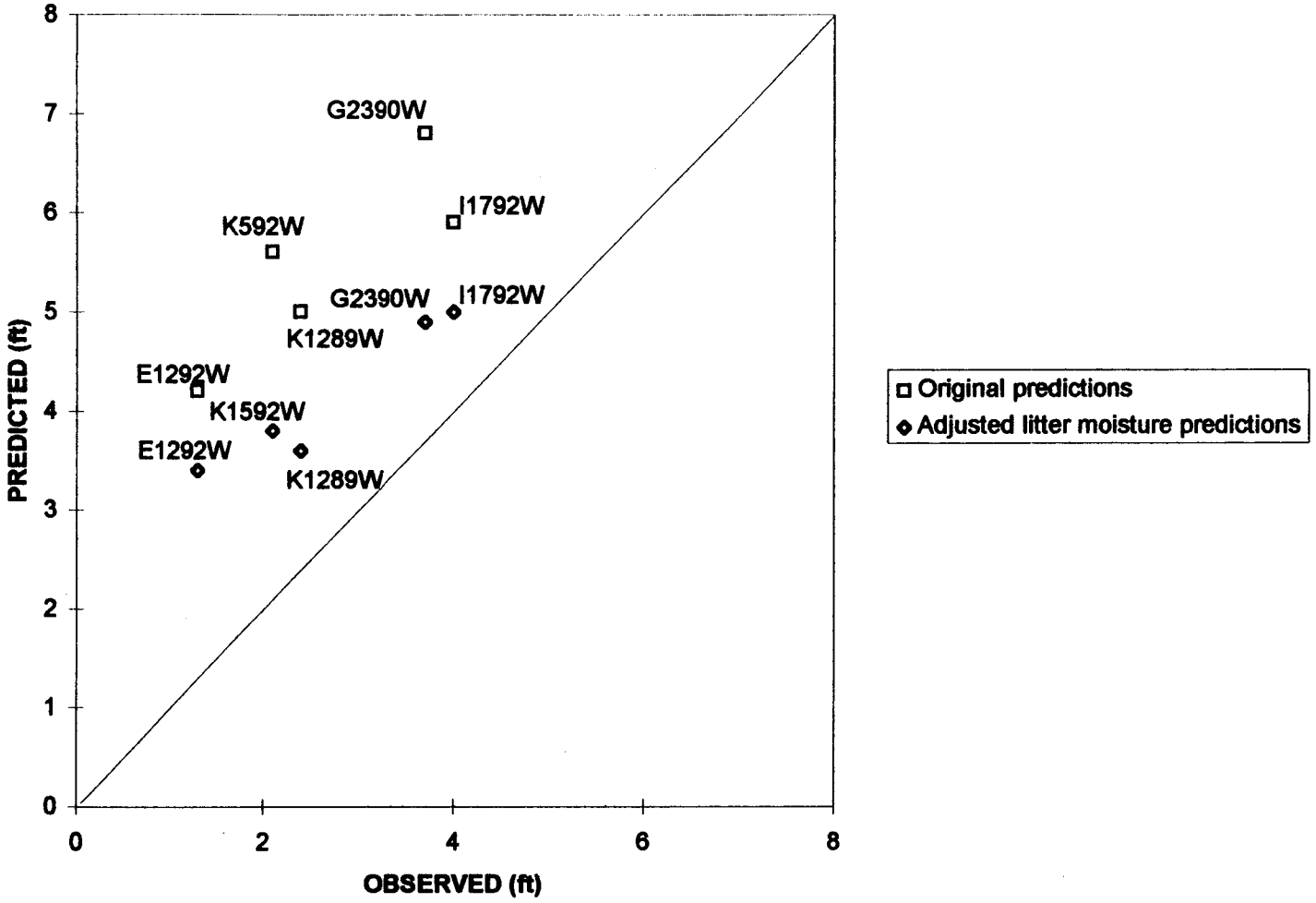

Figure 4.7: Comparison of original flame length predictions with those based on adjusted litter moisture.

4.4.2.2 Custom Fuel Models

The fuel models are the primary means by which the structure and properties of a fuel complex are represented. In examining the custom fuel models for the nine experimental plots (Figures C.1 to C.9) there are general trends which indicate the interval at which the plots were burned. The amount of dead fuel accumulations increased as the interval between prescribed burns increased, ranging from under 6 tons/acre for plot I1892S, a 2-year burn interval plot, to over 16 tons/acre for plot I1792W, which had not been burned previously. This is most notable in the 1-hour size class, resulting primarily from the larger amount of litter accumulations on plots that were burned less frequently. Live woody fuel loads ranged from 0.14 tons/acre for plot I1892S to 4.83 tons/acre for plot I1792W, however there was not a consistent increase over the increasing burn intervals. Fuel bed depths also increased, in general, with increasing burn interval, ranging from 0.14 to 1.43 feet. This is consistent with expectations, as the shrubs are allowed to grow longer between burns, which also causes a deeper litter layer. Also, for frequently burned plots, there are fewer shrubs to hold the litter in place, causing fall accumulations to be blown off the plots during the winter. No consistent effects on observed fire behavior were found as most of the above parameters varied between plots, although a general trend of increased fire behavior occurred as the burn interval increased.

As discussed in section 4.2.1.1, the number of times that each plot was burned prior to the burn of interest is also important. This also helps account for the low fuel loads in plot I1892S, as this plot was burned three times previous to the 1992 burn. Plots

that were burned once prior to the burn of interest, including plots K1289W, G2390W, and K1489S, would tend to have a higher standing dead load as the first burn tends to kill the live fuels which then remain standing for the second burn. From Table 4.3, plot K1489S did have the largest amount of standing dead fuel which corresponds to the high levels of fire behavior observed during the 1989 burn. However, there was no consistent trend in standing dead load with number of previous burns for the other plots.

With respect to seasonal differences between fuel models, live woody fuel loads were consistently lower during the summer than the winter. This results from the summer burning which retards the growth of the shrubs as they resprout (W. A. Patterson III, personal communication, 1996). Also, while the variability in summer live leaf and stem fuel moistures is accounted for in the environmental parameters, it may be beneficial to separate these fuel types within the fuel models. If the fuel loads for the leaves and stems are separated, then they can each be assigned different moisture contents instead of using the higher leaf moisture for the whole live load. A revised custom fuel model was constructed for each of the summer experimental and control plots, see Appendix E. The live stem load was accounted for as a live herbaceous load within the grass component with the corresponding shrub depth. The live leaf load was accounted for as a live woody load in the shrub component in order to account for the oils and waxes present in the leaves. The results of this analysis were surprising, as there was no change in predicted fire behavior for any of the summer experimental or control plots. This suggests that the fire prediction model may not account for the contribution of live fuels at moisture content

values over about 90% as found in the summer stems. Perhaps only at the lower winter stem moistures averaging 50% does the live load contribute to predicted fire behavior.

Seasonal changes can also exist within the chemical properties of a particular species, which would be represented by the mineral and heat content parameters within the fuel models. Recall that the total and effective mineral contents are held constant within the fuel models and have been found to be similar among most fuel types. For the heat content of the fuels, a value of 8,000 Btu/lb was used as an arbitrary estimation within the custom fuel models for each of the dead and live components of the winter and summer plots. This parameter, however, may actually fluctuate throughout the year, helping to account for the variations in fire behavior within this fuel complex. This has been found to be the case with Chamise, a major component of the flammable chaparral brush fields of southern California (Philpot, 1969b). The heat content of the leaves and stems of Chamise was found to increase over the months of May to October, by up to 600 Btu/lb. This increase was directly related to the ether extractive content of the fuel, typically found on or near the surface of the leaves and stems. The general cycle of ether extractives for the Chamise was a decrease over the period from January to May, then an increase by almost 4% dry weight, reaching its peak in the fall. This information was incorporated into a dynamic fuel model for the chaparral, where heat content was written as a time-dependent function (Rothermel & Philpot, 1973). Similar results of seasonal changes in heat content have been found for Douglas-fir and ponderosa pine, where a 10% increase occurred over the course of the summer (Philpot & Mutch, 1971). Thus, extreme fire behavior in the shrub understory of the pine - oak forests during the winter may be largely due to the

lower moisture contents of the live fuels, while an increase in ether extractives and heat content would allow for similar fire behavior at higher moisture contents during the summer months.

4.4.2.3 Fire Prediction Model

The above considerations suggest that the representation of the live fuels within the fuel and environmental parameters are most important in accounting for the distinction between winter and summer predictions. This raises concerns as to the extent to which the live fuels are assumed to contribute to the overall fire behavior within the fire prediction model. In previous studies with Tasmanian grasslands, it was found that the live fuels that burned during the experiments were often predicted not to burn by BEHAVE, resulting in several under-predictions (Marsden-Smedley & Catchpole, 1995a, 1995b).

Of the summer burn plots in the present study, K1489S had the most complete set of observations with respect to the type of vegetation burning. Areas with primarily litter and the shorter blueberry shrubs tended to produce flame lengths of 1.5 to 2.5 feet, although spread rates could not be distinguished from the data in these particular fuels. The addition of the huckleberry shrubs, however, produced flame lengths ranging from 5 to 11 feet, with corresponding spread rates of 6 to 12.5 ft/min. Thus, it appears that the live fuels in this particular plot are significantly contributing to the overall fire behavior.

If BEHAVE is assuming live fuels will not burn when they actually do, this may be due primarily to the prediction model ignoring the contribution of live fuels at the higher

moisture content levels found during the summer, and possibly even winter months. Similar to the dead fuels, there is a moisture of extinction calculated by the prediction model for live fuels, or the value of moisture content for which the live fuels will no longer contribute to the flaming front (Albini, 1976a, 1976b). This parameter is internal to the fire prediction model within BEHAVE and can not be altered by the user. It is based on the assumption that the live fuel moisture of extinction is linearly related to the "effective heat", Q_{ef}, produced by the burning dead fuel, defined as (Fosberg & Schroeder, 1971):

$$Q_{ef} = 1800[(1-\alpha)/\alpha](1-M_f/.3), \text{ [cal/g]} \qquad (4.2)$$

where α is the fraction of living fuel and M_f is the fuel moisture content expressed as a fraction. At the extinction moisture, there is just enough of this effective heat to raise the temperature of the live fuel to ignition. This corresponds to the heat of preignition which is a linear function of moisture content, see equation 2.9. Equating the two relationships for "effective heat" and heat of preignition (equations 4.2 and 2.9, respectively), allows the live fuel moisture of extinction to be written as a function of the dead fuel moisture content and the fraction of the total fuel load that is live. BEHAVE uses a modified version which incorporates all size classes and a different weighting parameter for the fuel loading of each component. The live fuel moisture of extinction, $M_{x,living}$, is written as (Albini, 1976b):

$$M_{x,living} = 2.9W'\left(1 - \frac{M'_{f,dead}}{M_{x,dead}}\right) - 0.226 \text{ [fraction} \geq M_{x,dead}\text{]}, \tag{4.3}$$

where,

$$W' = \frac{\sum_{dead} W_{0,j} \exp(-138/\sigma_j)}{\sum_{live} W_{0,j} \exp(-500/\sigma_j)}, \tag{4.4}$$

$$M'_{f,dead} = \frac{\sum_{dead} W_{0,j} M_{f,j} \exp(-138/\sigma_j)}{\sum_{dead} W_{0,j} \exp(-138/\sigma_j)}, \tag{4.5}$$

and

$W_{0,j}$ = oven-dry loading of size class j [tons/acre],

σ_j = surface-area-to-volume ratio of size class j [ft^{-1}],

$M_{f,j}$ = moisture content of size class j [fraction].

Equations 4.3 to 4.5 were inserted into a spreadsheet program for each of the nine experimental and two control plots of the present study, in order to calculate the live fuel moisture of extinction as calculated by BEHAVE, see Table 4.16.

Table 4.16: Calculated live fuel moisture of extinction.

Plot	Live Fuel Moisture of Extinction, %	No % Coverage Reduction for Load, %
K1289W	1462	974
E1292W	1171	779
K1592W	440	325
G2390W	1100	863
I1792W	493	404
I1892S	8511	4033
K1489S	1562	1107
K1492S	3159	1892
M1392S	4867	2702
TP01S	484	361
TP06S	1128	748

The values in column 2 represent the live fuel moistures of extinction when using the appropriate inputs from each of the eleven custom fuel models. These values are given as percentages, and so the calculated values of live fuel moisture of extinction range from 440% to over 8500%, for the eleven burn plots. This would indicate that the live fuels will be predicted to burn in all cases. The usefulness of these values is questionable as the moisture content of most live fuels probably never exceeds 300-400%, see Table D.1, and usually not over 200% for the pine - oak forests.

Equation 4.3 predicts high values of moisture of extinction when the fraction of live fuels is low. That is, when there is a lot more dead fuel than live fuel, it is assumed that there is a high amount of effective heat being produced to bring the live fuels to ignition. This effective heat is equal to the heat of preignition at very high values of moisture content, and therefore, a large moisture of extinction is predicted. Live fuel fractions for the nine burn plots ranged from 0.02 for plot I1892S (moisture of extinction

of 8500%) to 0.30 for plot K1592W (moisture of extinction of 440%). The effect of the small live fuel fractions may have been magnified when the live fuel loads were reduced in the custom fuel models depending on the percent coverage of the shrub component. For comparison, if 100% coverage is assumed and the un-reduced values of fuel loading for each size class are used, see Tables 4.2, 4.3 and 4.4, then the live fuel moistures of extinction are significantly reduced, as shown in the third column of Table 4.16. However, these alternative values are still generally well above 325%, and so this does not resolve the uncertainty of values given by equation 4.3.

These results indicate that the live fuels will contribute to overall fire behavior within the prediction model, and will continue to be predicted to burn until the ratio of live to dead fuel approaches a value of one or higher. This agrees with the assumption that both the live and dead fuels will burn when sufficient fine dead fuel exists and the dead fuel moisture content is low enough relative to its moisture of extinction (Albini, 1976b). Similarly, if the dead fuel is too moist or its load is too light relative to the live load, then only the dead fuel will burn, although the live fuel continues to act as a heat sink, absorbing heat from the advancing flame front and slowing the rate of spread. In the first case, where both are burning, each is producing a reaction intensity and the model simply adds them together. In the latter case, only a dead fuel reaction intensity is produced and the live fuels primarily affect the denominator, or heat sink portion, of the spread equation.

It appears that the live fuels are a key parameter within the pine - oak forest fuel complex. BEHAVE is predicting these live shrubs to burn, although the magnitude of their contribution appears to be very dependent on the season in which they are burned.

This corresponds to the moisture content of the live fuels, where the higher values during the summer produce a greater heat sink and decrease the predicted fire behavior. A more detailed analysis is necessary to examine how each of the live fuel parameters enter into the fire spread equations and what, if any, impact will uncertainties in measuring or estimating these parameters have on prediction outcomes. This applies to all of the fuel and environmental parameters, and a similar analysis would help to determine the relative importance of each, the effectiveness of their measurement process, and indicate possible sources of errors in fire behavior predictions. Such an analysis follows for the pine - oak forests in the form of a sensitivity study.

5. Analysis of BEHAVE

5.1 Sensitivity Study

A sensitivity study is an analysis of how changes in model parameters affect the results generated by the model (American Society for Testing and Materials [ASTM E1355], 1992). A complete sensitivity study of BEHAVE including all combinations of variations in input parameters would require an extremely large number of computer runs to view the effects on each fire behavior characteristic. The present analysis focuses only on changing each input parameter independently, while all others are held constant. Using the subprogram TSTMDL, the variations in predicted spread rates and flame lengths resulting from changes to single input parameters were evaluated in graphical form over the allowable range, as outlined by Burgan (1987) and Burgan and Rothermel (1984). These graphs provide a general display of the interaction between input parameters and fire behavior predictions. In order to analyze the sensitivity of BEHAVE to variations in input parameters, an interval of interest for each of the fuel and environmental parameters was established. These intervals were based on either the range of values present on the day of the burn, the estimated error in the data collection process, or other stated criteria. The corresponding variation in predicted spread rates and flame lengths was then evaluated.

The general guidelines for establishing the sensitivity of the model to, or relative importance of, each input parameter were based primarily on the degree of change in the

two fire behavior characteristics - spread rate and flame length. The degree of change in input parameter is calculated as: $(I_{upper} - I_{lower})/I_{lower}$, where I_{upper} and I_{lower} are the upper and lower values in the interval of interest. For example, if the 1-hr fuel load was varied between 1 and 3 tons/acre, the degree of change would be 2. The degree of change in output, or predicted fire behavior, is calculated as: $|O_{upper} - O_{lower}|/O_{lower}$, where O_{upper} and O_{lower} are the output values corresponding to the upper and lower input parameters, respectively. If an increase in 1-hr fuel load from 1 to 3 tons/acre produces a decrease in flame length from 4 to 2 feet, this is equivalent to a degree of change in output of 0.5. This provides a consistent method of evaluating each input parameter and, by evaluating the ratio of the degree of change of output to the degree of change of input, the input parameters can be ranked according to the fire prediction model's sensitivity to each. An analysis follows for each of the input parameters, including an establishment of the interval of interest, the corresponding variations in predicted spread rates and flame lengths, and the degree of change of both input and output parameters. The causes within the fuel and fire prediction models for the interactions between the important parameters will also be discussed. The input parameters will be ranked based on their impact on fire behavior predictions.

5.1.1 1-hr S/V Ratio

The 1-hr surface-area-to-volume ratios were not measured for the various fuels in this complex, so the accuracy of the values chosen is not known. The values used throughout each of the custom fuel models were 2000 and 1500 ft^{-1} for 1-hr litter and

shrub fuels, respectively. These values correspond to the mid-range of suggested values by Burgan and Rothermel (1984) for various grasses, broadleaved plants and conifer needles. It is assumed that actual values of 1-hr S/V ratio in the litter and shrub understories of the pine - oak forests would tend to fall within this range, although the variability between the various species is unknown. A large interval of interest was chosen for evaluation, 1000 to 3500 ft^{-1}, corresponding to a degree of change of 2.5.

For each of the custom fuel models, the predicted spread rates increased with increasing 1-hr S/V ratio, rising faster with the higher values, or finer fuels, see Figure 5.1 for typical behavior. Over the interval of interest, spread rates doubled on average, with degrees of change ranging from 0.7 to 1.8. For the winter burns where predicted fire behavior was higher than for the summer, the degrees of change had more practical significance.

For instance, over the interval of interest, spread rates for plot K1492S increased from about 0.5 to 1.5 ft/min, or a degree of 2.5. These spread rates fall in the lower end of the first hazard level as described in Table 3.2 and cause little concern. The practical significance is increased with plot K1592W, where spread rates were predicted to increase by a similar degree of 2.8, or approximately 5 to 14 ft/min, which includes the first and second hazard levels in Table 3.2. This suggests that when predicted spread rates are higher, errors in approximating the 1-hr S/V ratio can have a greater effect on the usefulness of spread rate predictions.

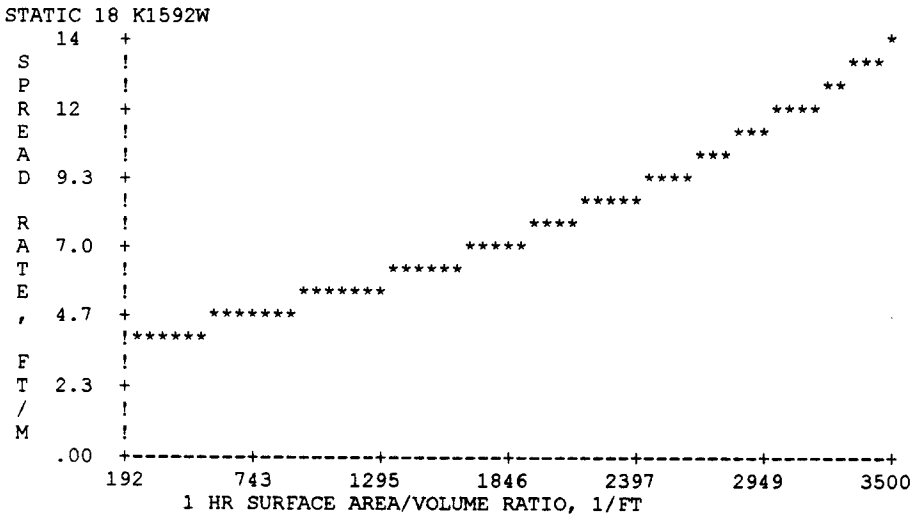

Figure 5.1: Predicted spread rate vs. 1-hr S/V ratio for plot K1592W.

As 1-hr S/V ratio was increased, predicted flame lengths increased initially, peaking at a S/V ratio between 500 to 1000 ft^{-1}. Flame lengths then decreased over the rest of the interval as shown in Figure 5.2. The interval of interest fell within this region of decrease in flame lengths, which was small, ranging from a degree of change of 0.1 to 0.3.

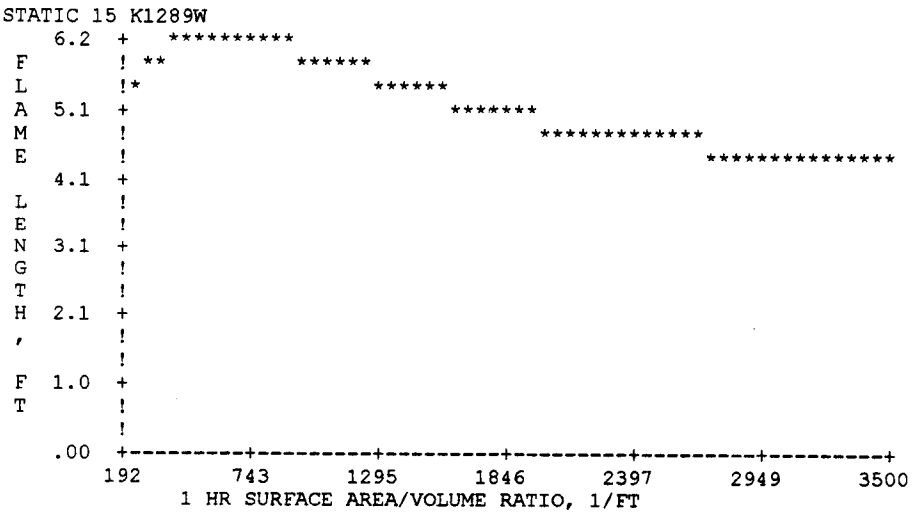

Figure 5.2: Predicted flame length vs. 1-hr S/V ratio for plot K1289W.

The interaction between spread rates and flame lengths with 1-hr S/V ratio is complex, as several of the parameters and weighting factors in the spread equation, equation 2.2, have been written in terms of this parameter. Whether or not spread rates and flame lengths increase or decrease with increasing 1-hr S/V ratio, depends greatly on the behavior of the potential reaction velocity, Γ', found in the reaction intensity term of equation 2.4 which can be written as:

$$I_R \approx \rho_b \delta h \Gamma' \eta_M \eta_s. \tag{5.1}$$

Recall from equations 2.12a-c that Γ' is written in terms of β/β_{op} and σ, and is at its maximum at β_{op}. For tightly packed fuel beds where $\beta/\beta_{op}>1$, as is the case for each of the burn plot fuel models, Γ' decreases with increasing 1-hr S/V ratio. This causes similar behavior in the reaction intensity.

The reaction intensity is in the numerator of the spread equation and therefore has a decreasing effect on the overall rate of spread.

$$R = \frac{I_R \xi (1 + \phi_w + \phi_s)}{\rho_b \varepsilon Q_{ig}} \text{ [ft / min]}, \tag{2.2}$$

This is overshadowed, however, as both the propagating flux ratio, ξ, and wind coefficient, ϕ_w, increase with increasing σ, thereby increasing the numerator of the spread equation, see equations 2.13 and 2.14a-d.

In the denominator of equation 2.2, the effective heating number, ε, is dependent on σ, as shown in equation 2.8. As σ increases, so does ε, resulting in an increase in the denominator. Overall, the effect of increasing 1-hr S/V ratio is an increase on predicted spread rates.

The behavior of predicted flame lengths to increases in 1-hr S/V ratio was very similar to the behavior of Γ' and I_R with changes in 1-hr S/V ratio. This can be seen by combining the relations for the heat per unit area and fireline intensity from equations 2.21 and 2.22 into equation 2.23 and writing flame lengths as:

$$F_L = 0.45(I_R R t_r/60)^{0.46}. \qquad (5.2)$$

From the above discussion, we know that the reaction intensity is decreasing, while the spread rate is increasing with increasing 1-hr S/V ratio. Overall, however, the effects of the reaction intensity overshadow this behavior along with the additional σ term in the denominator from $t_r = 384/\sigma$ (Andrews, 1986), causing the pattern found in Figure 5.2. The decrease over the interval of interest for each burn plot has been found to be small, which would result from the near square root exponent in equation 5.2.

Predicted spread rates are sensitive to variations in 1-hr S/V ratio, although flame lengths are not. Brown (1972) suggested that the contribution of these fine fuels may be overemphasized in the fire prediction model. This is consistent with results obtained for

grassland fuels (Gould, 1991) where the wide variability of possible values for S/V ratios leads to substantial errors in predictions.

5.1.2 Woody S/V Ratio

A value of 1350 ft^{-1} was used as an estimate for the live woody surface-area-to-volume ratio in each of the custom fuel models. Within the shrub component, this includes both the leaves and small stems of the live fuels. The variability in S/V ratio between these two components of the live fuels is not known and so the live woody S/V ratio was varied over the same interval as the 1-hr S/V ratio. Predicted spread rates generally decreased with increasing live woody S/V ratio, with the exception of plots K1289W and K1592W which decreased in spread rate over about half the range then increased slightly. The changes in predicted spread rates were small, averaging less than 0.5 ft/min, or degrees of change ranging from <0.1 to 0.3. Predicted flame lengths also decreased with increases in this parameter, with degrees of change ranging from <0.1 to 0.3.

The effects of this parameter on predictions can be explained qualitatively by the fact that, while the live fuels are contributing to fire behavior, they are also very wet and are absorbing heat from the advancing flame front. This effect is amplified as the S/V ratio increases and a larger fraction of these fuels must be heated to ignition. This is seen quantitatively with the effective heating number in equation 2.8, which is based on the finding that a larger fraction of a fuel particle is required to be heated to ignition as the fuel particle size gets smaller. This increases the heat sink portion of the spread equation

and overall, there is a decrease in predicted spread rates and flame lengths with increasing live woody S/V ratio.

The small increase in predicted spread rates over the range of about 2000 to 3500 ft^{-1} for plots K1289W and K1592W were not significant, although most likely due to the slightly higher windspeeds (Burgan & Rothermel, 1984). The increasing wind coefficient in the numerator of the spread equation would overcome the decreasing parameters, causing an overall increase in spread rate.

5.1.3 1-hr Fuel Load

In order to estimate an interval of interest for the total 1-hr fuel load, it was necessary to first estimate the accuracy of obtaining litter load values using the techniques mentioned in Chapter 4. Recall that four subplots of size 100 cm x 40 cm were chosen out of each of the 20 m x 20 m burn plots. From these subplots, the litter, standing dead and live woody fuel loads were computed for the entire plot. This could be viewed as sampling a population of 4 out of 1000 subplots. A simplifying assumption was made that the 1000 subplots make up a normally distributed population and that the 4 subplots are a random sample. This is reasonable when considering the litter load as it usually covers 100% of the plot and is relatively uniform.

The needed random sample size, n, for a specified half-width h_w, confidence coefficient $1-\alpha$, and planning value for the population standard deviation ω, is (Neter, Wasserman, & Whitmore, 1993):

$$n = \frac{z^2 \omega^2}{h_w^{\,2}}, \tag{5.3}$$

where $z = z(1-\alpha/2)$ is the percentile of the standard normal distribution, or the number of standard deviations away from the mean. Solving for h_w, we can estimate the accuracy of the litter load measurements by obtaining the width of the confidence interval around the population mean.

The confidence coefficient was chosen to be 0.95, commonly accepted in experimental methods. The planning value of the population standard deviation refers to the standard deviation that would be obtained if the entire population was sampled. No data of this type was available for comparison, and so sample standard deviations were first computed from the four litter load measurements taken for each of the burn plots. Each of the deviations were in close agreement between plots and so it was felt reasonable by the author to assume that the average of all of the sample standard deviations would closely represent the population standard deviation. This value was taken to be $\omega = 0.7$ tons/acre. From equation 5.3, with $n = 4$, $z = 1.96$, and $\omega = 0.7$, the half-width, h_w, of the 0.95 confidence interval was found to be approximately 0.7 tons/acre. With 95% confidence, the litter load estimates will be precise to ±0.7 tons/acre when sampling 4 out of 1000 subplots.

Since most of the shrub component of the total 1-hr fuel load was determined from the downed woody fuel inventory method, the accuracy was taken to be ±20%, as suggested by Brown (1974). Combining the precision of ±0.7 tons/acre for the litter load

and ±20% for the 1-hr shrub load, the overall interval of interest was computed for each of the burn plots, see Table 5.1.

Table 5.1: 1-hr fuel load intervals of interest.

Fuel model. Plot	Range (tons/acre) (degree of change)
14. I1892S	3.65 - 5.27 (0.4)
15. K1289W	4.22 - 5.98 (0.4)
16. K1489S	3.89 - 5.83 (0.5)
17. E1292W	3.75 - 5.57 (0.5)
18. K1592W	4.40 - 6.14 (0.4)
19. K1492S	4.46 - 6.30 (0.4)
20. M1392S	4.44 - 6.10 (0.4)
21. G2390W	5.65 - 7.47 (0.3)
22. I1792W	9.91 - 11.91 (0.2)

The effect of increasing 1-hr fuel load is similar for both predicted spread rates and flame lengths. Figure 5.3 shows the typical sharp increase which levels off toward a peak, then slowly decays. For each of the burn plots, the 1-hr fuel load intervals of interest tended to fall close to the peak, or stable portion of the curve, and so the variations in predicted fire behavior with increasing 1-hr fuel load were generally small. Spread rates were predicted to increase or decrease by less than 1 ft/min, and flame lengths by, at most, 0.5 ft. These corresponded to degrees of change in spread rates of <0.1 to 0.3, and flame lengths of 0.1 to 0.3.

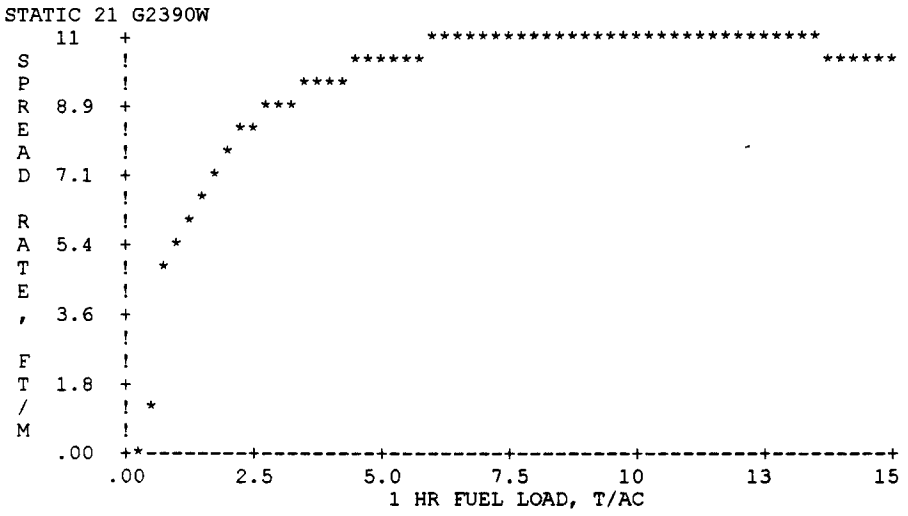

Figure 5.3: Predicted spread rates vs. 1-hr fuel load for plot G2390W.

The behavior of predicted spread rates and flame lengths to increasing 1-hr fuel load is governed primarily by the reaction intensity. This is caused by the dependence of reaction intensity on the oven-dry fuel load, w_o, through the reaction velocity term. Equation 2.12a can be approximated as:

$$\Gamma' \propto \Gamma'_{max} (w_o)^A \exp[A(1-w_o)]. \tag{5.4}$$

Over the range of 1-hr fuel loads, the reaction velocity increases with increasing fuel load until the optimum packing ratio is reached, followed by a decrease in the reaction velocity (Burgan, 1987). This pattern was followed closely by the predicted spread rates and flame lengths for each of the plots.

5.1.4 10-hr Fuel Load

For each of the custom fuel models, the predicted spread rates and flame lengths decreased with a corresponding increase in 10-hr fuel load. This is not, however, felt to be an important parameter to the pine - oak forests in this particular location. This is due to the extremely low values of this size-class (0-.24 tons/acre) in each of the fuel models, see Figures C.1 to C.9. During the 1992 downed woody fuel inventory of the 58 test plots, 10-hr fuel loads never exceeded 0.7 tons/acre.

5.1.5 100-hr Fuel Load

A reasonable interval of interest for the 100-hr fuel load was determined to be ±20%, as suggested by Brown (1974) for values determined by the downed woody fuel inventory. This corresponds to a degree of change averaging 0.5. Increasing this parameter caused a decrease in predicted spread rates and flame lengths, agreeing with the guidelines of Burgan and Rothermel (1984) on changing fuel load. The degree of change in predicted spread rates and flame lengths was small, ranging from <0.1 to 0.2. For plots E1292W, M1392S and I1792W, the actual values of 100-hr fuel load were very small (<0.7 Tons/Acre) as determined from the fuel inventory, and so they were not included in the sensitivity study, due to the lack of precision of the TSTMDL graphs when evaluating these small intervals of interest. The behavior of predictions to variations in 100-hr fuel load for these plots, however, was similar to the other plots.

The primary reason for the decrease in fire behavior with increasing 100-hr fuel load is the corresponding decrease in the characteristic S/V ratio for the entire plot

(Burgan, 1987). The addition of the larger fuels, which have a low S/V ratio, increases the weighting parameter for that size class, therefore decreasing the calculated characteristic value. The increasing S/V ratio along with increasing the fuel load in tightly packed fuels creates an overall reduction in predicted spread rates and flame lengths.

5.1.6 Live Woody Fuel Load

Although the live woody fuel load was determined by the same method as the litter load, it may not be acceptable to use the same simplified method of determining the precision of the estimates. While the litter layer usually covers 100% of the area, the live woody fuels average between 60 and 70% coverage. Also, the data included load estimates for both the leaves and stems of the live fuels along with different species which were highly variable between plots, and so estimating a population standard deviation would be difficult. Considering these non-uniformities and variabilities in this fuel component, it is unlikely that sampling 4 out of 1000 subplots could statistically represent the entire plot and fulfill the requirements of a standard normal distribution (Neter et al., 1993). From a lack of any historical data for this fuel complex, a precision of ±50% has been arbitrarily chosen as a possible worst case. This corresponds to a degree of change of about 2.0.

In general, predicted spread rates decreased with increasing live woody fuel load, with the exception of plot G2390W which has a slight initial increase before decaying. The behavior of predicted flame lengths appeared to be seasonally dependent, with summer flame lengths decreasing with increasing live woody fuel load, and winter flame

lengths increasing initially then decreasing. The changes in predicted fire behavior were small over the ±50% interval of interest, with virtually no change in flame lengths (a degree of change averaging <0.1). The decrease in spread rates was slightly higher, but only to a degree of up to 0.3.

The effects of increasing the live fuel load on predictions are similar to those with the dead fuels. The reaction velocity will increase to the optimum packing ratio, then decrease, causing similar behavior in the live fuel reaction intensity. The overall effect of each of the variables within the spread equation, however, depends on several interactions, including the change in the characteristic S/V ratio with increasing live load which also affects several variables. This effect will also vary between plots depending on the amount of live and dead fuels present in the fuel model.

There was, however, a seasonal difference in the effects of changing live fuel loads. This can be attributed mainly to the wide variation in live fuel moistures during the two seasons. It has been stated earlier that the live fuels appear to be acting mainly as a heat sink in the overall spread process, due to increases in the denominator of the spread equation with increasing live S/V ratio and fuel load. The magnitude of this effect, however, is going to vary between the seasons due to the live moisture content and its effect on the heat of preignition in the denominator of the spread equation. Recall, from equation 2.9 that:

$$Q_{ig} = 250 + 1{,}116M_f. \qquad (2.9)$$

During the summer months when the live leaf moistures averaged 160% and stems 90%, the overall fuel bed moisture content, M_f, is greater than that during the winter when live stem moistures averaged 50%. This produces a larger heat of preignition, and therefore a larger denominator, which dampens the effects of changing other variables. Similarly, the live fuel moisture damping coefficient, found in the live fuel reaction intensity, equation 2.4, is also different between seasons. The moisture damping coefficient, η_M, is written as (Rothermel, 1972):

$$\eta_M = 1 - 2.59\left(\frac{M_f}{M_x}\right) + 5.11\left(\frac{M_f}{M_x}\right)^2 - 3.52\left(\frac{M_f}{M_x}\right)^3. \qquad (5.5)$$

Assuming a live fuel moisture of extinction, $M_{x,living}$, of 400%, a live fuel moisture content during the winter would yield a value for η_M of about 0.75. However, a summer live leaf moisture content of 160% gives a value of about 0.55. The higher moisture contents during the summer produce a lower coefficient, which "dampens" the effects of the live fuel reaction intensity. Combining the effects of the lower fraction of the reaction intensity that is released during the summer, and the higher heat of preignition, creates a greater heat sink effect than in the winter, and hence the different behavior in predicted spread rates and flame lengths.

5.1.7 Fuel Bed Depth

The interval of interest for fuel bed depth was determined from the range of measurements of shrub depth taken before each burn, see Table 4.5. The minimum and maximum values of the huckleberry (Gaylussacia bacata) height were used since this was the dominant shrub species of the burn plots. Litter depths were held constant, as they were small compared to the overall depth. To calculate the interval of interest, the height values in Table 4.5 were multiplied by the percent coverage of the shrub component for each plot, and the characteristic fuel bed depth was then determined using the weighting procedure discussed in Chapter 2. Table 5.2 gives the range of fuel bed depth values determined for each burn plot.

Table 5.2: Fuel bed depth intervals of interest.

Fuel model. Plot	Range (ft) (degree of change)
14. I1892S	0.07 - 0.21 (2.0)
15. K1289W	0.39 - 0.83 (1.1)
16. K1489S	0.20 - 1.09 (4.5)
17. E1292W	0.40 - 0.90 (1.3)
18. K1592W	0.57 - 0.92 (0.6)
19. K1492S	0.17 - 0.35 (1.1)
20. M1392S	0.17 - 0.26 (0.5)
21. G2390W	0.64 - 1.60 (1.5)
22. I1792W	1.14 - 1.62 (0.4)

Predicted spread rates increased nearly linearly with increasing fuel bed depth, as shown in Figure 5.4 for plot K1289W. Degrees of change ranged from 0.7 to 6.0, resulting in wide variability in predicted spread rates over the possible range of depth values. For each of the summer plots, BEHAVE predicted fires to not spread at the minimum value of the interval of interest. The maximum values still under-predicted

spread rates for plots M1392S and K1489S over the whole range of observed values, see Figure 4.3. For the winter plots, the maximum value of the interval of interest for plot G2390W resulted in an over-prediction of about 10 ft/min (the difference between about 6 and 16 ft/min). This has some practical significance, when using the guidelines of Table 3.2, as the two values represent a very slow-moving fire close to the first hazard level, and a fire moving well into the second level.

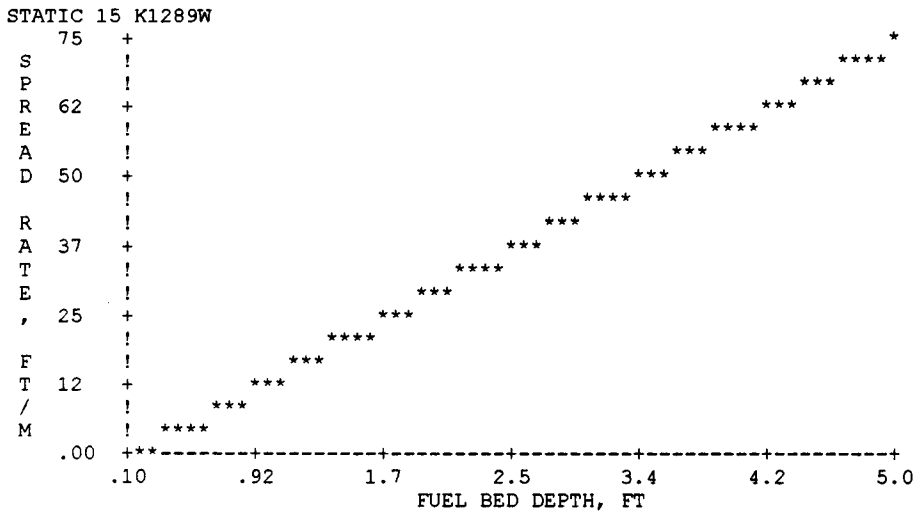

Figure 5.4: Predicted spread rates vs. fuel bed depth for plot K1289W.

Figure 5.5 shows the typical behavior of flame lengths to variations in fuel bed depth. There is a sharp increase in the beginning, lessening with higher values of depth. In general, due to the relatively small values for fuel bed depth, the interval of interest for each of the fuel models fell within this region of sharp increase, making flame lengths also sensitive to changes in this parameter. Degrees of change varied widely from about 0.5 to 15.0. Practically, the changes in flame lengths for the winter plots were of most significance, as they varied between the first and second hazard levels as outlined in Table

3.1. For instance, plot K1289W ranged from <2 up to 6.5 ft flame lengths over the interval of interest, which would have resulted in an over-prediction, see Figure 4.4. Plot K1592W was over-predicted for the entire interval of depth values. As in the spread rate case, the summer plots were predicted not to burn at the low end of the depth interval, and flame lengths were under-predicted over the whole ranged of observed values for plots M1392S and K1489S.

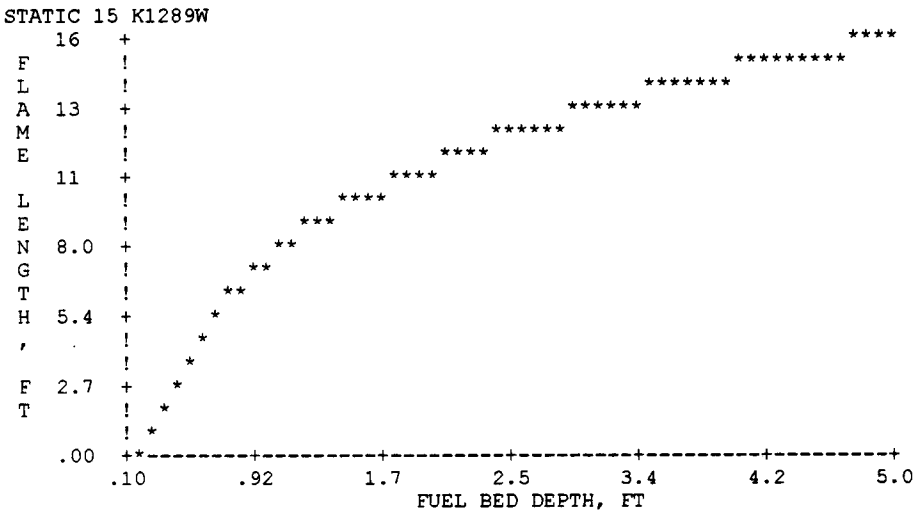

Figure 5.5: Predicted flame lengths vs. fuel bed depth for plot K1289W.

In order to analyze the dependence of predicted spread rates on fuel bed depth it is helpful to look at each of the terms in the spread equation to view their behavior as this parameter is varied. Recall from equation 2.13 that the propagating flux ratio was written as:

$$\xi = (192 + 0.2595\sigma)^{-1} \exp[(0.792 + 0.681\sigma^{.5})(\beta + 0.1)]. \qquad (2.13)$$

The packing ratio, β, is inversely proportional to the fuel bed depth so we have that $\xi \propto \exp(1/\delta)$. As δ increases the exponential term decreases causing a decrease in ξ, and the numerator of the spread equation. The potential reaction velocity also depends on δ, as seen in the packing ratio term of equation 2.12a:

$$\Gamma' = \Gamma'_{max} (\beta/\beta_{op})^A \exp[A(1-\beta/\beta_{op})]. \qquad (2.12a)$$

Each of the burn plots are at greater than optimum packing ratio, $\beta/\beta_{op} > 1$, making $1-\beta/\beta_{op} < 0$. This approaches zero as δ increases, and so the exponential term of equation 2.12a increases. The term $(\beta/\beta_{op})^A$ affects the magnitude of Γ'. Combining the effects on Γ' with the additional depth term in equation 5.1, there is a strong increase in reaction intensity with increasing fuel bed depth. A similar dependence is found with the wind coefficient, ϕ_w, which from equation 2.14a can be written,

$$\phi_w = CU^B \left(\frac{\beta}{\beta_{op}}\right)^{-E} \propto (\delta)^E, \qquad (5.6)$$

where E is a small exponent determined by equation 2.14d. The effects of increasing depth are amplified at higher wind speeds, as the wind coefficient is also directly proportional to this speed, U. Lastly, an additional depth term is found in the denominator

of the spread equation, as $\rho_b \propto 1/\delta$, causing an increase in spread rate. The combination of each of these terms produces an overall linear dependence of spread rates on fuel bed depth. The behavior of flame lengths to increasing fuel bed depth follows from $F_L \propto (R)^{1/2}$ in equation 5.2.

Predicted spread rates and flame lengths are sensitive to changes in fuel bed depth. During the winter, the amount of over-prediction could be accounted for by this parameter alone, as variations in depth typically produced predictions that covered the whole range of observed behavior. For spread rates, the plot with the greatest depth, G2390W, had the greatest over-predictions. Also, plots K1289W, K1492W and G2390W had slightly higher windspeeds than the other plots, increasing the sensitivity of predictions to depth changes. This suggests that when burning conditions are closer to optimum or extreme, such as with higher wind speeds, winter burning and taller shrubs, errors in estimating the fuel bed depth may produce the least accurate predictions. This is complicated even further by estimating the percent coverage of the fuel component, which alters the fuel bed depth measurement further. However, if the actual values of the huckleberry height were used, assuming 100% shrub component coverage, spread rates would be even more over-predicted. There is a more complicated interaction in this case, as the packing ratio of the fuel bed would also change with the increase in fuel load, and so a definite conclusion about the percent coverage reduction cannot be made.

For the summer burns, under-estimating depth could significantly under-predict fire behavior, or even predict the fire not to spread or produce flames when they actually will. Since most of the depth is governed by the live shrub height, reducing the depth is, in

effect, equivalent to compacting all of the wet fuels, which are acting as a heat sink and smothering the fire.

With these considerations, the effect of fuel bed depth on fire behavior predictions appears to be over-emphasized for this fuel complex. A similar conclusion was made under more controlled settings with grassland fuels (Gould, 1991). Grass fuel beds were constructed to various heights, loads and densities. It was found that observed rates of spread were not as sensitive to fuel bed depth as that predicted. Also, that there was no consistent relationship between observed flame lengths and fuel bed depths for the grass fuels, although the fire prediction model generally under-predicted them. Spread rates in the grassland study were under-predicted in low fuel bed depths (<0.15m or 0.5 ft), and over-predicted in higher depths (>0.25m or 0.8 ft) and higher wind speeds (>3.5 m/s or 8 mi/hr).

For the pine - oak forest, there is a clearer distinction between the seasons of the burns than between the fuel bed depths, and so a distinct transition between under- and over-predictions at certain depths cannot be made. However, as stated earlier, it does appear that greater depths do lead to greater over-predictions, as was the case for plot G2390W.

5.1.8 Moisture of Extinction

The interaction between moisture of extinction and predicted fire behavior depends largely on the moisture content of the dead fuels, and in particular the 1-hr fuels. Figure 5.6 shows the effect on spread rates of increasing the dead fuel moisture of extinction for

plot K1489S, where the 1-hr fuel moisture content was about 15%. For moisture of extinction values equal to or less than this value, predicted spread rates are zero. There is then a sharp increase in spread rates as this parameter is increased from about 15 to 20%, which then begins to level off. The greater the difference between fuel moisture and moisture of extinction, the greater the predicted spread rate. Similar behavior is found with predicted flame lengths.

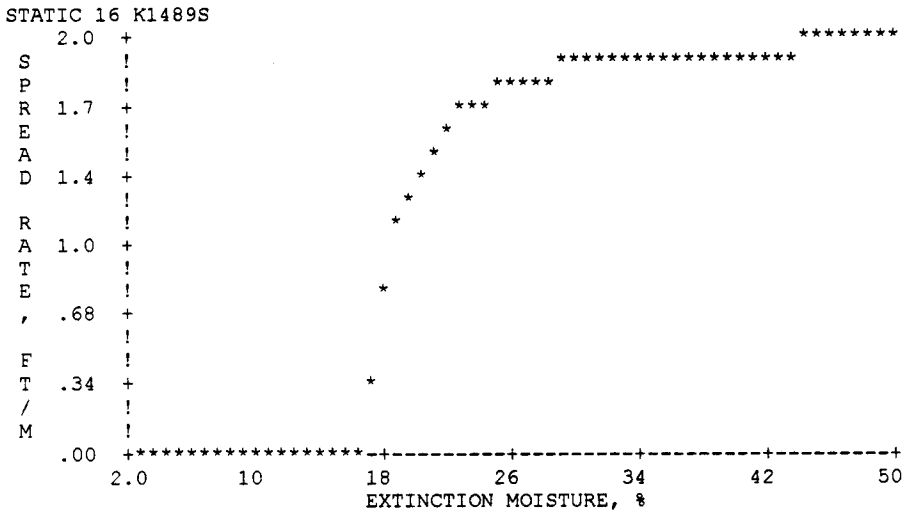

Figure 5.6: Predicted spread rates vs. dead fuel moisture of extinction for plot K1489S.

The values of moisture of extinction predicted by BEHAVE for each fuel model fell well outside of the steeply sloping portion of the curve, indicating a sufficiently large difference between fuel moisture (primarily 1-hr) and moisture of extinction. This also results in a low sensitivity of the fire prediction model to changes in moisture of extinction.

The moisture of extinction has not been determined under controlled experiments for the pine - oak forest fuel complex. A study was conducted under field conditions, however, where random litter beds were ignited under various moisture conditions to determine if the fire would spread (Patterson, 1996). A moisture of extinction of the litter was found to be approximately 20%. This is a much lower value than that predicted for the majority of the plots. However, values for plots G2390W, I1792W, TP01S, and TP06S were predicted to be closer to 20%. These plots tended to have higher fuel bed depths and lower packing ratios than the other plots. Also, with the exception of plot G2389W which was burned once before 1990, each plot represents untreated conditions. This suggests that actual moisture of extinction values may be predicted well by BEHAVE under untreated conditions, but may loose accuracy as the calculated packing ratios increase.

5.1.9 Heat Content

From equation 2.4, the reaction intensity is linearly related to the heat content, and so a similar dependence is seen with predicted spread rates and flame lengths. The slope of this relationship is governed by the magnitudes of the other parameters within the fire spread equations. Because this variable is unknown for this fuel complex, its general behavior was analyzed over the whole interval allowed by TSTMDL, 7000 to 12000 Btu/lb, or a degree of change of .7. The resulting increase in fire behavior for each plot ranged from a degree of 0.6 to 0.7 for spread rates, and 0.6 to 0.8 for flame lengths.

The results of changing the heat content are very predictable, as any variations in the parameter result in direct and close to equal variations in fire behavior characteristics. As discussed in Chapter 4, however, the value of 8,000 Btu/lb used for the pine - oak forest fuel complex may not be accurate and may change during the year, especially for the live fuels. The effect of changing either the live or dead heat contents to more accurately portray the fire behavior of these fuels will depend on the quantity of each of these two fuel components. From equation 2.18:

$$h_{complex} = f_{dead}h_{dead} + f_{hb}h_{hb} + f_{wd}h_{wd}. \qquad (2.18)$$

The contribution of each component's heat content will depend on the weighting parameter associated with it, which is dependent on the relative S/V ratio and fuel loading for that component. With the typically large accumulations of litter in the pine - oak forests, the uncertainties in this component's heat content could account for some of the uncertainties in predicted fire behavior. Similarly, in areas of high live fuel loads, knowing the seasonal variations in heat content may help to better predict the potential fire behavior of this fuel complex.

5.1.10 1-Hr Moisture Content

The interval of interest for 1-hr moisture content was chosen separately for each of the custom fuel models depending on the range of recorded values for the litter and 1-hr fuels on the day of the burn, see Table 4.7. For the fire behavior predictions, the litter

moisture was used, whenever possible, for the 1-hr moisture content. However, when considering both fuel classes, there were often large variations. It is reasonable to consider this whole interval when evaluating the sensitivity of the prediction model to this parameter and in determining the optimum values to be used in the future. The corresponding degrees of change ranged from 0.2 to 3.0.

As shown in Figure 5.7, increases in 1-hr moisture content decrease predicted spread rates until the moisture of extinction is reached (a value of 29% for plot G2390W). At this point, predicted fire behavior becomes zero. As can be seen from the figure, the most sensitive areas are in the low moisture range (~2-10%) and where values are close to the moisture of extinction (~20-30%). Over the intervals of interest, degrees of change in spread rates ranged from 0.2 to 0.6. The changes in predicted spread rates were not of much practical significance, as they did not vary between hazard levels, as indicated in Table 3.2.

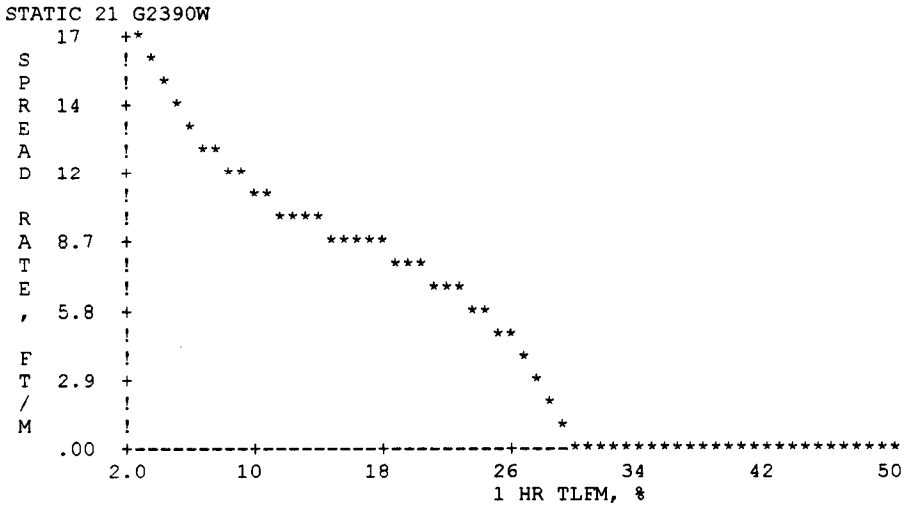

Figure 5.7: Predicted spread rates vs. 1-hr fuel moisture content for plot G2390W.

Predicted flame lengths decreased similarly with increasing 1-hr moisture content, reaching zero at the moisture of extinction, see Figure 5.8. The degrees of change ranged from 0.1 to 0.5. For summer burns, this corresponded to average decreases of about 0.5 ft, while for winter burns flame lengths decreased by up to 4 feet. The large interval of possible 1-hr fuel moisture values for plot I1792W resulted in flame length predictions ranging from about 4.5 to slightly over 9 ft. This is a large difference when considering the various interpretations of flame lengths found in Table 3.1.

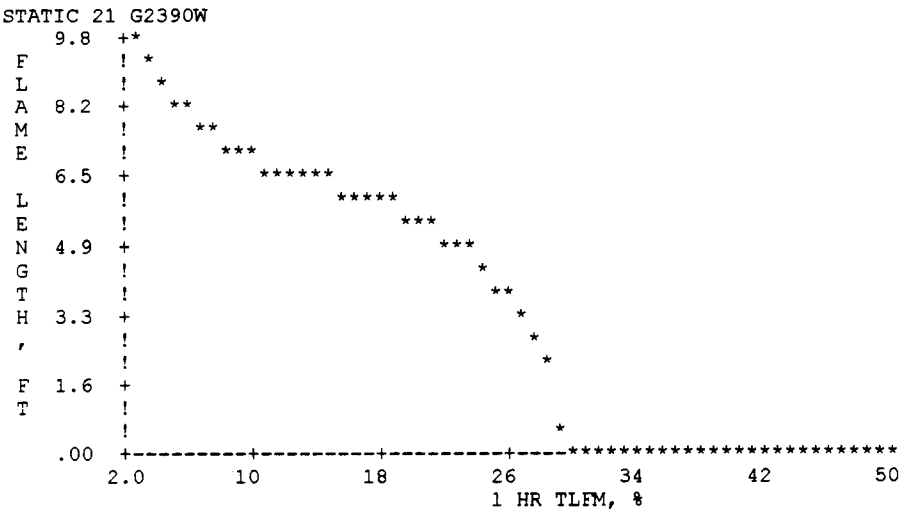

Figure 5.8: Predicted flame lengths vs. 1-hr fuel moisture content for plot G2390W.

The behavior of predicted spread rates and flame lengths to increases in 1-hr moisture content clearly shows the result of adjusting the litter moistures to account for the wintergreen surface fuels, as discussed in section 4.4.2.1. For plot G2390W, this corresponded to a range of 9.7 to 22.2%. In Figures 5.7 and 5.8, the curve levels out over this range, indicating a more stable region and a small change in predicted fire behavior. Similar behavior was found for the other winter plots when considering the difference

between litter moistures and adjusted moistures. Therefore, the use of an adjusted moisture content provides a means to fine tune fire behavior predictions without drastic changes.

The reasons for the decrease in spread rates with increasing 1-hr fuel moisture content are the effect that the variations have on the moisture damping coefficient and the heat of preignition, as discussed with the live woody fuel load parameter. Because the 1-hr fuels contribute the most to the characteristic fuel bed moisture content, their effect on these two variables are also the most significant. As the 1-hr fuel moistures increase, the characteristic fuel bed moisture content increases, and so the ratio M_f/M_x in equation 5.5 gets larger, decreasing η_M. This in turn reduces the dead fuel reaction intensity and the numerator of the spread equation. When $M_f = M_x$, the moisture damping coefficient, reaction intensity and spread rates equal zero. At the same time, the denominator is increasing as the heat of preignition increases causing an overall reduction in spread rates. These same reasons cause the similar decrease in predicted flame lengths.

5.1.11 10- and 100-Hr Moisture Content

No changes were predicted in fire behavior with a corresponding change in 10- and 100-hr moisture content.

5.1.12 Live Woody Moisture Content

As with the 1-hr moisture content, the live woody moisture content was varied over the range of measured values obtained on the day of the burn, see Table 4.7, ranging in degree of change from <0.3 to 1.3. Predicted fire behavior also decreased with

increasing live woody moisture content, although the change was not as dramatic as that which resulted with increasing 1-hr moisture content. This was due primarily to the lower fuel load of the live fuels and thus its lower contribution to the characteristic fuel bed moisture content.

The behavior of predicted fire behavior to changes in this parameter was largely season dependent. For summer burns, even though moisture contents varied widely between the live leaves and stems, there were minimal or no changes in predicted fire behavior. This effect increased slightly during the winter, although still to a small degree of change (<0.1). This is due primarily to the combination of lower live fuel loads and larger moisture content values during the summer, causing the prediction model to be less sensitive to changes in live fuel moisture. This supports the findings in Chapter 4 that separating the live leaf and stem loads within the fuel models during the summer does not affect the outcome of predictions.

5.1.13 Midflame Windspeed

The interaction between midflame windspeed and fire behavior was evaluated over the entire interval allowable, 0 to 18 mi/h. In general, predicted spread rates increased rapidly with increasing windspeed, especially for values over 3 mi/h, see Figure 5.9. Degrees of change ranged from 2.2 to 4.0, which resulted in spread rate increases of up to 11 ft/min per 1 mi/h increase in windspeed. Flame lengths increased in more of a linear fashion, with degrees of change ranging from 1.0 to 2.0, or up to a 1 foot increase per 1 mi/h increase in windspeed, see Figure 5.10. The exception to the above behavior was

plot I1892S, which was predicted to reach a maximum spread rate and flame length at a midflame windspeed of approximately 9 mi/h, holding constant at higher windspeeds. BEHAVE predicts fire behavior to reach a maximum when the effective windspeed, discussed in section 2.3.3, equals 1/100 of the reaction intensity (Burgan & Rothermel, 1984). This is based on findings that spread rates in grass fuels can actually decrease at windspeeds above a certain limit, due to wind forces being stronger than the heat transfer from the fire.

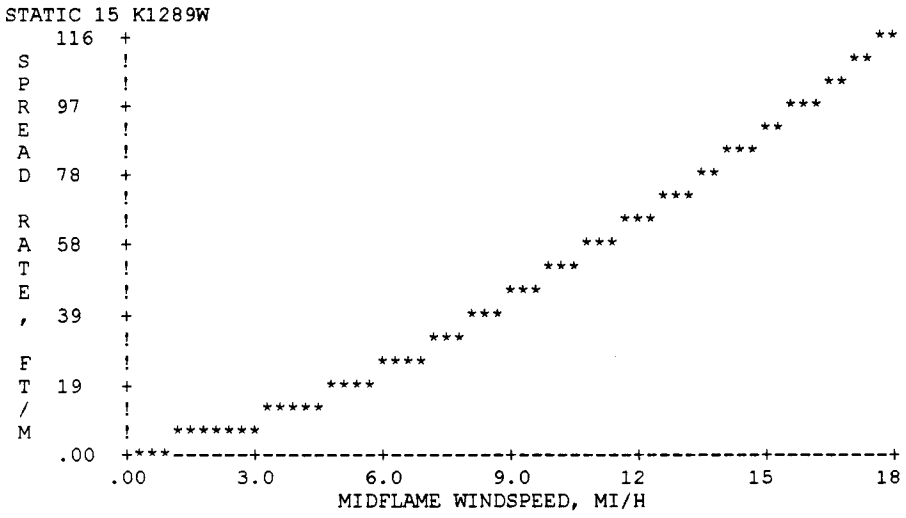

Figure 5.9: Predicted spread rates vs. midflame windspeed for plot K1289W.

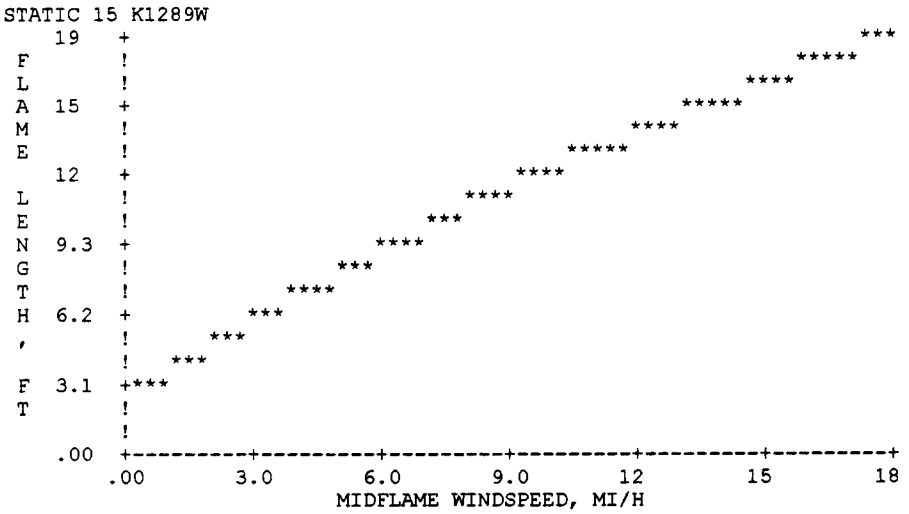

Figure 5.10: Predicted spread rates vs. midlflame windspeed for plot K1289W.

From equation 2.14a we see that the wind coefficient is proportional to the midflame windspeed, U, as $\phi_w \propto U^B$, where B is a number, dependent on σ and ranging from about 0.4 to 2.0. For large values of S/V ratio, the sensitivity of the spread equation to higher windspeeds is increased, as the wind coefficient becomes proportional to the square of the midflame windspeed. This effect is greatest in fuel beds at low packing ratios (Burgan, 1987).

This relationship has been examined in grass fuels (Gould, 1991), and it was found that observed rates of spread at various windspeeds suggested more of a linear (B = 1) relationship between spread rates and windspeed, as opposed to the "power of B" relationship as used in the prediction model. Spread rates were under-predicted for the grass fuels at low windspeeds and over-predicted at high wind speeds.

For the present study, observed fire behavior was compared to predictions evaluated over the range of recorded midflame windspeeds for each of the experimental

and control plots. This offers some indication as to the accuracy of the effect that the wind coefficient has on predicted fire behavior. If predicted spread rates at the upper range of midflame windspeed were well out of the range of observed fire behavior, then this may support the above findings that the power relationship within the coefficient is not applicable to every situation. Table 5.3 gives the results of this comparison.

Table 5.3: Observed vs. predicted fire behavior over range of midflame windspeeds.

		Observed		Predicted	
Plot	Midflame Windspeed	Spread Rates, ft/min	Flame Lengths, ft	Spread Rates, ft/min	Flame Lengths, ft
K1289W	0 - 5	2.0 - 6.5	1.0 - 4.0	2.2 - 18.18	2.8 - 8.2
E1292W	0 - 3.5		1.0 - 2.2		2.8 - 6.9
K1592W	0.7 - 6.2	1.5 - 12.0	1.3 - 3.5	2.2 - 17.17	3.2 - 8.6
G2390W	0 - 6	1.7 - 6.5	1.0 - 8.0	3.3 - 38.38	3.7 - 12.8
I1792W	0 - 3.5		3.0 - 5.0		4.4 - 11.0
I1892S	0 - 1.2	0.5 - 1.0	0.8 - 1.0	0.2 - 0.4	0.4 - 0.5
K1489S	0 - 5	6.0 - 12.5	3.5 - 11.0	1.1 - 10.10	1.8 - 5.4
K1492S	0 - 1.8	1.0 - 1.3	0.8 - 3.3	1.1 - 1.1	1.1 - 1.7
M1392S	0 - 1.8	1.1 - 5.0	1.2 - 2.8	0 - 1.1	0.8 - 1.3
TP01S	0 - 4.0	11.8 - 15	3.0 - 8.0	1.1 - 10.1	2.0 - 5.4
TP06S	2.0 - 4.0	20 - 26	3.0 - 7.0	5.5 - 11.11	4.3 - 6.3

From these results it can be concluded that, for the winter burns, the prediction model is very sensitive to changes in windspeed for this fuel complex. In fact, values of this parameter over as little as about 3 mi/h, appear to greatly over-emphasize the contribution of wind to overall fire behavior.

5.1.14 Slope

As suspected from the discussion of fire spread mechanisms in Chapter 2, predicted fire behavior increases with increasing slope. The increase is small for low

values (<30-50%), and then increases rapidly for higher values. This follows from the direct dependence of the slope coefficient on flame angle, see equation 2.15. This coefficient is also dependent on the packing ratio, although its effect is small (Burgan & Rothermel, 1984). Again, the one exception was plot I1892S, which was predicted to stop increasing at a slope of about 120%, then remain constant.

For each of the experimental plots, the slope was 0% and so there is little concern with the effects of slope for the majority of the research area. The small slope increases in the control plots, however, raise some concern as to the accuracy of the formulation of the slope coefficient. Spread rate and flame length predictions did not vary over the 7% increase in slope found on plot TP06S. However, there was an observed increase of approximately 6 ft/min in spread rates between the base of the slope and mid-slope. Fire behavior has also been observed to increase with slopes much less than 30% in previous prescribed burns in this fuel complex (W. A. Patterson, personal communication, 1996). The accuracy of the slope coefficient would have to be studied further with more supporting data.

5.2 Discussion

The fuel and fire prediction models contain a large number of parameters with complex interactions between each. The above analysis helps to isolate each of these parameters, evaluate their relative impact on fire behavior predictions, and identify potential strengths and weakness within the fuel and fire prediction modeling processes. This process can aid individuals involved in the management of these fuels through the use

of fire, by highlighting the parameters and data collection processes that require special attention in the future. Through this type of analysis, a better understanding of the modeling process is also obtained, along with a realization of how the future of fire modeling can improve.

5.2.1 Results of Sensitivity Study

Input parameters were varied based on data from each of the nine experimental plots in order to view any additional impact on the fire prediction model due to varying burn intervals or seasonal differences. The results are also applicable to the larger control plots as the behavior of fire predictions to variations in input parameters tended to be consistent and predictable. For instance, predicted spread rates are linearly related to fuel bed depth in every case and so similar behavior can be expected for the control plots.

In determining the importance of the input parameters, a process needs to be established which will place each parameter and its effects on fire behavior on the same scale, regardless of the size of the interval of interest. This will allow the parameters to be ranked with respect to their impact on fire behavior predictions. As discussed earlier, a ratio defined as the degree of change of the fire behavior characteristic to the degree of change of the input parameter was established. A higher ratio corresponds to a higher sensitivity of the fire prediction model to that parameter. Values of zero correspond to spread rates or flame lengths that did not change over the input parameter's interval of interest, and a blank indicates that the analysis was not possible for a particular plot.

Tables 5.4 and 5.5 give the results for the predicted spread rates and flame lengths, respectively.

Table 5.4: Ratios of degree of change of spread rate to input parameter.

Spread rate	I1892S	K1289W	K1489S	E1292W	K1592W	K1492S	M1392S	G2390W	I1792W	**Average**
1-hr S/V	.6	.3	.4	.4	.7	.6	.6	.3	.3	**.5**
Woody S/V	<.1	<.1	.1	.1	.1	.1	.1	0	0	**.1**
1-hr Load	.3	.1	.8	.3	.4	.1	.3	.2	.3	**.3**
100-hr Load	.3	.2	.2		.1	.1		.1		**.2**
Woody Load		.1	.1	.1	.2	.3		0	<.1	**.1**
Depth	3.0	3.5	2.3	3.9	1.6	5.7	9.4	1.7	1.3	**3.6**
Heat Content	1.0	.9	1.0	.9	.8	.8	.9	.9	.9	**.9**
1-hr Moisture	.4		.7	.2	.2	.3	.2	.6	.2	**.4**
Woody Moisture	0	.1	0	.2	.5	.1	0		.2	**.1**
Wind	2.2	2.1	4.0	2.1	2.2	2.2	2.9	2.4	2.3	**2.5**

Table 5.5: Ratios of degree of change of flame length to input parameter.

Flame Length	I1892S	K1289W	K1489S	E1292W	K1592W	K1492S	M1392S	G2390W	I1792W	**Average**
1-hr S/V	<.1	.1	.1	.1	<.1	.1	.1	.1	.1	**.1**
Woody S/V	.1	.1	.1	.1	.1	.1	<.1	.1	.1	**.1**
1-hr Load	.5	.2	.6	.4	.3		.3	.3	.5	**.3**
100-hr Load	.4	.2	.2		.2	.3		.1		**.2**
Woody Load		<.1	<.1	0	<.1	<.1		.1	<.1	**<.1**
Depth	3.0	2.2	3.4	1.3	1.5	.9	13.9	.8	.9	**3.1**
Heat Content	1.0	.9	.9	.8	.9	1.1	1.1	.9	.9	**1.0**
1-hr Moisture	.3		.7	.2	.2	.3	.2	.3	.2	**.3**
Woody Moisture	0	.1	0	.2	.3	0	0		.2	**.1**
Wind	.5	.4	.4	.4	.4	.4	.4	.4	.4	**.4**

As can be seen from Tables 5.4 and 5.5, the sensitivity study allows for the exclusion of a few of the input parameters. Variations in 10- and 100- hr fuel moisture content did not affect predicted fire behavior, and the 10-hr fuel load for this fuel complex was negligible. Thus, these parameters will not be considered in further analysis. Within the Lombard/Paradise Hollow research area, the slope was sufficiently small so that the fire prediction model did not recognize any changes in this parameter. While this insensitivity to small slope changes is questionable, for fire behavior prediction purposes this parameter does not need to be considered in this area. The moisture of extinction was also not included, as values predicted by the fire prediction model were not sensitive to changes and it was difficult to estimate an error in the model's calculation process. Several of the predicted values were found to be questionable based on field observations and so this parameter should be considered in the future.

The last column in Tables 5.4 and 5.5 provides the average ratios over all burn plots for each of the input parameters considered. From these values, the parameters were ranked in order of their relative impact on spread rate and flame length predictions, see Table 5.6.

Table 5.6: Ranking of input parameters.

Rate of Spread	Flame Lengths
Depth	Depth
Wind	Heat Content
Heat Content	Wind
1-hr S/V Ratio	1-hr Fuel Load
1-hr Moisture	1-hr Moisture
1-hr Fuel Load	100-hr Fuel Load
100-hr Fuel Load	Woody Moisture
Woody Moisture	1-hr S/V Ratio
Woody Fuel Load	Woody S/V Ratio
Woody S/V Ratio	Woody Fuel Load

For several of the variations in predicted fire behavior, the degrees of change may have been large, however there was little practical significance. For instance, with plot E1292W, the ratios of degree of change of fire behavior to fuel bed depth were 3.9 and 1.3 for spread rates and flame lengths, respectively. However, this was equivalent only to a maximum value of spread rates of 2.8 ft/min and flame lengths of 2.6 ft, having no practical significance when comparing to the hazard levels as outlined in Tables 3.1 and 3.2. Similarly, an error in estimating the 1-hr S/V ratio for plot K1592W would result in a spread rate range of 5 to 14 ft/min. While this does incorporate two hazard levels in Table 3.2, these spread rates are still of low importance. For the lower intensity fires often encountered in a prescribed burn, there may not be a need for careful measurement of most input parameters. However, under typical wildfire conditions, most commonly marked by higher winds and lower fuel moistures, the sensitivity of the model to variations in inputs may become more meaningful, and the variations in input parameters, along with the possible errors in estimating them, much more critical. This analysis follows.

5.2.1.1 Wildfire Conditions

Weather data were obtained for the Cape Cod National Seashore area in Massachusetts ranging from April 20 to November 1, 1993 (Weather information management system, 1993). The data were a compilation of National Fire Danger Rating System (NFDRS) reports, usually taken at 1:00 p.m. each day. The purpose of obtaining these reports was to get a sense of the weather trends in this area and, particularly, associated windspeeds. While this type of information would be better represented over a study of several years, only a rough approximation is necessary for the purposes of this analysis.

It was found that, over the recorded months, common values of windspeed tended to fall in these broad categories: low, 0-4 mi/h; medium, 7-13 mi/h; and high, 17-23 mi/h. These values represent a '20-foot windspeed', measured at a height of 20 feet above the ground at a weather observation station. The higher values tended to occur prior to or after a storm, or with the passing of a frontal system.

A 20-foot windspeed value of 20 mi/h was used in the analysis to represent an average high value that could be experienced in the Cape Cod area. For the purposes of the model, this value must be reduced to a midflame windspeed. To establish this value, the following correction factors were applied to the 20-foot windspeed, for exposed shrub fuels, as determined by the FIRE1 subprogram of BEHAVE, see Table 5.7.

Table 5.7: Correction factors to determine midflame windspeed from 20-foot values.

Plot	Exposed Fuel Wind Adjustment Factor	Midflame Windspeed
I1892S	0.4	8
K1289W, K1592W, K1489S, K1492S, M1392S	0.5	10
E1292W, G2390W, I1792W, TP01S, TP06S	0.6	12

From the guidelines in Table D.1 regarding ignition and fire behavior potential at various fine fuel moistures, and from the experience of fire managers familiar with the Cape Cod area (W. A. Patterson III, personal communication, 1996), a 1-hr fuel moisture value of 5% was used as an estimate of wildfire conditions. Recall that the 10- and 100-hr fuel moistures do not affect predicted fire behavior in this fuel complex, so they were held at their measured values for each plot.

The concern with a fire spreading through the pine - oak forests under these higher wind and lower fuel moisture conditions is the potential for the litter and shrubs to produce a hot enough fire to carry the flames into the overstory above. This has been the case in previous fires, such as the Long Island, NY and Plymouth, MA fires discussed in Chapter 1, where overall flame lengths have exceeded 100 feet, large areas have been burned in a short amount of time and even major highways have been insufficient in stopping the fire's spread. The control plots would best represent these natural conditions. The method used to construct their fuel models, based on historical data of fuel loading and size, and on-site approximations of such parameters as fuel height and moisture, would also be a realistic approach that fire managers might use to quickly obtain

fire behavior predictions. Under conditions of 1-hr moisture contents of 5% and midflame windspeeds of 12 mi/hr, BEHAVE predicts spread rates of 85 ft/min and flame lengths of 18 ft for plot TP01S, and spread rates of 75 ft/min and flame lengths of 16 ft for plot TP06S. These high flames create a great deal of concern as they would easily provide a sufficient exposure to ignite the pine and oak overstory. This type of behavior was seen in the prescribed burning of plot TP06S where flame heights of about 10 feet caused the crowning of individual, 40 foot pitch pines. The predicted spread rates are also of moderate hazard when considering the guidelines of Table 3.2. In fact, they may even be significantly under-predicted as was the trend for the spread rates under prescribed burn conditions discussed in Chapter 4.

In order to analyze any significant changes in the impact of each parameter on fire predictions under these wildfire conditions, a sensitivity study was conducted on each of the experimental plots under the above combined wind and moisture conditions. From the discussions earlier, we know that increasing the midflame windspeed and decreasing the 1-hr moisture content will increase predicted fire behavior. This follows since the wind coefficient is directly dependent on the windspeed, thereby increasing the numerator of the spread equation. It was demonstrated that midflame windspeeds as low as 3 mi/h tended to over-predict fire behavior in this fuel type, and so increasing to 8 - 12 mi/h should produce a dramatic rise in predicted values. Lowering the 1-hr fuel moisture will also raise the numerator of the spread equation by increasing the moisture damping coefficient, thereby allowing more reaction intensity to be released. The denominator will also be decreased, due to the direct dependence of the heat of preignition on fuel moisture.

Results of the sensitivity study showed a large overall increase in the level of predicted fire behavior over the intervals of interest, although the parameter ranking stayed the same in most cases. The one exception was the 1-hr S/V ratio which impacted predicted spread rates the most (above fuel bed depth and heat content) under these conditions. Table 5.8 shows the variations in predicted fire behavior over the intervals of interest for the three input parameters that affect predictions the most: 1-hr S/V ratio, fuel bed depth and heat content.

Table 5.8: Variations in predicted fire behavior over interval of interest.

	1-hr S/V ratio	Fuel Bed Depth		Heat Content	
Plot	Spread Rates, ft/min	Spread Rates, ft/min	Flame Lengths, ft	Spread Rates, ft/min	Flame Lengths, ft
I1892S	1.4 - 25	~0 - 10	2.9 - 4.8	4.9 - 8.2	1.6 - 2.7
K1289W	25 - 207	22 - 90	6.8 - 19	55 - 91	13 - 21
K1489S	18 - 173	5 - 77	1.9 - 15	40 - 66	10 - 17
E1292W	40 - 368	42 - 125	11 - 22	88 - 144	16 - 28
K1592W	20 - 166	26 - 65	8.3 - 17	44 - 72	13 - 21
K1492S	5 - 78	4.5 - 22	6.7 - 13	15 - 25	4.7 - 7.8
M1392S	7 - 73			14 - 25	4.2 - 6.9
G2390W	56 - 501	48 - 215	15 - 30	125 - 212	21 - 35
I1792W	80 - 732	165 - 248	30 - 39	187 - 306	31 - 51

We see that, while the degrees of change remained the same for fuel bed depth and heat content under these extreme condition, the increase in predicted fire behavior dramatically increased the practical significance of the variations. In this type of situation, uncertainties in estimating fuel bed depth can lead to a range of spread rates and flame lengths with a completely different interpretation. For instance, predicting fire in an area similar to plot K1289W under wildfire conditions, with fuel bed depth estimates ranging from 0.39 to 0.43 feet, could lead to predictions ranging from an easily controlled fire using handtools,

to one with moderate spread rates and large flame lengths producing erratic fire behavior and requiring large equipment to help suppress. The importance of determining the heat content of the fuels is also supported, as very different fire behavior is predicted over the range of possible values.

The wide range in predicted spread rates with increasing 1-hr S/V ratio supports the previous statement that increases in this parameter causes the prediction model to be more sensitive to higher windspeeds. The converse has actually been shown, where increasing the midflame windspeed caused the prediction model to be more sensitive to changes in 1-hr S/V ratio. This result is most apparent with plot I1792W, where the range of spread rates was 80 to over 700 ft/min over the range of 1-hr S/V ratios. While it is not likely that actual 1-hr S/V ratios would vary to this extent in the pine - oak forests, this extremely wide range of predicted spread rates suggests that even small variations will produce significantly different results. This plot represents burning under natural conditions as it had been untreated prior to 1992, and so the sensitivity analysis results can be generalized to the control plots. This suggests that under wildfire and natural fuel conditions, a large amount of judgment plays a key role in fire behavior prediction interpretations. Simply using average values for input parameters may not be sufficient to accurately portray the fire behavior potential of the fuel complex.

5.2.2 Conclusions About BEHAVE

The main purpose of this thesis was to evaluate the effectiveness of BEHAVE in predicting fire behavior in the flammable shrub understories of the northeastern pine - oak

forests. In order to do this, the necessary data have been obtained to construct site-specific fuel models for several plots that have undergone a series of prescribed burns. These fuel models, along with the recorded environmental data, have been used as input to the fire prediction model, and the results were compared to observations made during the prescribed burns. General trends were identified, followed by a detailed analysis of how each input parameter effects the outcome of predictions. The most important parameters were identified, and their impact was realized under possible wildfire conditions. From this information, several conclusions can be drawn about the data collection and fuel modeling processes, and the fire prediction model.

5.2.2.1 Data Collection

Several issues have been raised throughout the previous chapters regarding ranges in input variables and the possible errors in their measurement processes. For instance, fuel moisture values recorded on the day of the burn varied widely, suggesting large variations throughout each plot. Upon further analysis, however, it was found that the variations in 10- and 100-hr fuel moisture contents did not affect the outcome of fire behavior predictions at all. Similarly, variations in live woody fuel moistures during the summer affected predictions very little. The importance of this parameter increased during the drier, winter months, although overall its relative impact was small. The 1-hr moisture content was important, however, and recorded values also varied widely. This was mainly due to this parameter being composed of both leaf and needle litter fuels and 0-.25 inch fuel sticks. In the future, because the litter component comprises the majority of the 1-hr

size class, its moisture values should be taken as the 1-hr fuel moisture. The litter moistures did not vary considerably when considered separately from the 1-hr fuel stick measurements and so it appears that a sufficient number of samples were taken prior to the burns. In wildfire situations, the variations in these values should be used to help evaluate the range of possible fire behavior. For the winter plots, attention also needs to be paid to the inclusion of the wintergreen in the analysis of the litter moisture content. This was determined to be a useful method of fine-tuning fire behavior predictions and decreasing the amount of over-prediction for each plot. This will not help predictions during the summer, however, as fire behavior is already under-predicted and increasing 1-hr fuel moistures will only further these deviations.

The downed woody fuel inventory procedure was used to obtain the majority of the fuel load estimates during fuel model construction. This was found to be sufficient, assuming an error of ±20%, for the 1- (0-.25 inch sticks), 10- and 100-hr size classes. A different procedure, however, was used to estimate the litter and live fuel loads, through the collection of biomass plots. Where the litter load consistently covers 100% of the plot, this procedure worked well. An adjustment was made to account for litter accumulation during the winter between the fall biomass plot measurement and the following year's burn. The accuracy of this method was evaluated further by measuring the litter fall on three 2-year burn plots before the fall of 1995 and immediately before the spring 1996 burn (W. A. Patterson III, personal communication, 1996). It was found that actual litter accumulations over this period were close to the previously assumed adjustment, although over-estimated by about 0.4 tons/acre for two of the plots and 1.2

tons/acre for the third. On average, this would result in an over-estimation of litter load by about 15-25%. This agrees with the precision of about 20%, approximated in section 5.1.3, for fuel load estimates using a combination of the biomass plots and downed woody fuel inventory. Considering the relative importance of the 1-hr fuel load parameter, this over-estimate in litter load may partially account for over-predictions of fire behavior. As for the live fuel load estimates, it was determined that this measurement process was not sufficient to accurately represent the entire area, and so more, random collection points should be included. This may lead to larger values of live fuel load, which would actually reduce predicted fire behavior.

One problem with the downed woody fuel inventory process is a lack of litter depth measurements. At the present time, the method measures the depth of the duff layer and the height above the duff layer of the downed fuel, ignoring the litter layer, a major component of the fuel models. For many of the experimental plots where downed fuel loads were low, this approximation was sufficient, as the fuel depths corresponded to litter depths. This may not be as useful, however, in plots that have a significant downed woody fuel component. Such a measurement of litter depth could easily be incorporated into the inventory procedure, yielding the same degrees of accuracy, or better, as for the other measurements. Another parameter that needs careful measurement is the percent coverage of each of the fuel components within a fuel complex. This will directly affect the fuel load values, along with the fuel bed depth estimates. The model is very sensitive to each of these parameters.

Additional parameters that have not yet been determined for this fuel complex are the live and dead S/V ratios and heat contents. Most important of the two S/V ratios is the dead, or 1-hr value, due to its effect on predicted spread rates. Separate values need to be determined for the leaf litter and 0-.25 inch stick components, with a focus on the litter layer. Most likely, a range of possible values will be obtained, and the effect of this range on predictions will have to be determined. Ideally, the measurements would be relatively uniform throughout the fuel complex, and average values could be used. The live fuel S/V ratio affects predictions very little, and so only a rough estimate need be obtained. The heat content of the live and dead fuels can be a potentially more complex parameter, although very important in the fire prediction model. As discussed in Chapter 4, the value of this parameter may also change significantly throughout the year, and so may help account for some of the deviations of predictions from observed fire behavior.

5.2.2.2 Fuel Modeling

Once these data are obtained, it must be put into the fuel model in order to represent a particular fuel complex. It has been determined in Chapter 4 that the use of the standard NFFL fuel models 4-7 and 9 are insufficient in predicting fire behavior in this fuel complex. Thus, custom models must be created. For the purposes of the study, the fuel models were site-specific in order to account for plot variations and treatment effects.

The experimental and control plot fuel models were constructed slightly different with respect to the placement of the downed woody fuel. For the experimental plots, the litter component was comprised only of the leaf and needle fuel particles determined from

the biomass plots. The downed woody fuel was placed in the shrub component, along with the standing dead and live woody fuels. This separation of the litter layer is felt to be advantageous, as it allows for greater focus on the litter layer, which is the major carrier of the fire and has a different S/V ratio and depth than the rest of the fuel bed. For the control plots, the litter component was comprised of the leaf and needle fuel particles and the downed woody fuels. The shrub component only included the standing dead and live woody fuels. From the shrub component viewpoint, this method makes more sense, as it allows for greater focus on the standing dead which is important in this fuel complex, and the characteristics of the live fuels which are also a key factor. So, there is some confusion as to the placement of the downed woody fuels. Some of these fuels tend to fall within the leaf and needle layer, while others rest above the litter bed. For the pine - oak fuel complex, this issue would most likely not account for errors in predictions due to the relatively low amounts of downed dead fuel compared to the litter present on the plots.

5.2.2.3 Fire Prediction

When the custom fuel models, along with recorded environmental parameters, were used as input to the fire prediction model, a distinct pattern was found. The spread rates and flame lengths of the winter burn plots were over-predicted by the model, while fire behavior in the summer plots was under-predicted. It was concluded that the major contributing factor to this phenomenon was the presence of the live fuel component within the fuel and fire prediction models. According to the relationship for the live fuel moisture of extinction, the live fuels were predicted to burn well beyond their actual moisture

content values. When the contribution of the live fuels was analyzed further in Chapter 5, it was found that, while the live fuels are technically burning, they are also viewed as acting like a tremendous heat sink, absorbing the energy created by the burning of the dead fuels. This heat sink increases further during the summer months, when live fuel moistures, on average, almost triple.

The live fuel moistures alone were not enough to account for the large under-prediction of several of the summer plots, as variations in this parameter had little effect on predicted fire behavior. These effects were so small, it could almost be concluded that the live fuels were not being predicted to burn, although this is apparently not true according to the values of live fuel moistures of extinction, and most likely the small effects were also due to the low live fuel loads during the summer. Similarly, none of the other live fuel parameters had a significant effect on predictions. The effects of moisture did increase somewhat during the winter, most likely due to a combination of higher live fuel loads and lower moistures (less of a heat sink).

The live fuel moisture of extinction parameter causes a great deal of concern, and should be analyzed further. The calculation procedures for this parameter led to values of 400% to 8500%, with the majority well over 1100%. It was decided that the primary cause of these high values was the low amounts of live fuels in comparison with the dead fuel loads in each plot. A simple analysis was conducted on equations 4.3 to 4.5 in order to find what amounts of live fuel loads would cause the live fuels in each plot to be predicted not to burn, see Table 5.9. The live fuel loads were adjusted until the live fuel

moisture of extinction was roughly equivalent to the live fuel moisture contents recorded for each plot.

Table 5.9: Live fuel loads required to reach live fuel moisture of extinction.

Plot	1-hr Fuel Load (tons/acre)	Live Fuel Load (tons/acre)
I1892S	4.46	7
K1289W	5.10	30
K1489S	4.86	6
E1292W	4.40	14
K1592W	5.27	17
K1492S	5.38	9
M1392S	5.27	8
G2390W	6.56	32
I1792W	10.91	30
TP01S	5.91	3
TP06S	5.89	5

It is interesting to note that there is a seasonal difference in the ratio of the live to dead fuel load in order to reach the live fuel moisture of extinction. During the summer, the ratios ranged from about 0.5 to 1.7, while in the winter, ratios ranged from 2.7 to 5.9. This is interesting because there are no parameters within equations 4.3 to 4.5 that would distinguish these two seasons for this fuel complex. That is, there was no consistent difference in dead fuel moistures between seasons, nor was there a consistent difference in the amount of dead fuel present, the S/V ratios, or the dead fuel moistures of extinction. Very large amounts of live fuel are required in the winter plots to reach the live fuel moisture of extinction. For instance, plot K1289W would require a live load of about 30 tons/acre. The fuel bed depth for this plot was only about 0.5 ft. This would correspond to a live packing ratio of 1.7 and β/β_{op} of about 186.3. This suggests that the packing

ratio may be an important variable in the determination of the live fuel moisture of extinction parameter. Currently, it is accounted for indirectly, through the dead fuel moisture of extinction, which was correlated directly to packing ratio for the litter, grass and slash components. Another factor which the live fuel moisture of extinction does not take into account, is the potential behavior of various types of live fuels. It has been recognized that certain fuels, namely those containing waxes and resins on their leaves and stems, will burn more readily under higher moisture conditions (Burgan & Rothermel, 1984). Thus, basing the live fuel moisture of extinction on the theory that the moisture at which live fuels will burn is directly dependent on the heat given off by the dead fuels may be reasonable but may not be accounting for the ease of ignition and burning characteristics of various species.

While no recent work has been found by the author regarding the moisture of extinction of live fuels, there has been some work done focused on re-analyzing the heat of preignition parameter, which provides much of the basis for the calculations in equation 4.3. In experiments with 1/16-, 1/4- and 1 1/2-inch fuel sticks, it was found that heats of preignition were similar amongst the fuels at temperatures below 200 °C, agreeing with previous findings. However, above 200 °C, values varied considerably, suggesting that this parameter must take into account the different processes that are occurring at higher temperatures often found in the burning of forest fuels (ignition temperature is usually assumed to occur at 320°C) (Susott, 1984). Using the above results, the heat of preignition has been reformulated to incorporate the heat of pyrolysis, or flammable gas production, and the heat of vaporization (Wilson, 1990). While more study needs to be

conducted to verify the accuracy of these changes, any successful results may help in understanding the moistures at which fuels will not burn and, in particular, the behavior of live fuels at various moisture contents.

The fire behavior predictions obtained from BEHAVE for many of the burn plots of the present study were within reasonable accuracy for typical prescribed fire conditions and fuel management objectives. The general trend of the predictions, however, raises two major concerns. The fact that the summer burns were consistently under-predicted raises a question as to whether BEHAVE will be useful in predicting the potential fire behavior that has been observed during the summer in this fuel complex. Predictions were good for the standard low levels of summer fire behavior. However, when the observed fire behavior of plots K1489S, TP01S and TP06S demonstrated the huckleberry's potential to significantly increase fire behavior, predictions continued to remain at low levels, especially for spread rates. It appears that the heat sink effects of the fuel moistures during this season dominate the model predictions.

During the winter, the live shrubs appear to be less of an influence in both observed and predicted fire behavior. The main focus tends to be on the litter layer and the effects that the wintergreen has on its fire behavior. Uncertainties in estimating the fuel bed depth most likely account for the continued over-predictions. From a prescribed burn perspective, this is an error on the safer side, as it is better to over-estimate the fire potential of a fuel complex. This is only true to a certain extent, however, and there should be additional concern for the propensity of the prediction model to highly over-estimate fire behavior in untreated areas, marked by larger fuel accumulations and depths,

and under more extreme environmental conditions of higher windspeeds and lower fuel moistures. The potential of the fire prediction model to over-predict fire behavior during possible wildfire conditions was shown, particularly for the 1-hr S/V ratio, fuel bed depth and heat content parameters. A highly over-predicted fire in the winter or under-predicted fire in the summer will not allow fire behavior officers to accurately forecast the spread or potential of a wildfire, possibly leading to inaccurate estimates of suppression requirements, and compromising the many lives and property within the Cape Cod National Seashore area.

6. Conclusions

The field of wildland fire modeling is currently in a transitional period. The BEHAVE system of fuel modeling and fire behavior prediction has been well established for several years and widely used by land managers, fire behavior specialists and fire personnel to plan for prescribed burns, make land management decisions and forecast the behavior of wildfires. As new concepts and techniques are introduced to better understand the behavior of fire, several of the assumptions of BEHAVE have been questioned and new methods of fire prediction are being explored. The purpose of this thesis was to provide a thorough evaluation of BEHAVE that would analyze the theoretical and empirical basis of the model, identify its strengths and weaknesses and suggest alternative methods to model the complex phenomenon of a spreading wildfire.

The evaluation of the effectiveness of BEHAVE focused on the ability of the model to predict fire behavior in the pine - oak forest fuel complex. Chapter 1 provided a description of the potential fire behavior of this fuel complex through accounts of previous fires in similar fuels throughout the Northeast. The fuel complex of interest is located in Cape Cod National Seashore which has a significant wildland/urban interface and a large fuel load due to the exclusion of fire in the area over the past several years. Therefore, it is of great interest to introduce fire into this fuel complex as a fuel management tool, and to understand the behavior of a fire spreading through these fuels in order to improve the ability to predict its behavior.

Chapter 2 provided a more detailed description of the mathematical concepts and theoretical assumptions that govern the fire behavior predictions. It was found that a large number of parameters and empirical correlations were required to approximate the original theoretical equation of fire spread. The majority of the parameters that approximate the forward heat flux of the fire and the heat required to bring the unburned fuel to ignition were written in terms of measurable variables such as surface-area-to-volume ratio, packing ratio and moisture content. The concept of a fuel model was described where the physical and chemical characteristics of the various components of a fuel complex are represented. These fuel models provide the necessary parameters for the fire behavior predictions of BEHAVE. The rate of spread and various measures of intensity are predicted for a fire spreading through a homogeneous, porous fuel bed with constant properties and under constant environmental conditions.

A description of the pine - oak forest fuel complex followed in Chapter 3. The primary carriers of a fire spreading through these fuels are the litter and shrub components. During the dormant season when there are no leaves on the stems of the shrubs or the overstory, there is increased drying of the fuels below resulting in a high level of fire behavior. Fire behavior in the growing season is unique from the dormant season due to the presence of leaves on the shrubs and, in particular, the huckleberry. These leaves have a high extractive content which allows the shrubs to ignite and sustain burning at high moisture contents. While growing season burns are typically of lower fire behavior than the dormant season, there is still a potential for extreme fire behavior.

Hazard levels were developed in order to provide a basis of comparison for various magnitudes of flame lengths and spread rates.

Chapter 4 provided a comparison of fire behavior observations from prescribed burn studies in Cape Cod National Seashore with predictions obtained from BEHAVE. Custom fuel models were constructed for each of several experimental and control plots based on data collected prior to and on the day of the burn. There was a clear distinction in the results of the comparison between observed and predicted fire behavior based on the season in which the various plots were burned. The fire behavior of winter prescribed burns was consistently over-predicted, while the summer burns were consistently under-predicted.

In order to improve predictions for the winter burns, the 1-hr moisture content was adjusted to account for the high moisture content of the wintergreen which also lies within the surface fuels. This was found to be an effective means of fine-tuning the predictions during this season, although there was still a tendency to over-predict fire behavior. An attempt was also made to improve summer predictions by separating the live leaves and stems of the shrub component within the fuel model, in order to account for the large variations in moisture contents between these two parts of the shrub. Fire behavior predictions were unchanged by this adjustment of the fuel models, suggesting that the live fuels are not contributing to predictions for moisture contents over about 90%. According to the formulation for the live fuel moisture of extinction, however, the live fuels are predicted to burn, although the values calculated for this parameter did not appear to be reasonable. It was concluded that the representation of the live fuels within

the fuel and environmental parameters was most important in accounting for the distinction between winter and summer predictions.

The sensitivity study of Chapter 5 provided a detailed analysis of how individual parameters enter into the fire spread equations and the relative importance of each with respect to their impact on fire behavior predictions. This also allowed the effectiveness of data collection and measurement processes to be evaluated. It was found that fire behavior predictions were most sensitive to changes in fuel bed depth, midflame windspeed, heat content and 1-hr S/V ratio. The effects of this sensitivity become most critical under potential wildfire conditions when the levels of predicted fire behavior are higher, and so the fire prediction model was analyzed under conditions of lower fuel moistures and higher windspeeds. The importance of this additional analysis was that, under these conditions, predicted fire behavior for the control plots indicated the potential for the extreme fire behavior seen in previous wildfires and, in fact, may even be under-predicted. The sensitivity study for the experimental plots also indicated that a large amount of judgment would be necessary in predicting wildfire behavior, as small errors in estimating the 1-hr S/V ratio, fuel bed depth and heat content could lead to very different fire behavior predictions.

The primary reason for the under-predictions of summer fire behavior is the representation of the live fuels within the fire prediction model. Due to their high moisture contents, the overall fuel bed moisture is increased. The live fuels act as a great heat sink, increasing the amount of energy absorbed and decreasing the amount of energy released

from the flaming zone. The fire is essentially viewed as spreading through a uniform fuel bed full of very wet fuels which smother the fire.

During the winter, the effects of the live fuels have less of an influence on fire behavior within the fire prediction model. Observed fire behavior appears to depend primarily on the fire behavior of the surface fuels, including the litter and wintergreen. The huckleberry also enhances overall fire behavior by providing vertical fuels that also have a high extractive content in the fine stems of the shrubs. Due to the high sensitivity of the model to parameters such as fuel bed depth and 1-hr S/V ratio, it is most likely these fuel bed characteristics that would account for inaccuracies in predictions.

Fire prediction errors in the summer and winter appear to depend on very different reasons, with live fuel effects overwhelming the summer predictions and fuel bed characteristics causing deviations in winter predictions. The underlying cause in both cases, however, may be very similar. The pine - oak forests are a heterogeneous fuel complex with several different components. While fires spread mainly through only two of these components, the litter and shrubs, there appear to be separate mechanisms controlling the behavior of fires within each. This will be discussed further through an account of the prescribed burning of control plot TP06S.

6.1 Prescribed Burn Observations

The author was present during the prescribed burning of plot TP06S conducted in July, 1996 and several observations were made regarding the fire behavior in this fuel complex. Appendix A shows pictures which give an indication of the fuel bed

characteristics present on the day of the burn. The fire was ignited by a driptorch as a line fire across the full length of the plot down a draw between slopes A and B, see Figure 6.1. Fire behavior measurements were made on slope A which had a southwest aspect (slope facing southwest). Winds were blowing out of the southwest resulting in a head fire running up slope A. The fire behavior was very "good" during this burn. Flames averaged in the 3-7 ft range producing a very hot fire that was generally unapproachable and felt hot on bare skin from several feet away. Periodic flames approached about 10 ft, resulting in high scorch heights and the crowning of individual, 40-foot pitch pines.

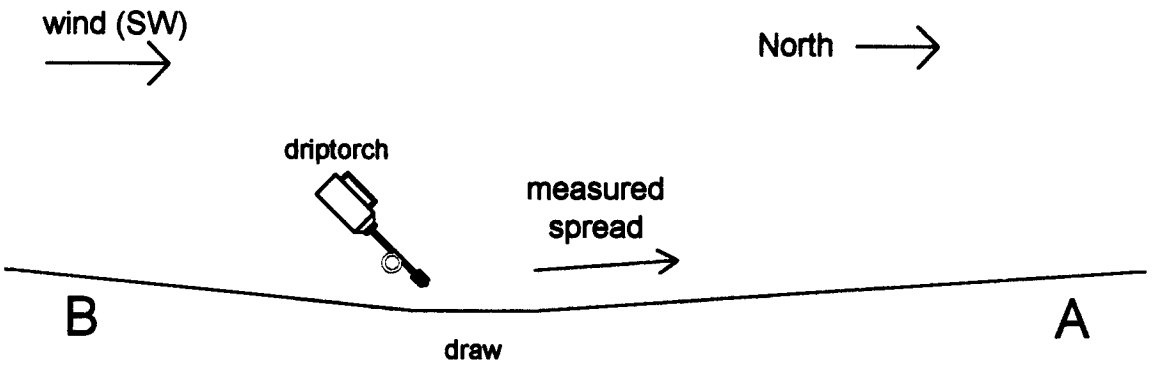

Figure 6.1: Cross-section of plot TP06S.

The fire spread readily through the litter layer with close to 100% consumption. Flame lengths were observed up to about 2 ft, providing sufficient exposure to at least ignite and kill all of the huckleberry. The amount of consumption of the huckleberry, however, varied throughout the plot. For the main head fire burning up slope A, all of the leaves and some of the small live stems were consumed. The fire burning in the opposite direction from the ignition line, toward slope B, spread along a flat portion of ground for up to 15-20 ft in the wider portion of the draw, then burned up slope B. In the flat

section, the fire was burning as a backfire against the wind. This resulted in the killing of the leaves of the huckleberry but with little consumption, resulting in the leaves remaining attached to the branches. As the fire burned up slope B, however, the leaves were consumed as with slope A, suggesting the slope effects dominated over the wind effects.

As the fire spread through the litter and shrubs, they often appeared to act as independent fire fronts. The fire spread through the litter underneath the shrubs as the shrubs were being preheated. Upon ignition of the shrubs, the fire fronts appeared to move closely together, although the litter fire front was often observed to be slightly ahead.

These simple observations suggest possible deviations from the assumptions made within the fire prediction model of BEHAVE. The litter and shrub components appear to be acting as two separate fuel beds, with the ignition of the shrubs dependent on the behavior of the litter. This is very similar to the ignition and spread mechanisms of a crown fire, where BEHAVE has problems in predicting fire behavior. When BEHAVE combines everything into one homogeneous fuel bed, these separate mechanisms are not accounted for. This also results in an assumption that the fire is spreading through a 'tightly packed' fuel bed which reduces predicted fire behavior. Observations of the actual fuel complex definitely did not seem tightly packed, as the leaves and needles lay softly on the ground with air space between, and the shrub layer, of course, is mostly air.

The important conclusions that can be made from this discussion include the fact that the ignition of the shrubs is largely dependent on the fire behavior within the litter layer. This agrees with the basis of the theory behind the live fuel moisture of extinction.

Also, the method used by BEHAVE to model complex fuel beds as one homogeneous bed does not appear to be effective for this fuel complex. During the summer, BEHAVE transforms the litter and shrubs into a fuel bed with uniform characteristics. This new fuel bed, with an equivalent depth, fuel loading, heat content, etc., becomes too wet and compact and so the fire is theoretically smothered producing low levels of fire behavior predictions. This is also the case during the winter, although the live fuels are not as overwhelming in the equivalent fuel bed. The analysis of wildfire conditions, however, showed that even small changes in the fuel bed depth of a winter plot produced very significant changes in predicted fire behavior. These results suggest that each component of this fuel complex has very different characteristics, including fuel-to-air ratios, moisture contents and fuel bed dimensions. Therefore, they would seem to be best treated as separate fuel beds. This would allow the burning behavior of each component to be analyzed according to its unique characteristics and its interaction with other components. Then, the overall fire behavior can be more effectively determined.

Additional work is needed in the area of modeling fires in heterogeneous fuel beds. Some work has begun in this area, comparing the behavior of fires in mixed fuel beds of excelsior and fuel sticks to predictions obtained from the mathematical model used in BEHAVE (Catchpole, Catchpole, & Rothermel, 1993). It was found that the experimentally measured fire behavior often differed from that predicted by BEHAVE. Problems with the model in mixed fuels include the weighting procedure based primarily on the S/V ratio, and the formulation for the reaction time, defined as the ratio of the reaction zone efficiency to the time for the fire front to burn through a reaction zone.

Mixed fuel fire behavior also appeared to be dependent on the presence of wind, which agrees with observations in the pine - oak forest fuel complex. This suggests that the use of the wind coefficient may not accurately portray the heat transfer mechanisms occurring during wind-aided spread. This work is part of an effort to produce a second generation fire danger/fire behavior system (Catchpole & Catchpole, 1995). This has included a complete re-evaluation of the heat transfer processes that are occurring in a wildfire and of the mathematical relations that govern their spread.

In the following section, a simple model will be introduced as a means of discussing the spread of fires through the pine - oak forests and similar fuel complexes. This will be done by establishing a fundamental relation for fire spread through a porous fuel bed, followed by a representation of the heat flux providing the forward heating of the fire. The important mechanism of fire spread between the litter and shrub components of the fuel complex will also be discussed, along with the possible experimental techniques for obtaining the material properties necessary to use this method of fire modeling.

6.2 Simple Model of Fire Spread

6.2.1 The Physical Model

The focus of this discussion will be the litter and shrub components of the pine - oak forests. Each of these fuel components will be treated as a separate fuel bed, with a focus on the litter layer. Figure 6.2 shows the physical model of a fire spreading through the litter layer, which is assumed to be a homogeneous, porous fuel bed composed of thermally thin fuel particles. The concept of a thermally thin material indicates that the

fuel temperature ahead of the flame is constant with depth (Pagni & Peterson, 1973). One-dimensional heating through the litter layer will be assumed in the absence of wind or slope effects. The flaming zone, assumed to be an infinitely long line fire of height, H_F, and depth, Δ, moves through the litter layer of depth, d, at a quasi-steady rate of spread, V.

The fuel ahead of the flames is assumed to ignite when it reaches an ignition, or pyrolysis, temperature, T_p. This unburned fuel is heated by various heat transfer mechanisms from the flames above the fuel and the flames within the fuel bed, as discussed in Chapter 2. In the absence of wind or slope, radiative heat transfer has been found to provide the largest fraction of the total energy transferred from the flaming zone to the unburned fuel (Pagni & Peterson, 1973). Observations from prescribed burns under these conditions indicate that radiation from the flames within the fuel bed is the dominant mode of heat transfer for fire spread through the litter layer.

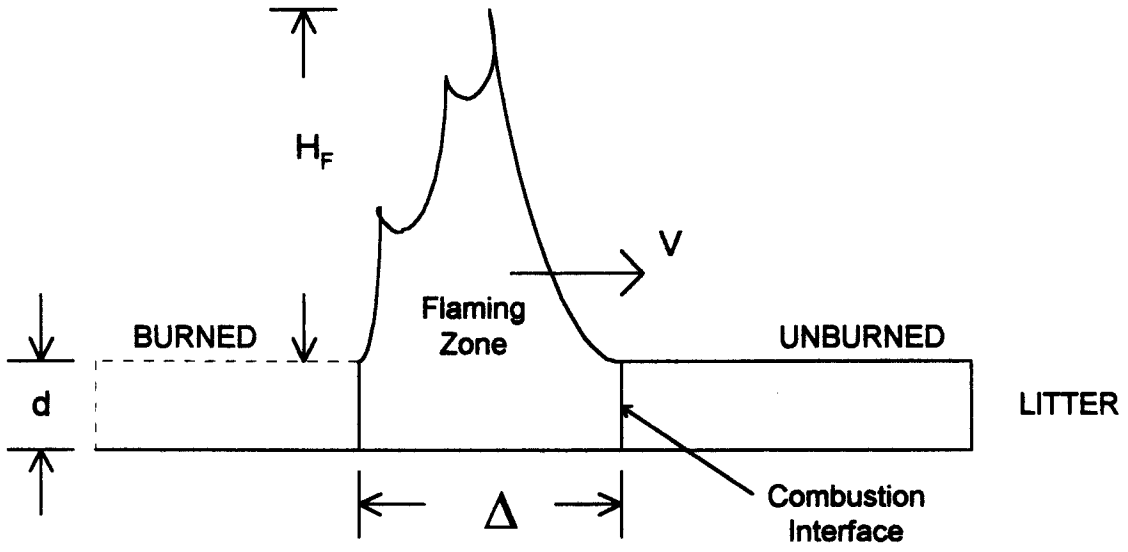

Figure 6.2: Idealized characterization of flame front moving through litter bed.

6.2.2 Energy Conservation

The conservation of energy principle for fire spread can simply be stated as follows: the rate of energy absorption to raise the unburned fuel to its ignition temperature must be equal to the rate of energy transfer from the flaming zone to the fuel bed. Williams (1977) expressed this concept of energy conservation through the 'fundamental equation of fire spread' written as:

$$\rho_b V \Delta h = \dot{q}_o'' \tag{6.1}$$

where,

ρ_b = fuel bed bulk density [kg/m^3],

V = quasi-steady rate of spread [m/s],

Δh = change in enthalpy as unit mass of fuel is raised from its initial temperature to its ignition temperature [kJ/kg],

$\dot{q}_o''$ = forward heat flux per unit area (energy per unit area per second transported across the combustion interface) [kW/m^2].

Enthalpy per unit mass, h, is a state variable used to represent the frequently encountered combination, h = (internal energy) + (pressure)*(volume) found in many thermodynamic processes (Cengal & Boles, 1994). In a constant pressure process (common for measurements in combustion systems), the heat withdrawn from the surroundings is equal to the increase in enthalpy of the system. When it is assumed that phase changes of the fuel prior to reaching the ignition temperature are negligible energetically, the change in enthalpy, Δh, can be approximated as (Williams, 1977):

$$\Delta h = c_s(T_p - T_o), \tag{6.2}$$

where,

c_s = specific heat of fuel bed [kJ/kg·K],

T_p = pyrolysis temperature [K],

T_o = initial temperature [K].

Therefore, if the rate of energy transfer from the flaming zone to the unburned fuel is known, then the rate of spread, V, can be expressed as:

$$V = \frac{\dot{q}_o''}{\rho_b c_s (T_p - T_o)} \quad \text{[m/s]}. \tag{6.3}$$

6.2.3 The Forward Flux

The forward flux, $\dot{q}_o''$, per unit area emitted from the flaming zone to the unburned fuel is similar to the propagating flux concept derived by Frandsen (1971). The source of this propagating flux was the reaction intensity, or heat release rate, defined by equation 2.3 as the product of the heat of combustion and mass loss rate per unit area of the fire front. A similar concept is used here, where it is assumed that the rate of spread of a fire depends on the size of the fire which, in turn, is dependent on the rate of heat release per unit area, $\dot{Q}''$, defined as (Drysdale, 1985):

$$\dot{Q}'' = \dot{m}'' \cdot \Delta H_c \quad \text{[kW/m}^2\text{]}, \tag{6.4}$$

where,

$\dot{m}''$ = mass loss rate per unit area of fire front [kg/m^2-s],

ΔH_c = effective heat of combustion [kJ/kg].

The heat release rate of the flaming zone is the product $\dot{Q}''\,\Delta(1)$ where we have assumed a unit length of the flaming zone.

The heat release rate is determined from the principle of oxygen consumption calorimetry, using the test apparatus discussed later. This empirical principle is based on the observation that, in general, the heat of combustion of any organic material is directly related to the amount of oxygen required for combustion. A measure of this rate of oxygen consumption can then be converted to a rate of heat release by assuming that approximately 13.1 MJ (megajoules) of heat are released per kg of oxygen consumed (Huggett, 1980). This has been found to be accurate within ± 5% or better for a wide range of conventional organic fuels. An effective heat of combustion is also obtained from the oxygen consumption apparatus. This parameter is distinguished from the gross, or net, heat of combustion obtained from the oxygen bomb calorimeter and used by BEHAVE. In the bomb calorimeter, a value for heat of combustion is obtained with nearly 100% combustion efficiency in pure oxygen. Oven-dry wood averages a gross heat of combustion of about 20 MJ/kg (Tran, 1992). In actual fires, however, char-forming materials such as wood undergo various modes of flaming and glowing combustion resulting in incomplete combustion. Therefore, the gross heat of combustion can exceed the effective value by as much as 25 - 50% (Janssens, 1995). Values for oven-dry wood are about 13 MJ/kg during flaming combustion which is of main interest in fire growth.

Of the total heat release rate of a fire, it has been found that the majority is convected upward into the fire plume and approximately 30% is released as radiant energy (Heskestad, 1995). Therefore, we have a known fraction, χ_r, of the heat of combustion that is radiated and so the rate of heat release of radiant energy of the flaming zone is (Drysdale, 1985),

$$\dot{Q}_r = \chi_r \dot{Q}'' \Delta(1) \quad [\text{kW}]. \tag{6.5}$$

We are interested in the heat transfer from the flames within the bed to the unburned fuel. Since we know the total rate of radiant heat release from the flaming zone, the amount that is released through the combustion interface within the fuel bed becomes merely a problem of determining a view factor, or the fraction of radiation leaving some surface which is intercepted by another (Incropera & DeWitt, 1990). This view factor can be represented as a fraction, χ_b, of the radiant heat release rate of the flaming zone. Then, the forward, radiative heat flux through the combustion interface is:

$$\dot{q}_r'' = \frac{\chi_b \chi_r \dot{Q}'' \Delta(1)}{d(1)}. \tag{6.6}$$

BEHAVE used a similar formulation where the propagating flux was written as a fraction of the reaction intensity that is actually received by the potential fuel. In order to calculate this fraction, or propagating flux ratio ξ, the no-wind propagating flux was experimentally determined from the relation $(I_p)_o = R_o \rho_b \varepsilon Q_{ig}$. Then, ξ was computed from the ratio of the no-wind propagating flux to the experimentally determined reaction intensity. Therefore, the rate of spread must be known first in order to later calculate the forward heat transfer. Also, the heat source and heat sink terms have been combined in

order to determine ξ. The method used to derive equation 6.6 separates these two processes. The forward heat transfer is written in terms of a direct measurement of the energy released from the fire. Its distribution into the unburned fuel bed can be calculated from view factors, which can be determined at any level of complexity. Then, from equations 6.3 and 6.6, the rate of spread can be determined by considering the separate processes of forward heat transfer and ignition,

$$V = \frac{\chi_b \chi_r \dot{Q}'' \Delta}{d\rho_b c_s (T_p - T_o)}. \tag{6.7}$$

The depth, Δ, of the flaming zone is defined by the product of the burn-out time, t_b, and rate of spread, V, or $\Delta = Vt_b$ (Thomas, 1995). The burn-out time is similar to the reaction time discussed in Chapter 2. It can be defined as the ratio of mass of fuel per unit area, m'', to mass loss rate per unit area, $\dot{m}''$ (Emmons, 1963). From equation 6.4 and $m'' = \rho_b d$,

$$t_b = \frac{\rho_b d \Delta H_c}{\dot{Q}''} \text{ [s]}. \tag{6.8}$$

If we substitute the relation for flaming zone depth $\Delta = Vt_b$ along with equation 6.8 into equation 6.7, we have,

$$\frac{\chi_b \chi_r \dot{Q}'' V \rho_b d \Delta H_c}{\dot{Q}'' d} = \rho_b c_s (T_p - T_o) V . \tag{6.9}$$

Then,

$$\chi_b \chi_r \Delta H_c = c_s (T_p - T_o) . \tag{6.10}$$

Equation 6.10 shows that the fraction, χ_b, of the radiant energy, $\chi_b \Delta H_c$, of the flaming zone is responsible for heating the unburned fuel to its ignition temperature. This result is expected based on the assumed mechanism of forward heat transfer.

6.2.4 Ignition of Huckleberry

The ignition of the huckleberry, or shrub component, of the fuel complex appears to be dependent on the amount of heat exposure provided by the litter layer. This would include the amount of convective and radiative energy of the fire, which is dependent on the heat release rate of the flaming zone. The most visible measure of this energy moving upward from the litter to the shrubs is the flame height.

The flame height, H_F, of a line fire where the length is much larger than the depth, Δ, has been found to be proportional to some power, n, of a dimensionless heat release rate per unit length of the flaming zone, based on experiments measuring flame spread over solids in the vertical and horizontal orientation (Hasemi, 1985). That is,

$$H_F = \gamma(\dot{Q}'^*)^n \Delta \quad [\text{m}], \tag{6.11}$$

where,

γ = parameter based on definition of flame height,

$\dot{Q}'^*$ = dimensionless heat release rate per unit length of flaming zone.

The value for n in equation 6.11 has been found to approach 2/3 for large values of $\dot{Q}'^*$ in line fires. Hasemi & Nishihata (1988) have supported this dependence of H_F/Δ on $(\dot{Q}'^*)^{2/3}$ for $\dot{Q}'^* < 3$ from experiments using burners to represent a rectangular (line) fire. The author took the experimental data of Hasemi and Nishihata and inserted it into a spreadsheet in order to determine a value for the parameter γ for line fires in the open. The data was curve-fitted for $\dot{Q}'^* < 3$ and a relationship of $H_F/\Delta = 4.5444(\dot{Q}'^*)^{0.6576}$ was found with $R^2 = 0.9938$. Therefore, an approximation of $\gamma = 4.5$ would be reasonable for line fires in the open with $\dot{Q}'^* < 3$. A curve fit of all of the data was also successful with $H_F/\Delta = 4.2975(\dot{Q}'^*)^{0.5816}$ and $R^2 = 0.9905$. Therefore, $\gamma = 4.3$ with n approaching 3/5 for $\dot{Q}'^* < 10$ The dimensionless heat release rate per unit length for a line fire is (Hasemi & Nishihata, 1988):

$$\dot{Q}'^* = \frac{\dot{Q}'}{\rho_\infty c_p T_\infty g^{1/2} \Delta^{3/2}}, \tag{6.12}$$

where,

$\dot{Q}'$ = heat release rate per unit length of the flaming zone [kW/m],

ρ_∞ = ambient air density [kg/m^3],

c_p = specific heat of air [kJ/kg·K],

T_∞ = temperature of ambient air [K],

g = acceleration of gravity [9.81 m/s^2].

The heat release rate per unit length of the flaming zone, $\dot{Q}'$, is similar to the fireline intensity discussed in Chapter 2 and can be written as the product of the heat release rate per unit area and the flaming zone depth. That is, $\dot{Q}' = \dot{Q}''\Delta$.

It is unknown exactly what flame heights would correspond to the ignition of the shrubs. However, it is suspected that this would depend on the ratio between the height of the shrubs and the flame height. For the prescribed burn of plot TP06S, it appeared that litter flame heights over between 1 and 2 ft were sufficient to ignite a fire within the 3 to 4 ft huckleberry.

Once ignition of the huckleberry occurs, then the shrubs are treated as a separate fuel bed with their unique geometry, moisture content, etc. Flame heights observed on plot TP06S often stayed within about a foot of the top of the shrub component. This suggests that, like the litter layer, heat transfer within this shrub fuel bed is most important in fire spread and heating from the flames above the bed would not be a major contributing factor in the absence of wind or slope effects. By determination of $\dot{Q}''$ for the shrubs, the

rate of spread and flame height can be determined from equations 6.7 and 6.11, respectively.

6.2.5 Change in Heat Transfer Mechanisms

There are instances when the heat transfer mechanisms responsible for fire spread will vary depending on the effects of wind and topography on the fire. These various modes of heat transfer may also vary in magnitude resulting in a faster or slower fire. An example of this effect is the difference between a fire spreading up a slope and a fire that is spreading down the slope. It is, of course, assumed that the fire spreading up the slope would be a much larger and faster fire than the fire backing down the slope. In this case, the upslope fire would propagate primarily by the means of radiation and convection. The downslope fire can be viewed as an opposed-flow fire, where the dominant means of heat transfer is often assumed to be gas-phase conduction. This is numerically defined as (Quintiere, 1995):

$$\dot{q}''_{cond} = \frac{k_g (T_f - T_p)}{L_c}. \tag{6.13}$$

where k_g is the gas-phase conductivity, T_f is the flame temperature and L_c is some preheating distance over which the forward flux acts.

As an example of the effects that varying heat transfer mechanisms will have on the rate of spread and flame properties using the concepts discussed earlier, consider two

cases of a fire spreading under the influence of slope effects. One fire is spreading up a slope and the other is backing down a similar slope, see Figures 6.3 and 6.4, respectively. No wind effects are considered. For simplicity, it is assumed that this slope is sufficient to cause a change in heat transfer mechanisms within the fuel bed when a fire changes from an upslope spreading fire to a fire backing down the slope. However, the change in flame angle is small so that heat transfer from the flames above the fuel bed will not be considered.

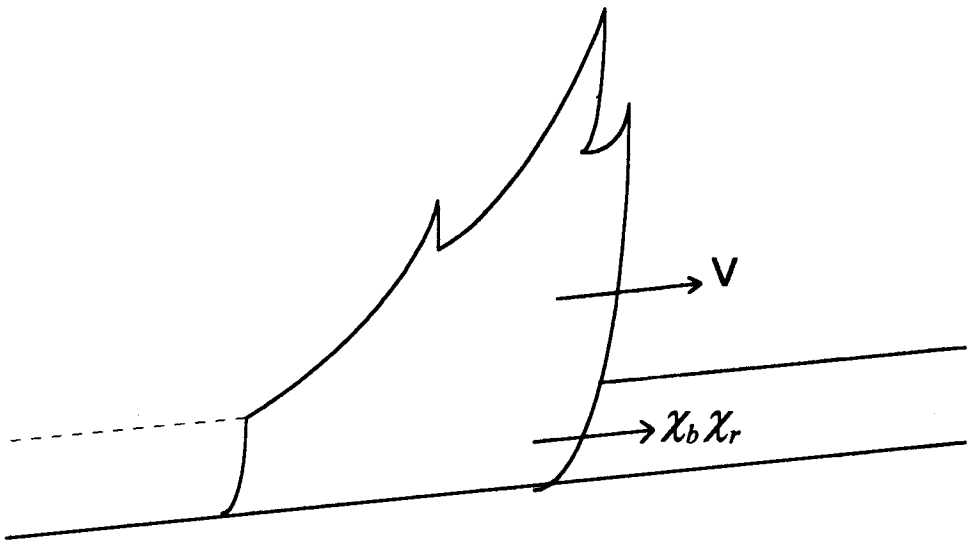

Figure 6.3: Fraction of heat release rate for upslope fire.

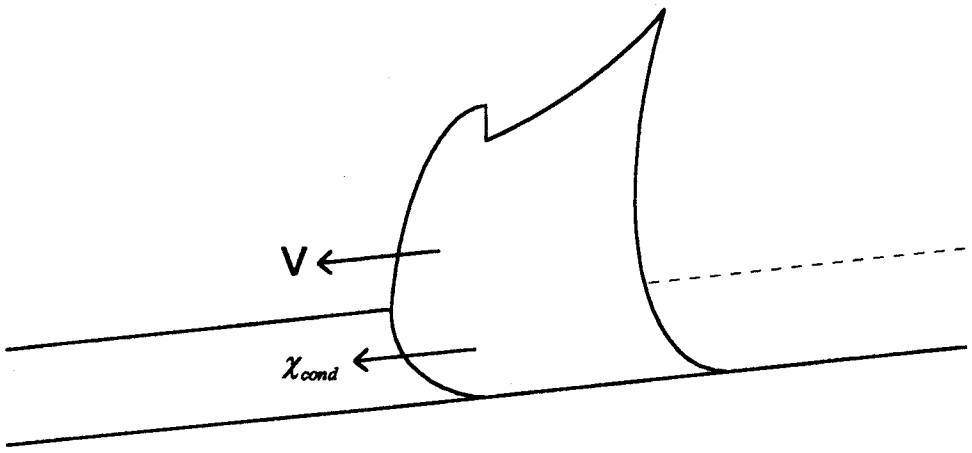

Figure 6.4: Fraction of heat release rate for downslope fire.

For the upslope fire of Figure 6.3, we will assume that the dominant heat transfer mechanism continues to be radiation and so we can estimate $\chi_r \approx 0.30$. The fraction of that radiant heat release rate that passes through the combustion interface can be determined from Figure 6.5, with an assumed control volume of height d, unit length and depth 2d. Assuming the duff layer acts as an insulator allowing no heat transfer to pass through and there is an equal exchange of radiant heat in and out of sides 4 and 5 due to an infinitely long flame front, then radiation can pass out of the flaming zone through sides 1, 2 and 3. If side 1 is in the direction of flame spread, then it accounts for 25% of the area that the radiation can pass through. Therefore, $\chi_b \approx 0.25$ and $\chi_b\chi_r \approx 0.08$ is the fraction of the total radiant heat release rate that passes through the combustion interface to heat the unburned fuel ahead.

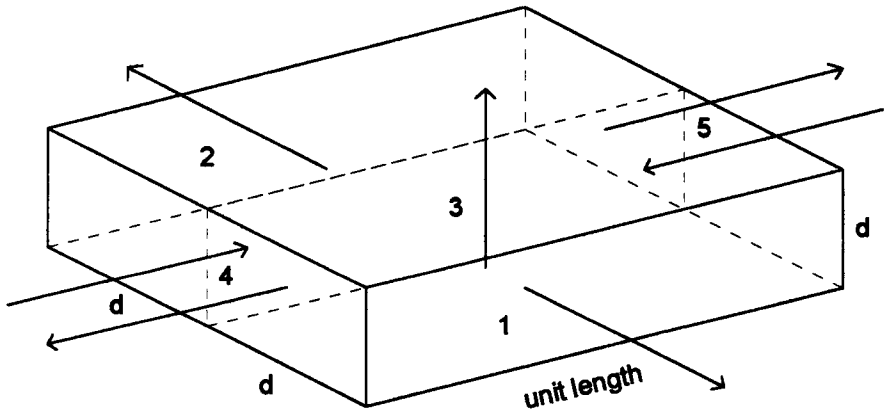

Figure 6.5: Control volume for radiant fraction of heat release rate through combustion interface.

In the case of the fire backing down the slope of Figure 6.4, the dominant mode of heat transfer is assumed to be gas-phase conduction. The forward flux to the unburned fuel that results from gas-phase conduction can be determined in detail from equation 6.13 or we can qualitatively reason that some fraction of the heat release rate that passes through the combustion interface heats the unburned fuel by this mechanism. In the absence of wind or slope effects, the contribution of gas-phase conduction to the total energy transferred to the fuel is about 20% and radiation accounts for about 80% (Pagni & Peterson, 1973). That is, gas-phase conduction contributes about ¼ that of radiation to the forward heat transfer. Therefore, the effects of gas-phase conduction in a backing fire can be assumed to be small compared to radiation in a head fire. For simplicity, if we assume that the fraction of the heat release rate that is transferred to the unburned fuel by gas-phase conduction, χ_{cond}, in a fire backing down a slope continues to be approximately

¼ that of the radiant transfer in the head fire up a slope, then we can estimate $\chi_{cond} \approx 0.02$, and the forward flux per unit area for the backing fire is:

$$\dot{q}''_{cond} = \frac{\chi_{cond}\dot{Q}''\Delta(1)}{d(1)}. \tag{6.14}$$

Since $\chi_{cond} << \chi_b\chi_r$, we can expect that the spread rate, flame height and depth of the down-slope fire should be less than the up-slope fire. From equation 6.4, we can write:

$$\dot{Q}'' = \frac{\dot{m}\cdot\Delta H_c}{\Delta(1)}, \tag{6.15}$$

where $\dot{m}$ is the mass loss rate of the flaming zone. This can be approximated by the relation for the mass flow rate through a control volume, or $\dot{m} = \rho_b V A_d$, where A_d is the cross-sectional area of the combustion interface. Then,

$$\dot{Q}'' = \frac{\Delta H_c \rho_b V d(1)}{\Delta(1)}, \tag{6.16}$$

or,

$$\dot{Q}'' = \Delta H_c \rho_b \left(\frac{d}{\Delta}\right) V. \tag{6.17}$$

The heat release rate per unit area and all of the fuel bed properties in equation 6.17 can be assumed to remain constant for both the up- and down-slope spreading fires. Therefore, if the spread rate increases as the fire spreads uphill, then the flaming zone depth must also increase in order to keep $\dot{Q}''$ constant. Similarly, as the fire slows down when spreading downhill, Δ must decrease. Since the flame height is also a function of $\dot{Q}''$ and Δ, then the faster spreading fire with a large flaming zone depth will also produce the greater flame heights.

In the case of enhanced forward heat transfer due to wind, we will not consider all of the additional mechanisms by which the unburned fuel is heated. Pagni and Peterson (1973) provide an excellent discussion of the various modes of heat transfer from the flames above and within the fuel bed and incorporate these into a model for fire spread through porous fuels that was in good agreement with forest fuel flame spread data. For illustrative purposes, we will consider radiant heating of the unburned fuel from the flames above the fuel bed. Again, we can write this forward flux as a function of the radiant heat release rate:

$$\dot{q}_f'' = \frac{aF\dot{Q}_r}{d(1)}, \tag{6.18}$$

where a is the fuel absorptivity, $\dot{Q}_r$ is determined from equation 6.5, and F is a view factor between the flame and a surface element at a distance y ahead of the flaming zone (Pagni & Peterson, 1973):

$$F = 0.5[1 - Z(1+Z^2)^{-0.5}], \tag{6.19}$$

$$Z = \frac{(x/L - \sin\theta)}{\cos\theta}, \tag{6.20}$$

where L is the flame length (= $H_F/\cos\theta$) and θ is the angle between the flame and the perpendicular to the fuel bed. The view factor, F, is similar to χ_b as it estimates the amount of the radiation that reaches a surface fuel element ahead of the flaming zone. It is simply related to the angle of flame tilt and the flame height which is again related to the heat release rate per unit area. The flame tilt angle, θ, has been empirically determined to be related to the windspeed, U_w, when the rate of spread is much less than U_w, by the relation $\theta = \tan^{-1}[1.4U_w(gL)^{-0.5}]$ (Pagni & Peterson, 1973).

This method of accounting for the heat transfer from the flames above the fuel bed to the unburned fuel differs from the wind and slope coefficients in BEHAVE which were multiplication factors that accounted for the additional propagating flux produced by wind and slope. The wind coefficient was experimentally determined from the ratio of the rate of spread in the presence of a heading wind to the no-wind rate of spread, $\phi_w = R_w/R_o - 1$ (Rothermel, 1972). The slope coefficient was determined similarly. Therefore, the coefficients are being calculated in a reverse direction, where the rates of spread are first

determined and then a relation will calculate what portion of that rate of spread was due to the effects of wind or slope. Equations 6.18 through 6.20 provide a means of estimating the forward heat transfer from the flames to the unburned fuel based on actual flame behavior and the geometry between the fuels and the flame. The power of this method of modeling the spread of fires is that each of the important mechanisms of heat transfer can be calculated separately and in detail. The driving force is calculated first, then its distribution by these various mechanisms can be determined. By knowing the amount and form of the energy that is supplied from the flaming zone, along with the energy required to bring the potential fuel to ignition, the rate of spread can then be calculated.

6.2.6 The Heat Release Rate

The key parameter in each of the above formulations for rate of spread and flame properties is the heat release rate. It is viewed as one of the most important parameters in determining the rate of fire growth, size of the fire and the threat to humans from exposure to fire and toxic gases (Tewarson, 1980). The heat release rate from large fires drives the flow which supplies air to the fire and influences the flame spread rate, spread pattern and fire plume behavior (Ohlemiller & Corley, 1990). Direct measurements of heat release rate versus time are used extensively as input to computer fire models designed to predict the response of buildings, furnishings and commodities to fire. Babrauskas and Grayson (1992) provide an excellent compilation of the history of this parameter, measurement techniques, experimental data and computer modeling applications.

The development of the principle of oxygen consumption calorimetry has brought significant advances in the measurement and application of heat release rates. A small scale test method based on this principle has been developed to determine the rate of heat release of materials under varying combustion conditions in air. The test instrument, called the Cone Calorimeter, determines fire properties such as rate of heat release per unit area, cumulative heat released, effective heat of combustion, time to ignition, mass loss rate, and properties of combustion such as smoke and toxic gases (American Society for Testing and Materials [ASTM E1354], 1992; Cox, Forcier, Jackson, & Jacoby, 1995). The apparatus utilizes a conical-shaped electrical heater which imposes a heating flux of up to 100 kW/m^2 on a horizontally- or vertically-oriented sample of size 100 mm x 100 mm x up to 50 mm thick. Samples are placed on a load cell to continuously monitor mass loss. All of the combustion products are collected in a duct where oxygen analyzers and other measurement devices are located. Larger-scale heat release rate apparatuses are also available where full-scale items or entire systems of materials, such as a room with various wall linings and furniture, can be tested (Babrauskas, 1992). The Cone Calorimeter has been utilized in order to determine the effective heats of combustion of duff and twig samples as part of a large scale fire experiment in Canada (Ohlemiller & Corley, 1990,1994; Quintiere, 1990). Such a small-scale test would appear to be useful in evaluating the behavior of the litter or duff layer to various conditions, as they are relatively uniform and can most likely be represented by small samples. For more complex fuel components such as the shrubs, a larger-scale apparatus may be necessary to yield applicable results to actual fuel bed conditions.

The Cone Calorimeter and other larger-scale devices provide a quantitative representation of the heat release rate and other parameters mentioned earlier as they vary with time. Figure 6.6 gives an illustration of the basic components of a typical heat release rate history (Mowrer & Williamson, 1990). Following an often negligible induction period, heat release rates usually exhibit an acceleratory growth period until a peak is reached. Depending on how quickly burnout begins, there may be a period of steady burning or there may be a distinct peak with an immediate decay. The tail portion of the curve usually denotes an extended period of low heat release rates where char formation and glowing combustion occur. The total energy released is the area under the time - heat release rate curve. Babrauskas (1995) shows heat release rate histories for several household items, flammable liquids, wood cribs and Christmas trees. When dried with heat lamps to simulate warm, dry room conditions, the Christmas trees typically had a large induction period followed a sharp growth period of less than 50 seconds to a peak. The decay period was equally fast, see Figure 6.7.

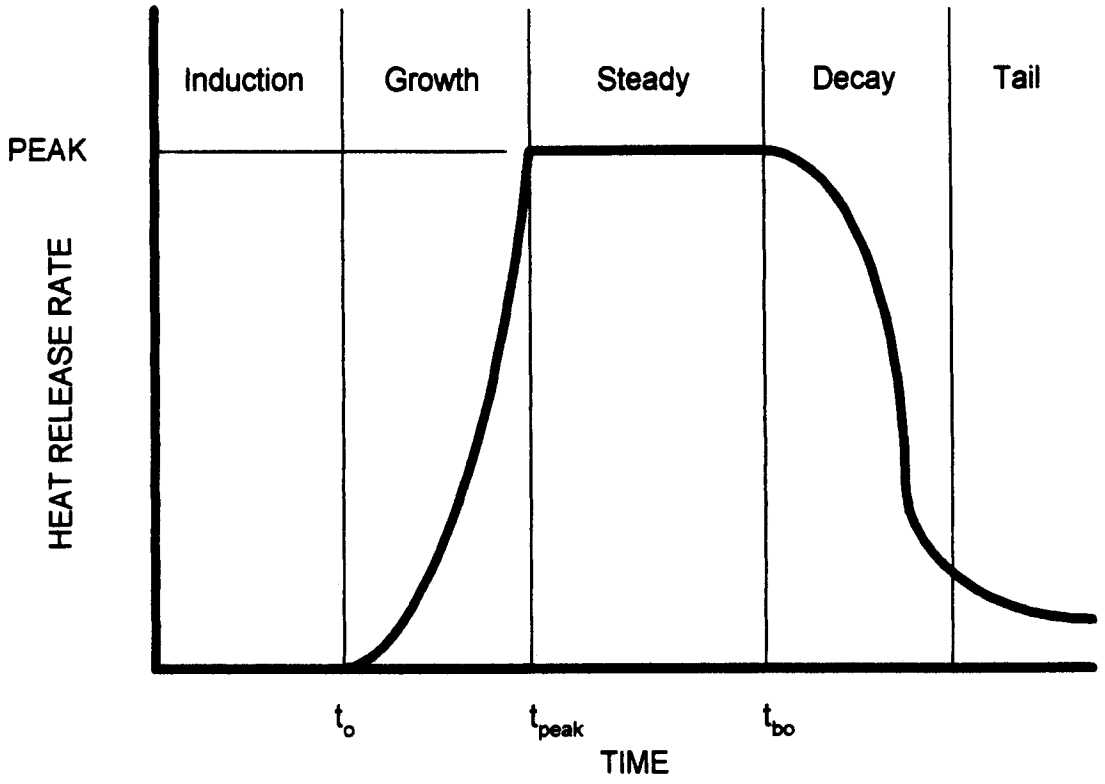

Figure 6.6: Example of heat release rate vs. time curve.

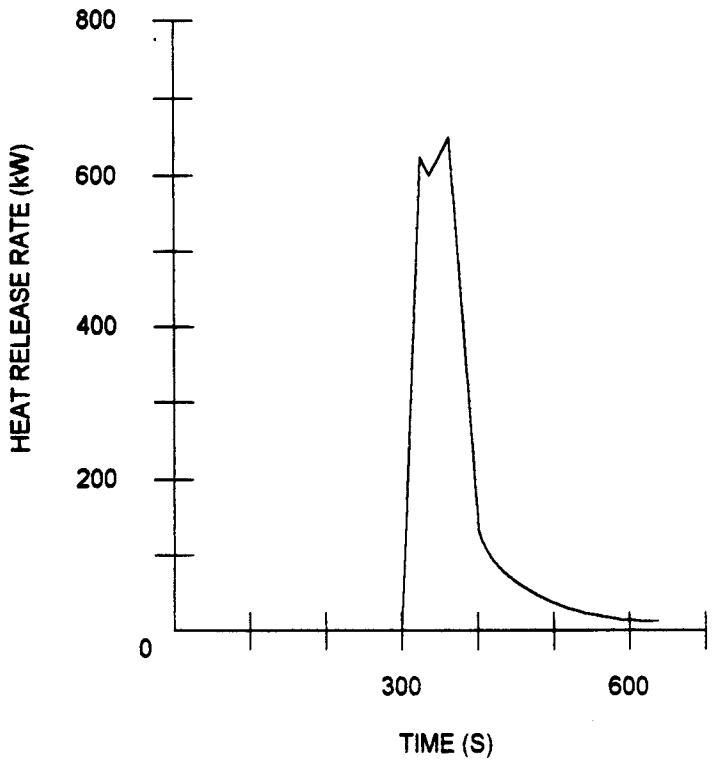

Figure 6.7: Heat release rate curve for a Christmas tree.

Once the heat release rate history is obtained, it must be characterized in order to be used in a predictive model. Mowrer and Williamson (1990) give various methods to model the growth and decay periods of a heat release rate history. Often, a power law relationship is used to describe the time-dependence of the fire growth where the heat release rate may increase with some power of the time since the start of the growth period. For instance, a t-squared representation of fire growth is often used where the heat release rate is written as, $\dot{Q} = \alpha(t - t_o)^2$, where t_o is the start of the growth period and α is the fire growth parameter. Depending on the application, a full heat release rate history may be useful which will include all aspects of the burning process of a material. Other

applications may only be interested in the peak value of the heat release rate or average values over a period of time.

6.3 Future Work

This discussion has demonstrated a simple model of flame spread to provide a theoretical basis for future work in this area of wildland fire modeling. The heat release rate parameter can be determined through experimental methods to give a quantitative, time-dependent history of the actual burning behavior of fuels or systems of materials. The fuels can be burned in as close to natural conditions as possible, especially in the larger scale calorimeters, and so the their heat release rates become a function of fuel type, size, moisture content and chemical composition. These parameters can be varied to view their effects on the effective heat of combustion and therefore the fire behavior of various fuel components. Such an analysis of fuels in the pine - oak forest fuel complex would prove very useful in understanding the fire behavior of these fuels.

Several important questions raised in previous chapters may also be answered about the fire behavior of the various fuel components. By obtaining heat release rate data of the live fuels at various moisture contents, the heat release rate parameter can be expressed as a function of the moisture content. This will directly show the various burning behaviors of the live fuels during the dormant and growing seasons. Exposing the litter and shrubs at various moisture contents to different levels of heat fluxes may also shed new light on the moistures of extinction of the live and dead fuels. By determining the potential heat release rates of the litter layer under various conditions, a quantitative

measure of the heat flux exposure to the shrubs will be obtained. This may provide a better understanding the ignition process and burning behavior of the shrubs and the fuel complex in general.

References

Albini, F.A. (1976a). Computer-based models of wildland fire behavior: A user's manual. Ogden, UT: USDA Forest Service, Intermountain Forest and Range Experiment Station.

Albini, F.A. (1976b). Estimating wildfire behavior and effects (General Technical Report INT-30). Ogden, UT: USDA Forest Service, Intermountain Forest and Range Experiment Station.

American Society for Testing and Materials [ASTM E1355]. (1992). Standard guide for evaluating the predictive capability of fire models. Philadelphia, PA: author.

American Society for Testing and Materials [ASTM E1354]. (1994). Standard test method for heat and visible smoke release rates for materials and products using an oxygen consumption calorimeter. Philadelphia, PA: author.

Anderson, H.E. (1983). Predicting wind-driven wild land fire size and shape (Research Paper INT-305). Ogden, UT: USDA Forest Service, Intermountain Forest and Range Experiment Station.

Andrews, P.L. (1986). BEHAVE: Fire behavior prediction and fuel modeling system - BURN subsystem, part 1 (General Technical Report INT-194). Ogden, UT: USDA Forest Service, Intermountain Forest and Range Experiment Station.

Andrews, P.L., & Chase, C.H. (1989). BEHAVE: Fire behavior prediction and fuel modeling system - BURN subsystem, part 2 (General Technical Report INT-260). Ogden, UT: USDA Forest Service, Intermountain Forest and Range Experiment Station.

Babrauskas, V. (1992). Full-scale heat release rate measurements. In V. Babrauskas & S.J. Grayson (Eds.), Heat release in fires (pp. 93-112). London: Elsevier Applied Science.

Babrauskas, V. (1995). Burning rates. In P. DiNenno, C. Beyler, R. Custer, W. Walton, J. Watts, D. Drysdale, & J. Hall (Eds.), The SFPE handbook of fire protection engineering (2nd ed., chap. 2-13). Quincy, MA: National Fire Protection Association & Society of Fire Protection Engineers.

Babrauskas, V., & Grayson, S.J. (Eds.). (1992). Heat release in fires. London: Elsevier Applied Science.

Bradshaw, L.S., Deeming, J.E., Burgan, R.E., & Cohen, J.D. (1984). The 1978 national fire-danger rating system: Technical documentation (General Technical Report INT-169). Ogden, UT: USDA Forest Service, Intermountain Forest and Range Experiment Station.

Brown, J.K. (1972). Field test of a rate-of-spread model in slash fuels (Research Paper INT-116). Ogden, UT: USDA Forest Service, Intermountain Forest and Range Experiment Station.

Brown, J.K. (1974). Handbook for inventorying downed woody material (General Technical Report INT-16). Ogden, UT: USDA Forest Service, Intermountain Forest and Range Experiment Station.

Burgan, R.E. (1987). Concepts and interpreted examples in advanced fuel modeling (General Technical Report INT-238). Ogden, UT: USDA Forest Service, Intermountain Forest and Range Experiment Station.

Burgan, R.E. (1988). 1988 revisions to the 1978 National Fire-Danger Rating System (Research Paper SE-273). Asheville, NC: USDA Forest Service, Southeastern Forest Experiment Station.

Burgan, R.E., & Rothermel, R.C. (1984). BEHAVE: Fire behavior prediction and fuel modeling system-FUEL subsystem (General Technical Report INT-167). Ogden, UT: USDA Forest Service, Intermountain Forest and Range Experiment Station.

Catchpole, E.A., & Catchpole, W.R. (1995). The second generation U.S. firespread model: Final report 1994 (INT-91558-RJVA). The University of New South Wales, Department of Mathematics and Statistics.

Catchpole, E.A., Catchpole, W.R., & Rothermel, R.C. (1993). Fire behavior experiments in mixed fuel complexes. International Journal of Wildland Fire, 3, 45-57.

Cengal, Y.A., & Boles, M.A. (1994). Thermodynamics: An engineering approach (2nd ed.). New York: McGraw-Hill, Inc.

Cox, A., Forcier, T., Jackson, R., & Jacoby, D. (1995). Operation and verification of the WPI cone calorimeter. Unpublished major qualifying project. Worcester Polytechnic Institute, Center for Firesafety Studies, Worcester, MA.

Crary, D.J., Jr. (1987). The effect of prescribed burning and mowing on fuels in Gaylussacia baccata communities. Unpublished master's project report, University of Massachusetts, Amherst.

Drysdale, D. (1985). An introduction to fire dynamics. New York: John Wiley and Sons.

Emmons, H.W. (1963). Fire in the forest. Fire Research Abstracts and Reviews, 5, 163-178.

Fahnestock, G.R. (1970). Two keys for appraising forest fire fuels (General Technical Report PNW-99). Portland, OR: USDA Forest Service, Pacific Northwest Forest and Range Experiment Station.

Fons, W.L. (1946). Analysis of fire spread in light forest fuels. Journal of Agricultural Research, 72, 93-121.

Fons, W.L., Bruce, H.D., & Pong, W.Y. (1959). A steady-state technique for studying the properties of free-burning wood fires. In W.G. Berl (Ed.), Proceedings of the First International Symposium on The Use of Models in Fire Research (pp. 219-234). Washington, DC: National Academy of Sciences-National Research Council.

Fosberg, M.A., & Schroeder, M.J. (1971). Fine herbaceous fuels in fire-danger rating (Research Note RM-185). Fort Collins, CO. USDA Forest Service, Rocky Mountain Forest and Range Experiment Station.

Frandsen, W.H. (1971). Fire spread through porous fuels from the conservation of energy. Combustion and Flame, 16, 9-16.

Golley, F.B. (1961). Energy values of ecological materials. Ecology, 42, 581-584.

Gould, J.S. (1991). Validation of the Rothermel fire spread model and related fuel parameters in grassland fuels. In N.P. Cheney & A.M. Gills (Eds.), Proceedings of the Conference on Bushfire Modelling and Fire Danger Rating (pp. 51-64). Canberra: Commonwealth Scientific and Industrial Research Organization.

Hasemi, Y. (1985). Thermal modeling of upward wall flame spread. In C.E. Grant & P.J. Pagni (Eds.), Fire Safety Science: Proceedings of the First International Symposium (pp. 87-96). Washington: Hemisphere Publishing Corporation.

Hasemi, Y., & Nishihata, M. (1988). Fuel shape effect on the deterministic properties of turbulent diffusion flames. In T. Wakamatsu, Y. Hasemi, A. Sekizawa, P.G. Seeger, P.J. Pagni, & C.E. Grant (Eds.), Fire Safety Science: Proceedings of the Second International Symposium (pp. 275-284). Washington: Hemisphere Publishing Corporation.

Haven, L., Hunter, T., & Storey, T. (1982). Production rates for crews using handtools on firelines (General Technical Report PSW-62). Berkeley, CA: USDA Forest Service, Pacific Southwest Forest and Range Experiment Station.

Heskestad, G. (1995). Fire plumes. In P. DiNenno, C. Beyler, R. Custer, W. Walton, J. Watts, D. Drysdale, & J. Hall (Eds.), The SFPE handbook of fire protection engineering (2nd ed., chap. 2-2). Quincy, MA: National Fire Protection Association & Society of Fire Protection Engineers.

Hough, W.A., & Albini, F.A. (1978). Predicting fire behavior in palmetto-gallberry fuel complexes (Research Paper SE-174). Asheville, NC: USDA Forest Service, Southeastern Forest Experiment Station.

Huggett, C. (1980). Estimation of rate of heat release by means of oxygen consumption measurements. Journal of Fire and Materials, 12, 61-65.

Incropera, F.P., & DeWitt, D.P. (1990). Introduction to heat transfer (2nd ed.). New York: John Wiley & Sons.

Janssens, M. (1995). Calorimetry. In P. DiNenno, C. Beyler, R. Custer, W. Walton, J. Watts, D. Drysdale, & J. Hall (Eds.), The SFPE handbook of fire protection engineering (2nd ed., chap. 3-2). Quincy, MA: National Fire Protection Association & Society of Fire Protection Engineers.

Kanury, M.A. (1995). Flaming ignition of solid fuels. In P. DiNenno, C. Beyler, R. Custer, W. Walton, J. Watts, D. Drysdale, & J. Hall (Eds.), The SFPE handbook of fire protection engineering (2nd ed., chap. 2-13). Quincy, MA: National Fire Protection Association & Society of Fire Protection Engineers.

Kelsey, R.G., Shafizadeh, F., & Lowery, D.P. (1979). Heat content of bark, twigs, and foliage of nine species of western conifers (Research Note INT-261). Ogden, UT: USDA Forest Service, Intermountain Forest and Range Experiment Station.

Maclean, N. (1992). Young men and fire. Chicago: University of Chicago Press.

Marsden-Smedley, J.B., & Catchpole, W.R. (1995a). Fire behaviour modelling in Tasmanian buttongrass moorlands I. Fuel characteristics. International Journal of Wildland Fire, 5, 203-214.

Marsden-Smedley, J.B., & Catchpole, W.R. (1995b). Fire behaviour modelling in Tasmanian buttongrass moorlands II. Fire behaviour. International Journal of Wildland Fire, 5, 215-228.

McFadden, R.D. (1995a, August 25). Fire races across eastern L.I., destroying homes. New York Times, pp. A1, B5.

McFadden, R.D. (1995b, August 27). Woodland fire finally tamed on Long Island. New York Times, pp. 1,35.

Mobley, H., Jackson, R., Balmer, W., Ruziska, W., & Hough, W. (1973). A guide for prescribed fire in southern forests (USDA Forest Service Pamphlet). Atlanta, GA: Southeastern Area S, and P.F.-2.

Mowrer, F.W., & Williamson, R.B. (1990). Methods to characterize heat release rate data. Fire Safety Journal, 16, 367-387.

National Wildfire Coordinating Group. (1989). Fireline handbook NWCG handbook 3. Washington, DC: Author.

Neter, J., Wasserman, W., & Whitmore, G. (1993). Applied statistics (4th ed.). Needham, MA: Allyn and Bacon.

Norum, R.A. (1982). Predicting wildfire behavior in black spruce forests in Alaska (Research Note PNW-401). Portland, OR: USDA Forest Service, Pacific Northwest Forest and Range Experiment Station.

Ohlemiller, T.J., & Corley, D.M. (1990). Estimation of the rate of heat release and induced wind field in a large scale fire (NISTIR 4430). Gaithersburg, MD: US Department of Commerce, National Institute of Standards and Technology.

Ohlemiller, T.J., & Corley, D.M. (1994). Heat release rate and induced wind field in a large scale fire. Combustion Science and Technology, 97, 315-330.

Pagni, P.J., & Peterson, T.G. (1973). Flame spread through porous fuels. In Fourteenth Symposium (International) on Combustion (pp. 1099-1107). Pittsburgh, PA: The Combustion Institute.

Patterson, W.A., III. (1996). [Prescribed burn studies, Cape Cod National Seashore]. Unpublished raw data.

Patterson, W.A., III, Saunders, K.E., & Horton, L.J. (1984). Fire regimes of Cape Cod National Seashore (Report OSS 83-1). Boston, MA: US Department of the Interior, Office of Scientific Studies.

Phillips, C.B., & Barney, R.J. (1984). Updating bulldozer fireline production rates (General Technical Report INT-166). Ogden, UT: USDA Forest Service, Intermountain Forest and Range Experiment Station.

Philpot, C.W. (1969a). The effect of reduced extractive content on the burning rate of aspen leaves (Research Note INT-92). Ogden, UT: USDA Forest Service, Intermountain Forest and Range Experiment Station.

Philpot, C.W. (1969b). Seasonal changes in heat content and ether extractive content of chamise (Research Paper INT-61). Ogden, UT: USDA Forest Service, Intermountain Forest and Range Experiment Station.

Philpot, C.W., & Mutch, R.W. (1971). The seasonal trends in moisture content, ether extractives, and energy of ponderosa pine and Douglas-fir needles (Research Paper INT-102). Ogden, UT: USDA Forest Service, Intermountain Forest and Range Experiment Station.

Quintiere, J.G. (1990). Canadian mass fire experiment, 1989 (NISTIR 4444). Gaithersburg, MD: US Department of Commerce, National Institute of Standards and Technology.

Quintiere, J.G. (1995). Surface flame spread. In P. DiNenno, C. Beyler, R. Custer, W. Walton, J. Watts, D. Drysdale, & J. Hall (Eds.), The SFPE handbook of fire protection engineering (2nd ed., chap. 2-14). Quincy, MA: National Fire Protection Association & Society of Fire Protection Engineers.

Rice, C.L., & Martin, R.E. (1985). Use of BEHAVE on shrublands at the urban interface. In L.R. Donoghue & R.E. Martin (Eds.), Proceedings of the 8th Conference on Fire and Forest Meteorology (pp. 270-275). Bethesda, MD: Society of American Foresters.

Richards, L.W. (1940). Effect of certain chemical attributes of vegetation on forest inflammability. Journal of Agricultural Research, 60, 833-838.

Rothermel, R.C. (1972). A mathematical model for predicting fire spread in wildland fuels (Research Paper INT-115). Ogden, UT: USDA Forest Service, Intermountain Forest and Range Experiment Station.

Rothermel, R.C. (1983). How to predict the spread and intensity of forest and range fires (General Technical Report INT-143). Ogden, UT: USDA Forest Service, Intermountain Forest and Range Experiment Station.

Rothermel, R. C. (1993). Mann Gulch fire: A race that couldn't be won (General Technical Report INT-299). Ogden, UT: USDA Forest Service, Intermountain Forest and Range Experiment Station.

Rothermel, R.C., & Anderson, H.E. (1966). Fire spread characteristics determined in the laboratory (Research Paper INT-30). Ogden, UT: USDA Forest Service, Intermountain Forest and Range Experiment Station.

Rothermel, R.C., & Philpot, C.W. (1973). Predicting changes in chaparral flammability. Journal of Forestry, 71, 640-643.

Shafizadeh, F., Chin, P., & DeGroot, W.F. (1977). Effective heat content of green forest fuels. Forest Science, 23, 81.

Susott, R.A. (1982). Characteristics of the thermal properties of forest fuels by combustible gas analysis. Forest Science, 28, 404-420.

Susott, R.A. (1984). Heat of preignition of three woody fuels used in wildfire modeling research (Research Note INT-342). Ogden, UT: USDA Forest Service, Intermountain Forest and Range Experiment Station.

Susott, R.A., DeGroot, W., & Shafizadeh, F. (1975). The heat content of natural fuels. Journal of Fire and Flammability, 6, 311-325.

Susott, R.A., Shafizadeh, F., & Aanerud, T.W. (1979). A quantitative thermal analysis technique for combustible gas detection. Journal of Fire & Flammability, 10, 94-104.

Tewarson, A. (1980). Heat release rate in fires. Fire and Materials, 4, 185-191.

Thomas, P.H. (1995). The growth of fire - Ignition to full involvement. In G. Cox (Ed.), Combustion fundamentals of fire (pp. 273-328). London: Harcourt Brace & Company.

Tran, H.C. (1992). Experimental data on wood materials. In V. Babrauskas & S.J. Grayson (Eds.), Heat release in fires (pp. 357-372). London: Elsevier Applied Science.

Weather information management system. (1993). Daily printout for station 191202, Marconi station, Cape Cod National Seashore, South Wellfleet, MA.

Williams, F.A. (1977). Mechanisms of fire spread. In Sixteenth Symposium (International) on Combustion (pp. 1281-1294). Pittsburgh, PA: The Combustion Institute.

Wilson, R.A. (1990). Reexamination of Rothermel's fire spread equations in no-wind and no-slope conditions (Research Paper INT-434). Ogden, UT: USDA Forest Service, Intermountain Forest and Range Experiment Station.

Woitkiewicz, M.D. (1996). Adjusted fuel moisture of Gaultheria procumbens and leaf litter - Effects on fire behavior. Unpublished manuscript, University of Massachusetts at Amherst, Department of Forestry and Wildlife Management.

Appendix A : Pine - Oak Forest Pictures

Figure A.1: Untreated area of the pine - oak forest fuel complex.

Figure A.2: Close-up of Gaylussacia baccata (huckleberry).

Figure A.3: Close-up of litter and surface fuels.

Figure A.4: Two years of growth on a winter plot burned every 4 years.

Figure A.5: One year of growth on summer plot burned every 3 years.

Figure A.6: Low intensity burn of summer plot burned every 2 years.

Figure A.7: Previously untreated plot TP06S to left of firefighters.

Figure A.8: Line fire ignition of plot TP06S. Fire spreading left.

Figure A.9: Head fire spreading through plot TP06S.

Figure A.10: Head fire spreading through plot TP06S.

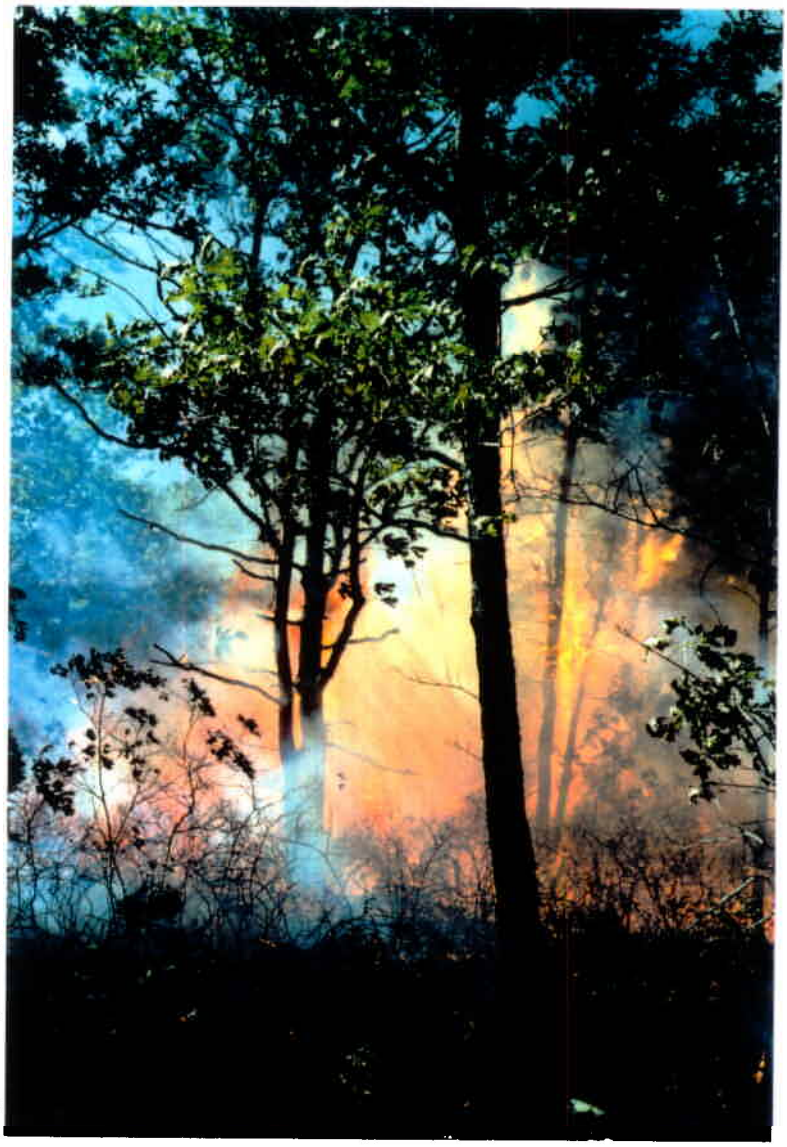

Figure A.11: Crowning of a 40-foot pitch pine.

Figure A.12: Backfire set at top of slope B in plot TP06S.

Figure A.13: Post-fire on slope A of plot TP06S.

Appendix B : Fire Behavior Hazard Levels

B.1 Flame Lengths

The visible flame lengths of a spreading fire correspond to the amount of heat felt by a firefighter on the fire lines (Andrews, 1986). A fire which has small flames can easily be extinguished with handtools or small amounts of water, while spreading fires with large flames will be difficult, if not impossible, to approach directly. Table 3.1 gives general interpretations of the various levels of flame length severity and their corresponding suppression tactical concerns (Andrews, 1986; National Wildfire Coordinating Group, 1989; Rothermel, 1983).

B.2 Spread Rates

It is also important to know the spread rate of a fire, as it will determine the type of ignition technique used in prescribed fires, the actions taken for suppression or the danger to those ahead of an advancing wildfire. Spread rates can also be correlated to the size and shape of a fire, which is information used to classify the type of fire, and the amount of resources and type of command structure required for wildfire suppression (National Wildfire Coordinating Group, 1989). The relative magnitudes of spread rates, however, are more difficult to interpret than flame lengths. A fire characteristics chart is available which relates the flame length, spread rate and heat per unit area to suppression interpretations similar to those in Table 3.1 (Rothermel, 1983). However, flame lengths are the major variable which separate the various levels of fire behavior, and so it is difficult to divide the spread rates into hazard levels using this method.

The primary concerns with a spreading wildfire or a prescribed fire that has burned beyond control are the speed with which the fire can be brought under control, and the safety of firefighting personnel. A more practical method of evaluating the consequences of spread rates may be to relate them to the speed with which firefighters are able to execute control and suppression tactics. For instance, a fire spreading at a low rate of spread would be equivalent to one which could be controlled easily by the construction of firelines, or fire breaks, around the perimeter of the fire. More moderate rates of spread would require the assistance of the faster, mechanical means of fireline construction, such as dozers or tractor-plows. The highest rates of spread may cause concern for firefighter safety, and so should be correlated to the speed with which a firefighter could escape a dangerous situation.

There are several factors that influence the speed with which a fire crew can construct a fireline. These include the type of vegetation, terrain and soil, weather and smoke conditions, and crew experience. Existing data available on production rates for crews using hand tools on firelines are highly variable (Haven, Hunter, & Storey, 1982). There are, however, general guidelines available to suppression personnel, which correlate line production rates to the 13 NFFL fuel models and crew experience levels (National Wildfire Coordinating Group, 1989).

To use these guidelines, the pine - oak forests will be approximated by a combination of NFFL fuel model 5, which accounts for the short shrub understory, and NFFL fuel model 9, which accounts for the pine - oak overstory. These approximations are solely for the purpose of estimating the difficulty in cutting line through the fuel

complex of interest. For a 20-person crew working over an extended period, line production rates average about 5 feet/min which is the lower value for fuel models 5 and 9. Faster production rates, averaging up to 30 ft/min, are achieved in the areas of only litter and timber fuels (fuel model 9), which may exist in the pine - oak forests where there are patches of no shrub understory. In an initial attack situation, where a narrow, incomplete line or "scratch line" is constructed in fuel model 5, production rates average up to 15 or 20 ft/min over a shorter period of time. Fires requiring the use of dozers or tractor-plows can be contained at the average rate of up to about 100 ft/min for fuel models 5 and 9. This corresponds to single pass line construction, or a single bulldozer constructing a fireline to mineral soil, one-blade wide, in near 0% slope (Phillips & Barney, 1984).

Besides the rate at which a fire can be contained, another major concern is the safety of firefighters and their escape from dangerous situations. Factors such as the slope and difficulty of the terrain are important in influencing the speed at which a person can move in a wildfire situation. The amount and type of vegetation is also important, although it is interesting to note that the majority of fatalities occur in light, flashy fuels on smaller fires (Rothermel, 1983). For example, the firefighters killed in Mann Gulch in 1949 were finally overcome on a 76% slope of primarily grass fuels. Their top running speed was estimated to be about 6.5 mi/h, which is roughly jogging speed in flat, level terrain (Maclean, 1992; Rothermel, 1993). For the present purposes, where the terrain of the pine - oak forests is relatively flat, an average walking speed of 3 mi/h (260 ft/min) will be assumed, and a jogging speed of 6 mi/h (530 ft/min).

The above rates of fireline construction and firefighter travel speed will be used to help categorize various levels of spread rate severity. Each level corresponds to some significant suppression action that may be taken or, under more extreme conditions, the speed at which firefighters would be able to react. Table 3.2 gives a general interpretation of the various levels of spread rate severity.

Appendix C : Custom Fuel Models

FUEL MODEL 14. PLOT I1892S

LOADS, S/V RATIOS, AND DEPTHS FOR INDIVIDUAL FUEL COMPONENTS

FUEL COMPONENT	********** LOADS **********					*** S/V RATIOS ****			DEPTHS
	1 HR	10 HR	100 H	HERB	WOODY	1 HR	HERB	WOODY	
LITTER	3.90	0.00	0.00	0.00	0.00	2000.	0.	0.	0.06
GRASS	0.00	0.00	0.00	0.00	0.00	0.	0.	0.	0.00
SHRUBS	0.56	0.08	1.22	0.00	0.14	1500.	0.	1350.	0.30
SLASH	0.00	0.00	0.00	0.00	0.00	0.	0.	0.	0.00

********** FUEL LOAD SUMMARY **********

**** FUEL COMPONENT ****			** TIMELAG CLASS *			
	DEAD	LIVE	CLASS	LOAD		
LITTER	3.90	0.00	------	-----	******	UNITS ******
GRASS	0.00	0.00	1 HR	4.46	LOAD	: T/AC
SHRUBS	1.86	0.14	10 HR	0.08	S/V	: 1/FT
SLASH	0.00	0.00	100 HR	1.22	DEPTH	: FT
TOTAL	5.76	0.14	TOTAL	5.76		

FINAL FUEL MODEL

STATIC 14. I1892S

LOADS, T/AC		S/V RATIOS, 1/FT		OTHER	
1 HR	4.46	1 HR	1951.	DEPTH, FT	0.14
10 HR	0.08	LIVE HERB	0.	HEAT CONTENT, BTU/LB	8000.
100 HR	1.22	LIVE WOODY	1350.	EXT MOISTURE, %	49.
LIVE HERB	0.00	SIGMA	1929.	PACKING RATIO	0.06047
LIVE WOODY	0.14			PR/OPR	8.85

Figure C.1: Plot I1892S custom fuel model.

FUEL MODEL 15. PLOT K1289W

LOADS, S/V RATIOS, AND DEPTHS FOR INDIVIDUAL FUEL COMPONENTS

FUEL COMPONENT	LOADS 1 HR	10 HR	100 H	HERB	WOODY	S/V RATIOS 1 HR	HERB	WOODY	DEPTHS
LITTER	4.20	0.00	0.00	0.00	0.00	2000.	0.	0.	0.04
GRASS	0.00	0.00	0.00	0.00	0.00	0.	0.	0.	0.00
SHRUBS	0.90	0.00	1.60	0.00	1.17	1500.	0.	1350.	1.14
SLASH	0.00	0.00	0.00	0.00	0.00	0.	0.	0.	0.00

FUEL LOAD SUMMARY

FUEL COMPONENT	DEAD	LIVE
LITTER	4.20	0.00
GRASS	0.00	0.00
SHRUBS	2.50	1.17
SLASH	0.00	0.00
TOTAL	6.70	1.17

TIMELAG CLASS	LOAD
1 HR	5.10
10 HR	0.00
100 HR	1.60
TOTAL	6.70

LOAD : T/AC
S/V : 1/FT
DEPTH : FT

FINAL FUEL MODEL

STATIC 15. K1289W

LOADS, T/AC		S/V RATIOS, 1/FT		OTHER	
1 HR	5.10	1 HR	1931.	DEPTH, FT	0.55
10 HR	0.00	LIVE HERB	0.	HEAT CONTENT, BTU/LB	8000.
100 HR	1.60	LIVE WOODY	1350.	EXT MOISTURE, %	61.
LIVE HERB	0.00	SIGMA	1843.	PACKING RATIO	0.02053
LIVE WOODY	1.17			PR/OPR	2.90

Figure C.2: Plot K1289W custom fuel model.

FUEL MODEL 16. PLOT K1489S

LOADS, S/V RATIOS, AND DEPTHS FOR INDIVIDUAL FUEL COMPONENTS

FUEL COMPONENT	LOADS 1 HR	10 HR	100 H	HERB	WOODY	S/V RATIOS 1 HR	HERB	WOODY	DEPTHS
LITTER	3.50	0.00	0.00	0.00	0.00	2000.	0.	0.	0.08
GRASS	0.00	0.00	0.00	0.00	0.00	0.	0.	0.	0.00
SHRUBS	1.36	0.04	2.29	0.00	0.71	1500.	0.	1350.	1.11
SLASH	0.00	0.00	0.00	0.00	0.00	0.	0.	0.	0.00

FUEL LOAD SUMMARY

FUEL COMPONENT	DEAD	LIVE
LITTER	3.50	0.00
GRASS	0.00	0.00
SHRUBS	3.68	0.71
SLASH	0.00	0.00
TOTAL	7.18	0.71

TIMELAG CLASS	LOAD
1 HR	4.86
10 HR	0.04
100 HR	2.29
TOTAL	7.18

LOAD : T/AC
S/V : 1/FT
DEPTH : FT

FINAL FUEL MODEL

STATIC 16. K1489S

LOADS, T/AC		S/V RATIOS, 1/FT		OTHER	
1 HR	4.86	1 HR	1887.	DEPTH, FT	0.65
10 HR	0.04	LIVE HERB	0.	HEAT CONTENT, BTU/LB	8000.
100 HR	2.29	LIVE WOODY	1350.	EXT MOISTURE, %	38.
LIVE HERB	0.00	SIGMA	1823.	PACKING RATIO	0.01744
LIVE WOODY	0.71			PR/OPR	2.44

Figure C.3: Plot K1489S custom fuel model.

FUEL MODEL 17. PLOT E1292W

LOADS, S/V RATIOS, AND DEPTHS FOR INDIVIDUAL FUEL COMPONENTS

FUEL COMPONENT	********** LOADS **********					*** S/V RATIOS ****			DEPTHS
	1 HR	10 HR	100 H	HERB	WOODY	1 HR	HERB	WOODY	
LITTER	3.60	0.00	0.00	0.00	0.00	2000.	0.	0.	0.04
GRASS	0.00	0.00	0.00	0.00	0.00	0.	0.	0.	0.00
SHRUBS	1.06	0.02	0.91	0.00	1.50	1500.	0.	1350.	1.44
SLASH	0.00	0.00	0.00	0.00	0.00	0.	0.	0.	0.00

********** FUEL LOAD SUMMARY **********

**** FUEL COMPONENT ****			** TIMELAG CLASS *				
	DEAD	LIVE	*	CLASS	LOAD	*	****** UNITS ******
LITTER	3.60	0.00	*	------	-----	*	****** UNITS ******
GRASS	0.00	0.00	*	1 HR	4.66	*	LOAD : T/AC
SHRUBS	2.00	1.50	*	10 HR	0.02	*	S/V : 1/FT
SLASH	0.00	0.00	*	100 HR	0.91	*	DEPTH : FT
	-----	-----	*		-----	*	
TOTAL	5.10	1.50	*	TOTAL	5.60	*	

FINAL FUEL MODEL

STATIC 17. E1292W

LOADS, T/AC		S/V RATIOS, 1/FT		OTHER	
1 HR	4.66	1 HR	1909.	DEPTH, FT	0.73
10 HR	0.02	LIVE HERB	0.	HEAT CONTENT, BTU/LB	8000.
100 HR	0.91	LIVE WOODY	1350.	EXT MOISTURE, %	55.
LIVE HERB	0.00	SIGMA	1801.	PACKING RATIO	0.01394
LIVE WOODY	1.50			PR/OPR	1.93

Figure C.4: Plot E1292W custom fuel model.

FUEL MODEL 18. PLOT K1592W

LOADS, S/V RATIOS, AND DEPTHS FOR INDIVIDUAL FUEL COMPONENTS

FUEL COMPONENT	LOADS 1 HR	10 HR	100 H	HERB	WOODY	S/V RATIOS 1 HR	HERB	WOODY	DEPTHS
LITTER	4.40	0.00	0.00	0.00	0.00	2000.	0.	0.	0.13
GRASS	0.00	0.00	0.00	0.00	0.00	0.	0.	0.	0.00
SHRUBS	0.87	0.09	1.60	0.00	3.05	1500.	0.	1350.	1.19
SLASH	0.00	0.00	0.00	0.00	0.00	0.	0.	0.	0.00

FUEL LOAD SUMMARY

FUEL COMPONENT	DEAD	LIVE
LITTER	4.40	0.00
GRASS	0.00	0.00
SHRUBS	2.56	3.05
SLASH	0.00	0.00
TOTAL	6.96	3.05

TIMELAG CLASS	LOAD
1 HR	5.27
10 HR	0.09
100 HR	1.60
TOTAL	6.96

LOAD : T/AC
S/V : 1/FT
DEPTH : FT

FINAL FUEL MODEL

STATIC 18. K1592W

LOADS, T/AC		S/V RATIOS, 1/FT		OTHER	
1 HR	5.27	1 HR	1936.	DEPTH, FT	0.72
10 HR	0.09	LIVE HERB	0.	HEAT CONTENT, BTU/LB	8000.
100 HR	1.60	LIVE WOODY	1350.	EXT MOISTURE, %	35.
LIVE HERB	0.00	SIGMA	1761.	PACKING RATIO	0.01995
LIVE WOODY	3.05			PR/OPR	2.71

Figure C.5: Plot K1592W custom fuel model.

FUEL MODEL 19. PLOT K1492S

LOADS, S/V RATIOS, AND DEPTHS FOR INDIVIDUAL FUEL COMPONENTS

FUEL COMPONENT	********** LOADS **********					*** S/V RATIOS ****			DEPTHS
	1 HR	10 HR	100 H	HERB	WOODY	1 HR	HERB	WOODY	
LITTER	4.30	0.00	0.00	0.00	0.00	2000.	0.	0.	0.08
GRASS	0.00	0.00	0.00	0.00	0.00	0.	0.	0.	0.00
SHRUBS	1.08	0.03	1.90	0.00	0.52	1500.	0.	1350.	0.55
SLASH	0.00	0.00	0.00	0.00	0.00	0.	0.	0.	0.00

********** FUEL LOAD SUMMARY **********

**** FUEL COMPONENT ****			** TIMELAG CLASS *		
	DEAD	LIVE	CLASS	LOAD	
LITTER	4.30	0.00	1 HR	5.38	
GRASS	0.00	0.00	10 HR	0.03	
SHRUBS	3.01	0.52	100 HR	1.90	
SLASH	0.00	0.00			
TOTAL	7.32	0.52	TOTAL	7.32	

****** UNITS ******

LOAD : T/AC

S/V : 1/FT

DEPTH : FT

FINAL FUEL MODEL

STATIC 19. K1492S

LOADS, T/AC		S/V RATIOS, 1/FT		OTHER	
1 HR	5.38	1 HR	1921.	DEPTH, FT	0.29
10 HR	0.03	LIVE HERB	0.	HEAT CONTENT, BTU/LB	8000.
100 HR	1.90	LIVE WOODY	1350.	EXT MOISTURE, %	43.
LIVE HERB	0.00	SIGMA	1875.	PACKING RATIO	0.03874
LIVE WOODY	0.52			PR/OPR	5.54

Figure C.6: Plot K1492S custom fuel model.

FUEL MODEL 20. PLOT M1392S

LOADS, S/V RATIOS, AND DEPTHS FOR INDIVIDUAL FUEL COMPONENTS

FUEL COMPONENT	********** LOADS **********					*** S/V RATIOS ****			DEPTHS
	1 HR	10 HR	100 H	HERB	WOODY	1 HR	HERB	WOODY	
LITTER	4.60	0.00	0.00	0.00	0.00	2000.	0.	0.	0.11
GRASS	0.00	0.00	0.00	0.00	0.00	0.	0.	0.	0.00
SHRUBS	0.67	0.11	0.19	0.00	0.28	1500.	0.	1350.	0.52
SLASH	0.00	0.00	0.00	0.00	0.00	0.	0.	0.	0.00

********** FUEL LOAD SUMMARY **********

**** FUEL COMPONENT ****			** TIMELAG CLASS *			
	DEAD	LIVE	CLASS	LOAD	******	UNITS ******
LITTER	4.60	0.00	1 HR	5.27	LOAD	: T/AC
GRASS	0.00	0.00	10 HR	0.11	S/V	: 1/FT
SHRUBS	0.97	0.28	100 HR	0.19	DEPTH	: FT
SLASH	0.00	0.00				
TOTAL	5.57	0.28	TOTAL	5.57		

FINAL FUEL MODEL

STATIC 20. M1392S

LOADS, T/AC		S/V RATIOS, 1/FT		OTHER	
1 HR	5.27	1 HR	1950.	DEPTH, FT	0.20
10 HR	0.11	LIVE HERB	0.	HEAT CONTENT, BTU/LB	8000.
100 HR	0.19	LIVE WOODY	1350.	EXT MOISTURE, %	40.
LIVE HERB	0.00	SIGMA	1926.	PACKING RATIO	0.04197
LIVE WOODY	0.28			PR/OPR	6.14

Figure C.7: Plot M1392S custom fuel model.

FUEL MODEL 21. PLOT G2390W

LOADS, S/V RATIOS, AND DEPTHS FOR INDIVIDUAL FUEL COMPONENTS

FUEL COMPONENT	********** LOADS **********					*** S/V RATIOS ****			DEPTHS
	1 HR	10 HR	100 H	HERB	WOODY	1 HR	HERB	WOODY	
LITTER	5.50	0.00	0.00	0.00	0.00	2000.	0.	0.	0.35
GRASS	0.00	0.00	0.00	0.00	0.00	0.	0.	0.	0.00
SHRUBS	1.06	0.24	2.29	0.00	1.52	1500.	0.	1350.	1.80
SLASH	0.00	0.00	0.00	0.00	0.00	0.	0.	0.	0.00

********** FUEL LOAD SUMMARY **********

**** FUEL COMPONENT ****			** TIMELAG CLASS *	
	DEAD	LIVE	CLASS	LOAD
LITTER	5.50	0.00	------	-----
GRASS	0.00	0.00	1 HR	6.56
SHRUBS	3.59	1.52	10 HR	0.24
SLASH	0.00	0.00	100 HR	2.29
TOTAL	9.09	1.52	TOTAL	9.09

****** UNITS ******
LOAD : T/AC
S/V : 1/FT
DEPTH : FT

FINAL FUEL MODEL

STATIC 21. G2390W

LOADS, T/AC		S/V RATIOS, 1/FT		OTHER	
1 HR	6.56	1 HR	1937.	DEPTH, FT	1.05
10 HR	0.24	LIVE HERB	0.	HEAT CONTENT, BTU/LB	8000.
100 HR	2.29	LIVE WOODY	1350.	EXT MOISTURE, %	29.
LIVE HERB	0.00	SIGMA	1844.	PACKING RATIO	0.01450
LIVE WOODY	1.52			PR/OPR	2.05

Figure C.8: Plot G2390W custom fuel model.

FUEL MODEL 22. PLOT I1792W

LOADS, S/V RATIOS, AND DEPTHS FOR INDIVIDUAL FUEL COMPONENTS

FUEL COMPONENT	********** LOADS **********					*** S/V RATIOS ****			DEPTHS
	1 HR	10 HR	100 H	HERB	WOODY	1 HR	HERB	WOODY	
LITTER	9.40	0.00	0.00	0.00	0.00	2000.	0.	0.	0.46
GRASS	0.00	0.00	0.00	0.00	0.00	0.	0.	0.	0.00
SHRUBS	0.89	0.10	0.74	0.00	2.72	1500.	0.	1350.	3.32
SLASH	0.00	0.00	0.00	0.00	0.00	0.	0.	0.	0.00

********** FUEL LOAD SUMMARY **********

**** FUEL COMPONENT ****			** TIMELAG CLASS *			
	DEAD	LIVE	CLASS	LOAD	******	UNITS ******
LITTER	9.40	0.00	1 HR	10.29	LOAD	: T/AC
GRASS	0.00	0.00	10 HR	0.10	S/V	: 1/FT
SHRUBS	1.73	2.72	100 HR	0.74	DEPTH	: FT
SLASH	0.00	0.00				
TOTAL	11.13	2.72	TOTAL	11.13		

FINAL FUEL MODEL

STATIC 22. I1792W

LOADS, T/AC		S/V RATIOS, 1/FT		OTHER	
1 HR	10.29	1 HR	1967.	DEPTH, FT	1.38
10 HR	0.10	LIVE HERB	0.	HEAT CONTENT, BTU/LB	8000.
100 HR	0.74	LIVE WOODY	1350.	EXT MOISTURE, %	29.
LIVE HERB	0.00	SIGMA	1870.	PACKING RATIO	0.01440
LIVE WOODY	2.72			PR/OPR	2.06

Figure C.9: Plot I1792W custom fuel model.

FUEL MODEL 23. PLOT TP06S

LOADS, S/V RATIOS, AND DEPTHS FOR INDIVIDUAL FUEL COMPONENTS

FUEL COMPONENT	********** LOADS **********					*** S/V RATIOS ****			DEPTHS
	1 HR	10 HR	100 H	HERB	WOODY	1 HR	HERB	WOODY	
LITTER	5.74	0.12	0.30	0.00	0.00	2000.	0.	0.	0.46
GRASS	0.00	0.00	0.00	0.00	0.00	0.	0.	0.	0.00
SHRUBS	0.15	0.00	0.00	0.00	0.93	1500.	0.	1350.	2.11
SLASH	0.00	0.00	0.00	0.00	0.00	0.	0.	0.	0.00

********** FUEL LOAD SUMMARY **********

**** FUEL COMPONENT ****			** TIMELAG CLASS *				
	DEAD	LIVE	*	CLASS	LOAD	******	UNITS ******
LITTER	6.16	0.00	*	1 HR	5.89	LOAD	: T/AC
GRASS	0.00	0.00	*	10 HR	0.12	S/V	: 1/FT
SHRUBS	0.15	0.93	*	100 HR	0.30	DEPTH	: FT
SLASH	0.00	0.00	*				
TOTAL	6.31	0.93	*	TOTAL	6.31		

FINAL FUEL MODEL

STATIC 22. TP06S

LOADS, T/AC		S/V RATIOS, 1/FT		OTHER	
1 HR	5.89	1 HR	1990.	DEPTH, FT	0.71
10 HR	0.12	LIVE HERB	0.	HEAT CONTENT, BTU/LB	8000.
100 HR	0.30	LIVE WOODY	1350.	EXT MOISTURE, %	23.
LIVE HERB	0.00	SIGMA	1926.	PACKING RATIO	0.01463
LIVE WOODY	0.93			PR/OPR	2.14

Figure C.10: Plot TP06S custom fuel model.

FUEL MODEL 24. PLOT TP01S

LOADS, S/V RATIOS, AND DEPTHS FOR INDIVIDUAL FUEL COMPONENTS

FUEL COMPONENT	********** LOADS **********					*** S/V RATIOS ****			DEPTHS
	1 HR	10 HR	100 H	HERB	WOODY	1 HR	HERB	WOODY	
LITTER	5.74	0.12	0.30	0.00	0.00	2000.	0.	0.	0.46
GRASS	0.00	0.00	0.00	0.00	0.00	0.	0.	0.	0.00
SHRUBS	0.17	0.00	0.00	0.00	1.07	1500.	0.	1350.	2.44
SLASH	0.00	0.00	0.00	0.00	0.00	0.	0.	0.	0.00

********** FUEL LOAD SUMMARY **********

**** FUEL COMPONENT ****			** TIMELAG CLASS *				
*	DEAD	LIVE *	*		*		
*	-----	----- *	* CLASS	LOAD	*		
* LITTER	6.16	0.00 *	* ------	-----	*	****** UNITS	******
* GRASS	0.00	0.00 *	* 1 HR	5.91	*	LOAD : T/AC	
* SHRUBS	0.17	1.07 *	* 10 HR	0.12	*	S/V : 1/FT	
* SLASH	0.00	0.00 *	* 100 HR	0.30	*	DEPTH : FT	
*	-----	----- *	*	-----	*		
* TOTAL	6.33	1.07 *	* TOTAL	6.33	*		

FINAL FUEL MODEL

STATIC 22. TP01S

LOADS, T/AC		S/V RATIOS, 1/FT		OTHER	
1 HR	5.91	1 HR	1989.	DEPTH, FT	0.79
10 HR	0.12	LIVE HERB	0.	HEAT CONTENT, BTU/LB	8000.
100 HR	0.30	LIVE WOODY	1350.	EXT MOISTURE, %	24.
LIVE HERB	0.00	SIGMA	1916.	PACKING RATIO	0.01344
LIVE WOODY	1.07			PR/OPR	1.96

Figure C.11: Plot TP01S custom fuel model.

Appendix D : Environmental Parameter Interpretations

Table D.1: Fire severity related to fuel moisture chart.

Relative Humidity, %	1-hr Fuel Moisture, %	Ignition and Spotting Potential, General Burning Conditions
> 60	>20	Very little ignition; some spotting may occur with winds above 9mi/h.
45-60	15-19	Low ignition hazard; campfires become dangerous; glowing brands cause ignition when relative humidity is <50%.
30-45	11-14	Medium ignition hazard; matches become dangerous; "easy" burning conditions.
26-40	8-10	High ignition hazard; occasional crowning, spotting caused by gusty winds; "moderate" burning conditions.
15-30	5-7	Quick ignition, rapid buildup, extensive crowning and spotting; fire moves up bark of trees igniting aerial fuels; long distance spotting in pine stands; dangerous burning conditions.
<15	<5	All sources of ignition dangerous; aggressive burning, spot fires occur often and spread rapidly; extreme fire behavior probable; critical burning conditions.

Table D.2: Guidelines for estimating live fuel (foliage) moisture content.

Stage of Vegetative Development	Moisture Content, %
Fresh foliage, annuals developing, early in growing cycle.	300
Maturing foliage, still developing with full turgor.	200
Mature foliage, new growth complete and comparable to older perennial foliage.	100
Entering dormancy, coloration starting, some leaves may have dropped from stem.	50
Completely cured.	<30 Treat as a dead fuel.

Table D.3: Modified Beaufort scale for estimating windspeeds.

Windspeed, mi/h	Nomenclature	Characteristics
≤ 3	Very Light	Smoke rises nearly vertically; small branches of bushes sway; tall grasses and weeds sway and bend in wind; wind vane barely moves.
4 - 7	Light	Trees of pole size in the open sway gently; wind felt distinctly on face; wind flutters small flag.
8 - 12	Gentle Breeze	Trees of pole size in the open sway very noticeably; tops of trees in dense stands sway; wind extends small flag; few crested waves form on lakes.
13 - 18	Moderate Breeze	Trees of pole size in the open sway violently; whole trees in dense stands sway noticeably; dust is raised in the road.
19 - 24	Fresh	Branchlets are broken from trees; inconvenience is felt in walking against the wind.
25 - 31	Strong	Tree damage increases with occasional breaking of exposed tops and branches; progress impeded when walking against wind; light structural damage to buildings.
32 - 38	Moderate Gale	Severe damage to tree tops; very difficult to walk into wind; significant structural damage occurs.
≥ 39	Fresh Gale	Surfaced strong Santa Ana; intense stress on all exposed objects, vegetation, buildings; canopy offers virtually no protection; wind flow is systematic in disturbing everything in its path.

Appendix E : Revised Summer Custom Fuel Models

FUEL MODEL 14. PLOT I1892S

LOADS, S/V RATIOS, AND DEPTHS FOR INDIVIDUAL FUEL COMPONENTS

FUEL COMPONENT	********** LOADS **********					*** S/V RATIOS ****			DEPTHS
	1 HR	10 HR	100 H	HERB	WOODY	1 HR	HERB	WOODY	
LITTER	3.90	0.00	0.00	0.00	0.00	2000.	0.	0.	0.06
GRASS	0.00	0.00	0.00	0.04	0.00	0.	1350.	0.	0.30
SHRUBS	0.56	0.08	1.22	0.00	0.10	1500.	0.	1350.	0.30
SLASH	0.00	0.00	0.00	0.00	0.00	0.	0.	0.	0.00

********** FUEL LOAD SUMMARY **********

**** FUEL COMPONENT ****			** TIMELAG CLASS *				
	DEAD	LIVE	*	CLASS	LOAD	******	UNITS ******
LITTER	3.90	0.00	*	1 HR	4.46	LOAD	: T/AC
GRASS	0.00	0.04	*	10 HR	0.08	S/V	: 1/FT
SHRUBS	1.86	0.10	*	100 HR	1.22	DEPTH	: FT
SLASH	0.00	0.00	*				
TOTAL	5.76	0.14	*	TOTAL	5.76		

FINAL FUEL MODEL

STATIC 14. I1892S

LOADS, T/AC		S/V RATIOS, 1/FT		OTHER	
1 HR	4.46	1 HR	1951.	DEPTH, FT	0.14
10 HR	0.08	LIVE HERB	1350.	HEAT CONTENT, BTU/LB	8000.
100 HR	1.22	LIVE WOODY	1350.	EXT MOISTURE, %	49.
LIVE HERB	0.04	SIGMA	1929.	PACKING RATIO	0.06047
LIVE WOODY	0.10			PR/OPR	8.85

Figure E.1: Plot I1892S revised custom fuel model.

FUEL MODEL 16. PLOT K1489S

LOADS, S/V RATIOS, AND DEPTHS FOR INDIVIDUAL FUEL COMPONENTS

FUEL COMPONENT	********** LOADS **********					*** S/V RATIOS ****			DEPTHS
	1 HR	10 HR	100 H	HERB	WOODY	1 HR	HERB	WOODY	
LITTER	3.50	0.00	0.00	0.00	0.00	2000.	0.	0.	0.08
GRASS	0.00	0.00	0.00	0.29	0.00	0.	1350.	0.	1.11
SHRUBS	1.36	0.04	2.29	0.00	0.42	1500.	0.	1350.	1.11
SLASH	0.00	0.00	0.00	0.00	0.00	0.	0.	0.	0.00

********** FUEL LOAD SUMMARY **********

**** FUEL COMPONENT ****			** TIMELAG CLASS *			
	DEAD	LIVE	CLASS	LOAD		
LITTER	3.50	0.00	------	-----	******	UNITS ******
GRASS	0.00	0.29	1 HR	4.86	LOAD	: T/AC
SHRUBS	3.68	0.42	10 HR	0.04	S/V	: 1/FT
SLASH	0.00	0.00	100 HR	2.29	DEPTH	: FT
	-----	-----		-----		
TOTAL	7.18	0.71	TOTAL	7.18		

FINAL FUEL MODEL

STATIC 16. K1489S

LOADS, T/AC		S/V RATIOS, 1/FT		OTHER	
1 HR	4.86	1 HR	1887.	DEPTH, FT	0.65
10 HR	0.04	LIVE HERB	1350.	HEAT CONTENT, BTU/LB	8000.
100 HR	2.29	LIVE WOODY	1350.	EXT MOISTURE, %	37.
LIVE HERB	0.29	SIGMA	1823.	PACKING RATIO	0.01744
LIVE WOODY	0.42			PR/OPR	2.44

Figure E.2: Plot K1489S revised custom fuel model.

FUEL MODEL 19. PLOT K1492S

LOADS, S/V RATIOS, AND DEPTHS FOR INDIVIDUAL FUEL COMPONENTS

FUEL COMPONENT	********** LOADS **********					*** S/V RATIOS ****			DEPTHS
	1 HR	10 HR	100 H	HERB	WOODY	1 HR	HERB	WOODY	
LITTER	4.30	0.00	0.00	0.00	0.00	2000.	0.	0.	0.08
GRASS	0.00	0.00	0.00	0.24	0.00	0.	1350.	0.	0.55
SHRUBS	1.08	0.03	1.90	0.00	0.28	1500.	0.	1350.	0.55
SLASH	0.00	0.00	0.00	0.00	0.00	0.	0.	0.	0.00

********** FUEL LOAD SUMMARY **********

**** FUEL COMPONENT ****			** TIMELAG CLASS *		
*	DEAD	LIVE *	*		*
*	-----	----- *	* CLASS	LOAD	*
* LITTER	4.30	0.00 *	* ------	-----	*
* GRASS	0.00	0.24 *	* 1 HR	5.38	*
* SHRUBS	3.01	0.28 *	* 10 HR	0.03	*
* SLASH	0.00	0.00 *	* 100 HR	1.90	*
*	-----	----- *	*	-----	*
* TOTAL	7.32	0.52 *	* TOTAL	7.32	*

****** UNITS ******

LOAD : T/AC
S/V : 1/FT
DEPTH : FT

FINAL FUEL MODEL

STATIC 19. K1492S

LOADS, T/AC		S/V RATIOS, 1/FT		OTHER	
1 HR	5.38	1 HR	1921.	DEPTH, FT	0.29
10 HR	0.03	LIVE HERB	1350.	HEAT CONTENT, BTU/LB	8000.
100 HR	1.90	LIVE WOODY	1350.	EXT MOISTURE, %	42.
LIVE HERB	0.24	SIGMA	1875.	PACKING RATIO	0.03874
LIVE WOODY	0.28			PR/OPR	5.54

Figure E.3: Plot K1492S revised custom fuel model.

FUEL MODEL 20. PLOT M1392S

LOADS, S/V RATIOS, AND DEPTHS FOR INDIVIDUAL FUEL COMPONENTS

FUEL COMPONENT	********** LOADS **********					*** S/V RATIOS ****			DEPTHS
	1 HR	10 HR	100 H	HERB	WOODY	1 HR	HERB	WOODY	
LITTER	4.60	0.00	0.00	0.00	0.00	2000.	0.	0.	0.11
GRASS	0.00	0.00	0.00	0.13	0.00	0.	1350.	0.	0.52
SHRUBS	0.67	0.11	0.19	0.00	0.16	1500.	0.	1350.	0.52
SLASH	0.00	0.00	0.00	0.00	0.00	0.	0.	0.	0.00

********** FUEL LOAD SUMMARY **********

**** FUEL COMPONENT ****			** TIMELAG CLASS *			
*	DEAD	LIVE *	*		*	
*	-----	----- *	* CLASS	LOAD	*	
* LITTER	4.60	0.00 *	* ------	-----	*	****** UNITS ******
* GRASS	0.00	0.13 *	* 1 HR	5.27	*	LOAD : T/AC
* SHRUBS	0.97	0.16 *	* 10 HR	0.11	*	S/V : 1/FT
* SLASH	0.00	0.00 *	* 100 HR	0.19	*	DEPTH : FT
*	-----	----- *	*	-----	*	
* TOTAL	5.57	0.29 *	* TOTAL	5.57	*	

FINAL FUEL MODEL

STATIC 20. M1392S

LOADS, T/AC		S/V RATIOS, 1/FT		OTHER	
1 HR	5.27	1 HR	1950.	DEPTH, FT	0.20
10 HR	0.11	LIVE HERB	1350.	HEAT CONTENT, BTU/LB	8000.
100 HR	0.19	LIVE WOODY	1350.	EXT MOISTURE, %	39.
LIVE HERB	0.13	SIGMA	1925.	PACKING RATIO	0.04204
LIVE WOODY	0.16			PR/OPR	6.14

Figure E.4: Plot M1392S revised custom fuel model.

FUEL MODEL 23. PLOT TP06S

LOADS, S/V RATIOS, AND DEPTHS FOR INDIVIDUAL FUEL COMPONENTS

FUEL COMPONENT	LOADS					S/V RATIOS			DEPTHS
	1 HR	10 HR	100 H	HERB	WOODY	1 HR	HERB	WOODY	
LITTER	5.74	0.12	0.30	0.00	0.00	2000.	0.	0.	0.46
GRASS	0.00	0.00	0.00	0.75	0.00	0.	1350.	0.	2.11
SHRUBS	0.15	0.00	0.00	0.00	0.18	1500.	0.	1350.	2.11
SLASH	0.00	0.00	0.00	0.00	0.00	0.	0.	0.	0.00

FUEL LOAD SUMMARY

FUEL COMPONENT	DEAD	LIVE
LITTER	6.16	0.00
GRASS	0.00	0.00
SHRUBS	0.15	0.93
SLASH	0.00	0.00
TOTAL	6.31	0.93

TIMELAG CLASS	LOAD
1 HR	5.89
10 HR	0.12
100 HR	0.30
TOTAL	6.31

LOAD : T/AC
S/V : 1/FT
DEPTH : FT

FINAL FUEL MODEL

STATIC 22. TP06S

LOADS, T/AC		S/V RATIOS, 1/FT		OTHER	
1 HR	5.89	1 HR	1990.	DEPTH, FT	0.71
10 HR	0.12	LIVE HERB	1350.	HEAT CONTENT, BTU/LB	8000.
100 HR	0.30	LIVE WOODY	1350.	EXT MOISTURE, %	21.
LIVE HERB	0.75	SIGMA	1925.	PACKING RATIO	0.01463
LIVE WOODY	0.18			PR/OPR	2.14

Figure E.5: Plot TP06S revised custom fuel model.

FUEL MODEL 24. PLOT TP01S

LOADS, S/V RATIOS, AND DEPTHS FOR INDIVIDUAL FUEL COMPONENTS

FUEL COMPONENT	********** LOADS **********					*** S/V RATIOS ****			DEPTHS
	1 HR	10 HR	100 H	HERB	WOODY	1 HR	HERB	WOODY	
LITTER	5.74	0.12	0.30	0.00	0.00	2000.	0.	0.	0.46
GRASS	0.00	0.00	0.00	0.87	0.00	0.	1350.	0.	2.44
SHRUBS	0.17	0.00	0.00	0.00	0.20	1500.	0.	1350.	2.44
SLASH	0.00	0.00	0.00	0.00	0.00	0.	0.	0.	0.00

********** FUEL LOAD SUMMARY **********

**** FUEL COMPONENT ****			** TIMELAG CLASS *		
	DEAD	LIVE	CLASS	LOAD	
LITTER	6.16	0.00	------	-----	****** UNITS ******
GRASS	0.00	0.87	1 HR	5.91	LOAD : T/AC
SHRUBS	0.17	0.20	10 HR	0.12	S/V : 1/FT
SLASH	0.00	0.00	100 HR	0.30	DEPTH : FT
TOTAL	6.33	1.07	TOTAL	6.33	

FINAL FUEL MODEL

STATIC 22. TP01S

LOADS, T/AC		S/V RATIOS, 1/FT		OTHER	
1 HR	5.91	1 HR	1989.	DEPTH, FT	0.79
10 HR	0.12	LIVE HERB	1350.	HEAT CONTENT, BTU/LB	8000.
100 HR	0.30	LIVE WOODY	1350.	EXT MOISTURE, %	21.
LIVE HERB	0.87	SIGMA	1916.	PACKING RATIO	0.01344
LIVE WOODY	0.20			PR/OPR	1.96

Figure E.6: Plot TP01S revised custom fuel model.